Targeting the ERβ/HER oncogenic network in lung cancer: synergistic antitumor interaction and potentiation of anti-PD1 efficacy

A DISSERTATION

SUBMITTED TO THE FACULTY OF THE GRADUATE SCHOOL OF THE

UNIVERSITY OF MINNESOTA

Abdulaziz A. Almotlak

IN PARTIAL FULFILLMENT OF THE REQUIERMENTS FOR THE DEGREE OF

DOCTOR OF PHILOSOPHY

Advisor: Jill M. Siegfried

April 2020

Acknowledgments

Since graduation form college then practicing pharmacy profession, my passion has been always to develop scientific ideas and work to speed up medical discovery in oncology field. My sincere thanks and gratitude to Allah (God) for provided me this great opportunity to pursue my graduate education. I have had many hard times and difficulties throughout the journey but Allah made it easy for me. All praise and thanks to Allah Almighty who gave me the strength and patients to accomplish this work.

I would like also to thank Dr. Jill Siegfried for giving me the opportunity of working under her supervision and guidance. So grateful for the amazing scientific discoveries we were able to explore. She guided me throughout the 5 years in a really amazing way. She taught me how to be an independent investigator and help me out to develop the skills needed to be a scientist, A real one. Words cannot and will not describe the sincere gratitude I have for everything she did for me over the last 5 years. SO THANK YOU DR. SIEGFIRED.

I am also so grateful for Dr. Mariya Farooqui. She provided me a tremendous amount of technical experiences. She was involved in every scientific adventure I went through. Without her support and guidance, things would be much more complicated and very challenging. Special thanks to Christian Njatcha, and Jose Gomez-Garcia. I would like also to thank my thesis committee for the support and guidance. Their questions and comments were very valuable toward the completion of mydissertation

I would lastly acknowledge the funding support provided by the government of Saudi Arabia and Imam Abdulrahman bin Faisal University.

I dedicate my thesis work to my beloved parents Abdullah Almotlak and Sabah Alhathal whose love and prayers during the day and praying during night of day and night made my journey possible. To my beloved wife Norah Alakeel, who has witnessed my every failure and victory throughout this journey. Thank you for all the sacrifices you took to make me happy. I also dedicate this body of work to every lung cancer patient who is still fighting the disease or those who lost the battle.

Abstract

Lung cancer is the leading cause of cancer related mortality in the United States, accounting for more than 142,000 estimated deaths in 2019. The major subtype of lung cancer is non-small cell lung cancer (NSCLC), which represents 85% of all cases. Despite the advancement in understanding the molecular basis of NSCLC, the 5-year survival rate is less than 20%. The current treatment strategies for advanced stage patients rely on molecularly-targeted therapies, cytotoxic chemotherapy and immunotherapeutic agents. Because of the complexity and heterogeneity of lung tumors, intrinsic and acquired resistance mechanisms ultimately result in failure to respond to these therapies and early relapse. Combinatorial strategy that involves targeting multiple aspects of tumorigenesis may represent a new avenue for therapeutic intervention in lung cancer management.

Estrogen signaling has been frequently shown to be an important mediator of lung cancer progression and metastasis. In a non-genomic fashion, ER mutually interacts with human epidermal growth factor receptors (HERs) to promote lung cancer proliferation and growth. Targeting ER signaling with the antiestrogen fulvestrant has shown moderate activities in preclinical models of lung cancer. The reciprocal interaction between ER and EGFR could limit the activity of using anti-ER agent alone. In a phase II clinical trial, combining fulvestrant with the selective EGFR tyrosine kinase inhibitor erlotinib showed an enhanced activity over erlotinib alone and improved the survival outcomes in NSCLC patients. However, the improvement in overall median survival was modest.

Recent retrospective clinical analysis demonstrated that genes contained in the prediction analysis of microarray 50 (PAM50) provide prognostic information in high

ERβ+ lung cancer patients. The 7-gene model includes c-Myc, MIA, CXXC5, FGFR4, Grb-7, FOXC1, and PgR. In high-risk patients, who tend to have a poor prognosis and short median survival, c-Myc, MIA, CXXC5, FGFR4, Grb-7, FOXC1 are overexpressed and PgR is downregulated. Importantly, the 7-gene model described one interacting network that includes ER and HER2/HER3 as the top upstream regulators for the 7-gene panel. In fact, a significant association between ERβ and HER2 expression was found, in which 70.2 % of ERβ-positive cases were positive for HER2 compared to 34.5% of ERβ-negative cases. HER3, when analyzed with HER2, showed also positive association with ERβ. These observations suggest that ERβ and HER2/HER3 pathways define lung tumors with very aggressive biology, indicating that blocking both pathways could be more efficacious than either one of them alone. These observations also could explain why the magnitude of response was modest when fulvestrant was combined with erlotinib, as erlotinib has weak activities against HER2 and HER3. Combining a pan-HER inhibitor such as dacomitinib (inhibits EGFR, HER2 and HER4) with fulvestrant could be more efficacious than either agent alone and could produce a gene signature that predicts better clinical outcomes in NSCLC.

Immune checkpoint inhibitors have changed the treatment paradigm for several solid tumors, including lung cancer. Antibodies that target programmed death receptor 1(PD1) or its ligand (PD-L1) have proven great efficacy for certain patients with lung cancer. Patients who respond to these agents tend to have durable effects and longer survival outcomes; however, only 20-29% of patients are predicted to respond. Several combination strategies are being evaluated clinically to maximize the efficacy of these agents and improve the response rate. Preclinical evidence found that the ER blocker

fulvestrant effectively sensitizes lung cancer cells to T cell and natural killer (NK) cell mediated cytotoxicity effects. In addition, estrogen signaling is a critical mediator for myeloid derived suppressor cells (MDSCs), which are largely known for their immunosuppressive effects. Evidence also demonstrated that EGFR inhibitors possess dual immunomodulatory effects that include upregulation of major histocompatibility complex I and II (MHC I and II), inducing the recruitment of immune cells, and inhibiting other tyrosine kinases essential for immune cells function. Synergy was observed when EGFR TKI and PD1 inhibitor was combined in an- EGFR-mutant model. Altogether, these previous observations encouragingly support the hypothesis that use of triple therapy (fulvestrant, pan-HER TKI and an immune checkpoint blocker) will be a promising treatment approach for lung cancer. Testing this hypothesis is the subject of this dissertation.

To evaluate the therapeutic potential of combining ER blocker with pan-HER in NSCLC, we chose fulvestrant, as an antiestrogen, and dacomitinib, as a tyrosine kinase inhibitor that targets EGFR, HER2, and HER4. We first evaluated the efficacy of this combination in three different human NSCLC cell lines and assessed the ability of this treatment approach to produce a gene signature that predicts better clinical outcomes. We utilized three different cell lines that represent three different categories of NSCLC population; EGFR-mutant, KRAS-mutant and EGFR and KRAS wild-type. Next, we investigated the immunomodulatory effects of this combination treatment on macrophages and CD8+ T cells in vitro. We used a novel syngeneic lung cancer model (FVBW-17/FVB-N) to evaluate the therapeutic effectiveness of fulvestrant-dacomitinib in combination with a mouse anti-PD1.

Major results

The combination of fulvestrant and dacomitinib significantly suppressed NSCLC cell growth in vitro and produced a combination index < 0.5, indicating strong synergy. The combination also showed potent downregulation of HER activity and marked decrease in amphiregulin (AREG) and neuregulin (NRG1-β1) expression. Importantly, the combination, but not single agents, completely reversed the gene signature associated with poor prognosis. C-Myc, MIA, CXXC5, FGFR4, FOXC1 and Grb7 were downregulated and PgR was upregulated following the combination treatment. The combination significantly reduced c-Fos, JunB and pCREB DNA-binding activities. The c-Fos/Ap-1 inhibitor t-5224, but not CBP-CREB inhibitor, was able to partially mimic the effects of the combination in reversing the gene signature. In vivo, the combination treatment demonstrated a robust synergistic antitumor effect in NSCLC cell lines that were engrafted subcutaneously in immunodeficient mice. Tumor regression was observed in the majority of tumors following the combination treatment. A drastic decrease in HER activity and downstream signaling were observed with the combination, along with a significant decrease in AREG and NRG1-β1 expression. In situ proximity ligation assay revealed a significant decrease in the active dimerization of both p-HER2/p-HER3 and p-HER2/p-EGFR dimers following the combination treatment. Additionally, the gene signature was also completely reversed by the combination but not with single agents. In the EGFR mutant model, the survival of mice was improved after treatment discontinuation, tumors that recurred were less aggressive, and two mechanisms of resistance commonly associated with HER TKIs were blocked.

To evaluate the immunomodulatory effects of the combination, bone marrow-derived macrophages and CD8+ T cells were treated with the combination. Surprisingly, macrophages lost their phagocytic function and behave more like M2-macrophages by expressing high IL-10, CD206 and PD1 following the combination treatment. Mechanistically, dacomitinib induced downregulation of phospho-Syk, and fulvestrant was not able to overcome this effect. In CD8+ T cells, the combination impaired the function of T cells, induced high PD1 expression, and severally reduced IFN-ϒ and TNF-α production. These debilitating effects were mostly attributed to the downregulation of Src Family kinases activities, as less phospho-SFK Y416 was detected following the combination treatment. In vivo, adding anti-PD1 antibody to the combination treatment enhanced the immune function and improved the antitumor effects. In a sequential approach, where anti-PD1 was administrated after the combination treatment, the average tumor volume was 4-fold less than placebo and this effect was synergistic. In comparison, the triple therapy given concomitantly showed a 2-fold decrease compared to placebo. Sequential triple therapy was also significantly better than concomitant triple therapy. None of the drugs alone show any sign of activities. Interestingly, after one week of administrating fulvestrant and dacomitinib, tumors showed high immune cell infiltration (inflamed tumor microenvironment), with relatively high PD1 expression on CD8+ T cells. In contrast, the concomitant triple therapy showed a significant increase in CD8+ T cells infiltration but with a decrease in PD1 expression, and fewer M2 macrophages.

Conclusion and Significance

Retrospective analysis of NSCLC patients revealed that the interaction between HER2/HER3 and ERβ contributes to poor outcomes in NSCLC patients with high ERβ expression. Here, we report that targeting ERβ with the antiestrogen fulvestrant, along with targeting multiple HER pathways with the pan-HER TKI dacomitinib produced synergistic antitumor effects in preclinical models of human ERβ+ NSCLC. The robust antitumor effect seen was accompanied by the ability of this combination treatment to produce a gene signature that predicts better clinical outcomes. The 7-gene model could serve as a predictive tool for identifying patients who will more likely respond to the treatment. These data strongly support its clinical use, giving the fact that both drugs are clinically used for cancer patients.

Convincing evidence also suggest an immunomodulatory effect of ER signaling and HER pathways. The combination of fulvestrant and dacomitinib suppressed phagocytic macrophages and CD8+ T cell functions and upregulated PD1 expression. These effects were largely contributed by dacomitinib for its inhibitory effects on Syk and Src kinases on immune cells and might limit the clinical utility of the fulvestrant/dacomitinib combination. However, the ability of the combination to turn the TME into an inflamed microenvironment with upregulated PD1 could potentiate the tumor-mediated killing effects by immunotherapy. The synergistic antitumor effect observed with adding anti-PD1 in a sequential manner after the administration of fulvestrant and dacomitinib is highly encouraging. The significance of these observations is that the triple therapy has shown excellent antitumor effects in a highly aggressive tumor model that is unresponsive to immune checkpoint inhibitor alone or fulvestrant-dacomitinib combination. The clinical usefulness of this approach can have therapeutic

applications for other solid tumor models, particularly in tumors that are less inflamed and are unlikely to respond to immune checkpoint inhibitors.

Table of Contents

List of Tables

Tables in Material and Methods:

List of figures

Focus of Research figure:

Chapter 3 figures

Chapter 4 figures

Chapter 1: General background

Lung cancer epidemiology and pathophysiology

Lung cancer is the leading cause of cancer related mortality for both men and women in the United States and worldwide (1). In 2019, there were 228,150 cases diagnosed with lung cancer and 142,670 deaths. Despite the advances in understanding its biology, lung cancer remains the most aggressive type of cancer with an estimated five-year survival rate that is less than 21% (2). Lung cancer mortality rate is far more than colon, pancreatic, and breast cancer deaths rate combined (1). The poor survival rate is attributed to the fact that more than 70% of cases are diagnosed with advanced stage disease when most of the treatment options are less effective. In fact, in early stage localized disease, the five-year survival rate is 60% (3). This indicates the need for both new treatment strategies with improved efficacy and early detection strategies as well.

Tobacco smoking is the major cause of all main types of lung cancer. It has been estimated that nearly 90% of cases were attributed to smoking (4). Continuous smokers are at 20-50 fold risk of developing lung cancer than never smokers, and that risk decreases among ex-smokers. Although cigarettes are the main tobacco product, other common forms of tobacco such as hookah and pipes were shown to cause lung cancer as well (4). Other life-style behaviors might also increase the risk of developing lung cancer. These include smoking marijuana or using electronic cigarettes. Lung cancer has been also associated with exposure to some environmental factors such as asbestos and air pollution (5,6). In fact, secondhand smoke, also known as environmental tobacco smoke, exhibits a 20-30% increased risk of developing lung diseases including lung cancer (4).

Although lung cancer has been widely associated with tobacco exposure, never-smokers can also develop lung cancer. A positive family history of lung cancer is a risk factor for lung cancer development (7). This was shown after careful consideration of smoking status. Several genome-wide association (GWA) studies have identified distinct genetic signatures in different chromosomal regions that increase the chance of lung cancer development. These abnormalities were shown to drive lung cancer independent of smoking status through many genetic, epigenetic and signaling driven mechanisms such as the ERBB protein family (EGFR, HER2, HER3 and HER4) (8,9, 10). In fact, the number of non-smokers diagnosed with lung cancer continues to increase accounting for 20-25% of all lung cancer cases and predominantly affecting women (11,12, 13).

Lung cancer represents a group of very aggressive, highly invasive, rapidly metastasizing and histologically and molecularly heterogeneous disease. Clinically, it is broadly categorized into two major subtypes: small cell lung cancer (SCLC) (accounts for 15% of all lung cancer cases) and non-small cell lung cancer (NSCLC) that account for 85% of all lung cancer cases (6). SCLCs exhibit a neuroendocrine phenotype by expressing different neuroendocrine transcription factors that arise mostly in the proximal airways of the lung. The most common subtype NSCLC is further subclassified into adenocarcinoma, squamous cell carcinoma and large cell carcinoma. Adenocarcinoma tumors mostly arise in the peripheral bronchi from alveolar Type II cells and account for 40% of all lung cancer cases. Squamous cell carcinomas account for 20-35% of all lung cancer cases and tend to arise in the main bronchi form a cell of origin differentiated as Clara cells expressing CCl10 (14). Large cell carcinomas, also known as NSCLC not otherwise specified (NSLC-NOS) and account for 10% of all lung cancer cases, are

highly undifferentiated and poorly characterized subtype that behave similarly to small cell cancers and arise in the proximal location with high tendency of invasion and metastasis (15). These different subtypes of lung cancer are molecularly distinct, and thus, are driven by distinct genetic and epigenetic programs. As a result, treatment plans are tailored based on the genetic testing, histology and staging of the disease.

Lung cancer major genetic aberrations

Recent advances in molecular diagnostics and mutational analysis have revolutionized our understanding of the biology of lung cancer at a deeper molecular scale. Lung cancer, as revealed by next-generation sequencing technologies, is characterized by a high mutational burden compared with many other malignancies (16). Several large sequencing studies have consistently established that lung cancer is a molecularly heterogeneous type of disease. For instance, several receptor tyrosine kinases were frequently found to be mutated in lung adenocarcinomas, but are rarely detected in squamous cell carcinomas (17). Furthermore, studies revealed that lung cancer developed in never-smokers is molecularly distinct than current-smokers. Cytosine to thymidine transitions are more common among never-smoker patients, where tumors in smokers are enriched for cytosine to adenine transversions (16). The most common genetic alterations reported in lung cancer are somatic mutation in the tumor protein 53 (*TP53*), Kristen Rat Sarcoma viral oncogene (*KRAS*), epidermal growth factor receptor (*EGFR*), gene amplification in the hepatocyte growth factor receptor (*MET*), anaplastic lymphoma kinase (*ALK*) and serine threonine protein kinase 11 (*STK11*). Other rare mutations include mutations in ROS1 tyrosine kinase proto-oncogene (*ROS1),* fibroblast growth

factor receptor 1 (*FGFR1*) and Janus kinase 2 (*JAK2*) (18). Some of these altered genes have been successfully targeted by small molecule inhibitors such as epidermal growth factor tyrosine kinase inhibitors (EGFR-TKIs), which have provided clinically meaningful efficacy and acceptable toxicity. However, lung tumors are more often characterized by co-existence of these mutations, which indicates the intratumoral heterogeneity in response to current therapeutic agents.

KRAS is one member of the RAS family of proto-oncogenes that include NRAS and HRAS. Ras proteins are intracellular guanine binding proteins that belong to GTPases family enzymes and play a critical role in controlling cell proliferation and survival. In the quiescent cell state, Ras is guanosine diphosphate (GDP) bound and upon signal activation by upstream tyrosine kinase receptors, GDP switches to GTP that allow Ras to activate downstream pathways including the mitogene-activated protein kinase (MAPK) and the phosphatidylinositol-3-kinase pathway (PI3K). This switch is tightly regulated by additional proteins, including the guanine nucleotide exchange factors (GEFs), which attenuate the affinity of Ras to GDP and favor GTP binding, and the GTPase-activating proteins (GAPs), which accelerate the GTPase activity of Ras leading it to an inactive state (19). It has been estimated that 20-40% of lung cancer cases are KRAS mutant tumors (20). Most of these mutations are found in exon 2 and 3 and involve amino acid substitution. These mutations impair the GTPase activity leading to a sustainable activation state of Ras. The most common isoform of KRAS mutation is G12C (substitution of glycine at codon 12 by cysteine) and accounts for 35% of all KRAS mutations in lung cancer. Other detected mutations include G12D and G12V (21). Different mutant forms may be associated with distinct biological behavior (21). In

addition, co-occurring mutations are frequently observed in KRAS mutant tumors and include *TP53* (40%) and *STK11* (30%) (21). As a result, different clinical outcomes are observed in this heterogeneous population. Although for decades, KRAS mutation was considered undruggable, new horizons have been recently explored and showed some clinical activity. This includes tackling the mutant G12C form by direct inhibitors that target the novel cysteine residue, ARS-1620 and AMG510 (22,23). However, these agents are more likely to develop resistance and new treatment strategies are needed to further improve their efficacy.

Another common genetic alteration includes the amplification and overexpression of MET oncogene. MET is a receptor tyrosine kinase for hepatocyte growth factor (HGF) ligands. It is overexpressed in about 60% of lung cancer and amplified in 5% of the cases (24). High phosphorylation and protein expression have been observed in malignant tissues compared to normal tissues and correlate with advanced disease stage and poor prognosis (24). MET amplification represents a bypass resistance mechanism in 5-20% of lung cancer cases progressed on EGFR targeted therapy (25). Several targeting strategies have been explored to tackle MET oncogenic signaling in lung cancer. These include using monoclonal antibodies that target either the receptor or the ligand, and using small molecule inhibitors that target the kinase activity of the receptor. Although MET is overactive in the majority of lung tumors, only patients with the gene amplification were responding to MET inhibitors (24). The amplification does predict a high response rate as compared to non-amplified MET. However, combination strategies could be the key to enhance the response rate and improve the efficacy.

Other rare mutations are the structural rearrangements in ALK and ROS1 that are detected in 5 and 2% patients with lung cancer respectively (26). The ALK most common in fusions rearrangements occur in the intracellular domain with the terminal end of echinoderm microtubule-associated protein-like 4 (EML4), which results from an inversion in chromosome 2p whereby intron 13 of EML4 is fused to intron 19 of ALK. The fused protein EML4-ALK is constitutively active and associated with cell proliferation and survival by activating the downstream pathways MAPK, PI3K and the signal transducer and activator of transcription 3 (STAT3) pathway. Similar to ALK, ROS1 intact tyrosine kinase protein fused with a partner gene leading to constitutive activation of downstream signaling (27). These mutations render the tumor very sensitive to tyrosine kinase inhibitors. Those inhibitors showed potent antitumor activity with favorable clinical outcomes. As a result, several ALK and ROS1 tyrosine kinase inhibitors are approved by the Food and Drug Authority (FDA) as a first-line treatment option for this disease (28).

Epidermal growth factor receptors (HERs) signaling pathway

The EGF family of receptors consists of four receptors, EGFR/ERBB1, HER2/ERBB2, HER3/ERBB3, and HER4/ERBB4. These receptors are structurally similar but with distinct properties, including variations in tyrosine kinase activity, ligand binding ability and differential downstream activity. HERs are transmembrane receptors that consist of three main domains; extracellular ligand domain, transmembrane domain, and intracellular tyrosine kinase domain (29). There are more than 10 identified growth factors like ligands that bind to HERs and activate them and initiate their downstream

signaling pathways. EGF, amphiregulin (AREG), transforming growth factor alpha (TGF-α) and epigen (EPG) can bind to EGFR. Epiregulin (ERP), heparin-binding EGF-like growth factor (HB-EGF) and betacellulin (BTC) bind to both EGFR and HER4. Neuregulins 1 and 2 (NRG1/2) bind to HER3 and HER4, while NRG3/4) bind to only HER4 (30). However, HER2 lacks a ligand binding activity and it relies on the heterodimerization with other HERs, mostly with HER3. After binding to the receptors, this leads to conformational changes and homo or heterodimerization with other members of HER family. These structural changes are followed by phosphorylation of the intracellular kinase domain, which subsequently creates a site for adaptor protein to bind and induce the downstream signaling pathways MAPK, PI3K and STAT3 (31). Depending on the pathway, the end result is cell proliferation, survival, and inhibition of apoptosis.

Dysregulation of HER activity has been linked to human cancer pathogenesis. Many epithelial tumors harbor mutations in EGFR or HER2 and to a lesser extent HER3 receptors (32). Overexpression of the *EGFR* gene has been detected in 40-80% of both squamous and adenocarcinoma NSCLC cases (33). While the overexpression was thought to predict responsiveness to anti-EGFR therapy, only patients with EGFR mutations significantly responded (34). EGFR mutations are reported in 32.2% of NSCLC patients (35). Most of these mutations occur between exon 18-21, with the L858R point mutation in exon 21 and E746_A750 deletion in exon 19 being the most prevalent (36). Both of these mutations result in changes near the ATP site, which leads to enhanced catalytic activity and autocatalysis of the tyrosine kinase that occur even in the absence of ligands. Numerous epidemiological studies showed that these mutations

were commonly seen among females and never smokers compared to male and current smokers NSCLC patients (37).

HER2 genetic alteration has been also described in lung cancer. Both HER2 amplification and gene mutation have been detected. Gene amplification is found in 10-20% and in-frame insertion mutation is observed in 2-4% of NSCLC patients (38, 39). These patients tend to have very aggressive disease and shorter survival. HER2 has no known ligand that directly binds to it; however, it becomes constitutively active upon homo o heterodimerization with either EGFR or HER3. The preferred partner for HER2 is HER3 and this heterodimer produces a very potent pro-tumorigenic effect in cancer cells (40, 41). On the other hand, the overexpression of HER3 is found in 32% of NSCLC (42). HER3 has a weak kinase activity and its oncogenic effect is induced upon dimerization with EGFR or HER2 (32). Hyperactivation of HER3 signaling is one of many bypass mechanisms that have been shown to drive resistance to EGFR tyrosine kinase inhibitors (EGFR TKI) (43). High production of NRG1 ligands, which preferably bind to HER3, by somatic gene fusion in *NRG1* has been recently reported in some NSCLC patients (44). Several combination strategies that involve combining EGFR TKIs with anti-HER3 monoclonal antibodies are explored and undergoing clinical testing.

The discovery of EGFR biological role in lung cancer tumorigenesis has led to the development of EGFR targeted agents. These agents act by reversibly or irreversibly binding to the ATP site at the tyrosine kinase of EGFR, which inhibits the phosphorylation and subsequently the induction of the downstream oncogenic cascade (45). Gefitinib was the first agent discovered to tackle EGFR activity. It was originally tested in an unselected population of NSCLC patients, considering the fact that EGFR is

overexpressed in the majority of cases. However, it appeared later that only patients with EGFR mutations responded to the therapy compared to conventional chemotherapeutic agents (46). Other agents were discovered and showed similar activities such as erlotinib, and afatinib (47). A second generation of EGFR TKIs was then developed that showed significantly better antitumor effects in clinical studies compared to the first generation. Dacomitinib is an irreversible tyrosine kinase inhibitor and it has potent activity against HER2 and HER4 kinases compared to the first generation molecules gefitinib and erlotinib. In ARCHER1050 phase III clinical study, dacomitinib showed significantly better progression and overall survival compared to the first generation TKI gefitinib (48). As a result, several of these EGFR TKIs are approved by FDA for first-line treatment of NSCLC with EGFR activating mutations. However, patients eventually develop acquired resistance to EGFR TKI through different mechanisms. In 50% of the cases, a second mutation in the EGFR kinase domain (T790M) is developed that results from a substitution of methionine (M) by threonine (T) at position 790 of exon 20 (45). This led to the discovery of EGFR TKI that selectively target both the sensitizing mutations and the secondary mutation (T790M). Osimertinib is now approved for first line treatment of EGFR mutant NSCLC. Other resistance mechanisms reported involve activation of HER2:HER3 signaling, MET overexpression, the tumor suppressor PTEN loss and PI3K overactivation (49). This suggests that targeting one pathway is often overcome by other perturbed pathways that will restore cell proliferation and survival signaling. Additionally, wild-type EGFR tumors do not respond magnificently as the mutant EGFR tumors, even though the majority of NSCLC tumors are characterized by

hyperactivated EGFR signaling. Combination strategies are a key approach to enhance the response rate and prevent or attenuate the resistance mechanisms.

Role of estrogen signaling in lung cancer

Although lung cancer was considered mostly a health problem among men, in the last few decades more women are actually diagnosed with lung cancer. The incidence and mortality rates have decreased among men compared to women (6). While the habit of smoking is increasing among women, which explains the increase in the incident rate, nearly 53% of the women diagnosed are never-smoker compared to 15% in men (50). This indicates that other factors are contributing to lung cancer development. Indeed, several epidemiological studies have linked estrogen signaling to lung cancer development and progression. High circulating endogenous estrogen has been associated with worse clinical outcomes in premenopausal women and men (51). High expression of estrogen receptors, predominantly the beta form (ERβ) and aromatase, the rate-limiting enzyme necessary for converting androgen to estradiol, were also observed in lung tumor tissues compared to the healthy ones (51). Additionally, the Women's Health Initiative (WHI) controlled trial demonstrated that women who were taking combined hormonal replacement therapy (HRT) (estrogen plus progestin) were more likely to die from lung cancer compared to placebo (52, 53). All these epidemiological findings support a role for estrogen signaling in lung cancer development.

Estrogen Receptor Biology

ER is a ligand-inducible transcription factor that belongs to the nuclear hormone receptor family. It is characterized into two main types; estrogen receptor alpha (ERα) encoded by the *ESR1* gene and estrogen receptor beta (ERβ) encoded by *ESR2* (54). The distribution of these receptors is a tissue-specific. ERα is more predominant in breast, ovary and endometrial tissues while lung, bone, brain and testes express ERβ. In cancer, the oncogenic effect of estrogen is mediated by ERα in breast carcinomas and by ERβ in lung cancer (55). Both receptors share the same structure, containing a transcription active domain (A/B domain), DNA binding domain (DBD), a flexible hinge region (D domain), and a ligand-binding domain (E/F domain) (54). Activated ER can mediate its physiological function by mainly through two main approaches; a nuclear-based signaling (genomic pathways) and a membrane-based signaling (non-genomic). In the classical approach, the endogenous estrogen 17-βestradiol (E2) binds to the ER receptors and leads to homodimerization and translocation to the nucleus. This ER complex along with cofactors and corepressors will bind to the DNA at the estrogen receptor element (ERE) to mediate the transcription of several ER target genes. The transcription activity is also mediated independently to ERE where ER complex has been shown to bind to different DNA binding sites of other transcription factors such as activator protein 1 (AP-1) simulating protein 1 (SP1) and nuclear factor κ B (NF κB) (56). E2 can also bind to membrane-bound ERs present in the cellular membrane as monomers. ER:E2 complex will rapidly transactivate kinase pathways either by inducing growth factor ligand release or by associating with several cytoplasmic kinases such as MAPK and PI3K (56).

Estrogen signaling in lung cancer

In lung cancer, estrogen signaling is active and mediates a pro-tumorigenic effect through mainly non-genomic pathways by predominantly ERβ (57). Five different ERβ isoforms have been identified in lung cancer cells. However, only ERβ1 is functionally active (51). 60-80% of NSCLC patients show a high expression of ERβ (51, 58). Different epidemiological studies associated high ERβ expression with worse clinical outcomes in both women and men with lung cancer. Expression of aromatase was also detected in malignant lung tissues compared to healthy tissues, and correlates also with poor prognosis (58). E2 has been shown to induce NSCLC proliferation by transactivating EGFR that leads to inducing MAPK and Akt pathways. This effect is mainly through promoting EGFR ligands release, including HB-EGF, AREG and TGF-α., which they induce homo or heterodimerization of HERs (58). E2 also promotes NSCLC cell angiogenesis by inducing vascular endothelial growth factor (VEGF) secretion (58). HGF, a ligand for MET receptor, has been shown to be induced by E2 in lung fibroblasts (59). In addition, E2 facilitates NSCLC cell migration by stimulating CXCL12/CXCR4 pathway (60). In mouse xenografts with NSCLC and tobacco carcinogen-induced lung cancer models, E2 significantly increased tumor growth and augmented the lung tumor burden, and the antiestrogens fulvestrant and the aromatase inhibitor anastrazole, were able to partially inhibit these effects (58). These observations suggest that estrogen signaling is active and antiestrogens that are used in breast cancer could be repurposed for lung cancer treatment.

Estrogen receptor and HER cross-talk in lung cancer

Although the accumulating evidence suggest estrogen signaling potentiates lung tumorigenesis, the antitumor effect observed with ER inhibitors in lung cancer was

modest. One mechanism was the bidirectional cross-talk between ER and EGFR pathways in lung cancer. Upregulation of EGFR signaling was observed after longer exposure to fulvestrant in NSCLC cell lines, and the EGFR TKI gefitinib upregulated ERβ expression as well (61). Clinical evidence demonstrates that high expression of cytoplasmic ERβ predicts poor response to EGFR TKI in EGFR-mutant NSCLC (62). This mechanism was previously reported in breast cancer cells, and EGFR/HER2 and HER2/HER3 hyperactivation are capable of driving resistance to endocrine therapies (63). Combining gefitinib with fulvestrant significantly suppressed NSCLC cell proliferation in vitro and decreased tumor volume by 60% in mouse xenografts (61). In a phase II clinical trial, the combination of the EGFR TKI erlotinib and fulvestrant showed improved efficacy and good tolerability in EGFR wild-type NSCLC patients (64). However, the antitumor effect could be further improved if HER2/HER3 signaling was also inhibited in combination with estrogen antagonist. HER2/HER3 signaling is weakly affected by the first-generation TKIs gefitinib and erlotinib. HER2/HER3 could be a driving resistance mechanism for both EGFR TKI and antiestrogen alone, and using a pan-HER TKI in combination with fulvestrant might further improve the clinical outcomes in lung cancer treatment.

HER2/HER3 signaling mediates the strongest oncogenic signaling among HER family of receptors in cancer cells (40-41). In fact, co-expression of ERβ and HER2/HER3 receptors defines lung tumors with very aggressive biology and predicts poor clinical outcomes in NSCLC patients (65). High ERβ tumors are more likely to be positive for both HER2 and HER3. Using the prediction analysis of microarrays 50 (PAM50), a common predictive tool used in breast cancer, seven genes, when analyzed

together, consistently showed correlation with progression free survival and overall survival. Six of those genes were upregulated and one was downregulated in high risk patients. The six genes include c-*Myc*, Melanoma inhibitory activity (*MIA*), CXXC finger protein 5 (*CXXC5*), fibroblast growth factor receptor 4 (*FGFR4*), growth factor receptor bound protein 7 (*Grb-7*) and forkhead box C 1 (*FOXC1*) were upregulated, and the one that was downregulated is progesterone receptor gene (*PgR*). Interestingly, the seven-gene model predicted one interacting network that includes ER and HER2/HER3 pathways, which means these two pathways define a subset of patients with poor survival and aggressive cancer. This suggests that combining anti-ER with pan-HER TKI that inhibits EGFR, HER2, HER3 and HER4, could be more efficacious than either agents alone or the anti-ER EGFR TKI combination, and the 7-gene model could serve as a predictive tool for evaluating and predicting the response.

Tumor-immunology in lung cancer

The field of tumor microenvironment (TME) has been evolving rapidly in the last few decades. Along with tumor cells, noncancerous cells are a major component of the TME and play a pivotal role in dictating tumor progression. Mounting evidence demonstrates that in addition to the tumor mutation burden and neoantigenes presentation, the cross-talk between cancer cells and immune cells at the tumor bed is a major regulatory mechanism for tumor outgrowth. To avoid the initial attack and elimination by immune cells, tumor cells evolve rapidly and acquire multiple immunosuppressive mechanisms and recruit immunosuppressive immune cells to escape the immune-surveillance (66). The presence of certain immune cells at the tumor site

predicts the prognosis of NSCLC patients. High infiltration of cytotoxic T lymphocytes (CD8+ T cells) and the anti-tumorigenic phenotype of macrophages (M1) correlate with better PFS and OS compared to regulatory T cells (Treg) and the pro-tumorigenic macrophages (M2) in NSCLC (67). This indicates the importance of analyzing the TME in evaluating any combination treatment strategies in cancer treatment.

In addition to reducing immunogenicity, one of the major mechanisms acquired by the tumor cells to escape the immune elimination process is by inducing programmed death-1/ligand-1 (PD1/PD-L1) pathway in immune cells. PD1, a major inhibitory checkpoint protein, is a transmembrane glycoprotein expressed on T cells and many other immune cells (66). Its expression correlates with an exhaustion phenotype and predicts lower anti-tumor response. Two main ligands, PD-Ll and PD-L2, have been identified that bind to PD1 and initiate apoptotic signaling in immune cells. Most NSCLC tumors express PD-L1, as a mechanism of immunosuppression (68). Another mechanism is by secreting immunosuppressive cytokines that allow the recruitment of immunosuppressive cells to the tumor bed such as Tregs or myeloid derived suppressor cells (MDSCs). For instance, secreting VEGF, CCL2 or IL-10 could drive the TME toward an immunosuppressive phenotype (69). Agents that target the PD1/PD-L1 axis showed great efficacy in reinvigorating the anti-tumor immune response and shifting the TME from an immunosuppressive to immune-stimulatory phenotype. Five monoclonal antibodies that target either the receptor or the ligand are now approved by the FDA for wide-range of malignancies, including NSCLC. However, their efficacies in NSCLC, as monotherapy, are limited for 20-25% of NSCLC patients (71, 72). Combining immune checkpoint blockade with cytotoxic chemotherapeutic agents showed an enhanced response rate even

in tumor types insensitive to immunotherapeutic agents alone (73). The need for new treatment approaches that take into account multiple aspects of tumorigenesis is highly warranted and could provide better efficacy and safety profiles.

CD8 T cells antitumor immune response

The ultimate goal of the adaptive immune system during immunosurveillance is to eliminate tumor cells. Cytotoxic lymphocytes CD8 T cells, in addition to natural killer (NK) cells, are the main players in mediating this effect. CD8 T cells are a specialized subset of lymphocytes that provide fundamental defensive mechanisms against intracellular pathogens and tumor cells. Efficient CD8 T cells priming requires three main signals: stimulation of T cell receptor (TCR) with major histocompatibility complex (MHC) class I peptide that is presented by antigen presenting cells (APCs), engagement of stimulatory receptors CD28 with CD80/86, and secretion of cytokines such as IL-12 and interferons. Activated CD8 T cells are recruited to the tumor site in response to various secreted chemokines such as CXCL9, 10 and 11 (74). The interaction between TCR and the antigenic-peptide MHC leads to destroying target cells (tumor cells). The cell killing mechanism is elicited by granule exocytosis, which involves releasing perforin and granule-associated enzymes (GZM), or via the death ligand/death receptor system (74).

In addition to co-stimulatory signals, co-inhibitory signals are also expressed by activated CD8 T cells. This normal physiological mechanism helps maintain homeostasis and prevent excessive immune response (74, 75). One of these is the expression of PD1

(75). This immunomodulatory mechanism is propagated in cancer to evade the anti-tumor immune response of CD8 T cells (75). High PD-L1 expression will induce T cell apoptosis in mechanisms that involve dephosphorylating kinases in TCR signal, PI3k downregulation, induction of Smad3 and inhibiting Bcl-xl expression (76). Therefore, agents that target either PD1 or PD-L1 have been shown to have an enhanced effect on CD8 T cells trafficking, activation and anti-tumor response.

Role of macrophages in tumor progression

Macrophages are part of the innate immune defense system and play a major role in regulating tumor progression. These highly plastic myeloid immune cells provide a set of immune defense functions that help maintain hemostasis in tissues, including wound healing following tissue damage and resolving and mounting infection (77). Cancer causes excessive vasculature and tissue damage that creates a high inflammatory microenvironment (78). One of the major causes of this excessive inflammation is due to the high infiltration of macrophages and other leukocytes during the tumor progression. These infiltrating leukocytes are capable of switching between two states, classically activated macrophages (M1) that exhibits anti-tumorigenic properties, or they polarize to an M2 phenotype, which is associated with more pro-tumorigenic effects (77). During tumor progression, tumor-associated macrophages (TAMs) are educated by the TME and skewed away from the M1 towards M2 phenotype. M1 phenotype is characterized by high IL-12, inducible nitric oxide synthase (iNOS), and high tumor necrosis factor alpha (TNFα) (77). These reactive oxygens and nitrogens along with inflammatory factors confer immune response that facilitates tumor cell killing. Conversely, M2 state is

characterized by high IL-10, Arginase1 (Arg1), and mannose receptor c-type 1 (Mrc1) known as or CD206. These factors promote the pro-tumorigenic effect by aiding tumor invasion and suppressing other effector immune cells (77). However, the concept of M1/M2 phenotype is not a black and white, and growing evidence suggest that these leukocytes are plastic and can express markers from both phenotypic category. In vivo, this plasticity is highly complex due to the variety of external stimuli and the complexity of the tumor microenvironment (77). An increasing amount of evidence suggests that TAMs express high PD1, and that expression correlates with lower phagocytic activities and higher pro-tumorigenic effects (79). TAMs also express PD-L1, which further contributes to an immunosuppressive TME. Inhibiting PD1/PD-L1 axis reverses this phenotype and triggers macrophage-mediated antitumor activity (79).

Signaling transduction mediated by non-receptors tyrosine kinases in immune cells

Role of Src Family Kinase (SFKs) in regulating T cells immune response

The response of innate and adaptive immune systems to stimuli is regulated by a complex network of intracellular signal transduction pathways. The activation of T cell immune response relies primarily on lymphocyte-specific tyrosine kinase (Lck) for early activation and propagation of TCR pathways (80). Lck belongs to the family Src family kinases (SFKs) that are expressed in epithelial, immune cells and a wide range of other cells. After antigen recognition bound to MHC, propagating TCR-CD3 signal relies on the phosphorylation by Lck at specific sites on immunoreceptor tyrosine-based activation motif (ITAM). Phosphorylated ITAMs recruit zeta-chain-associated protein kinase of 70

kDa (ZAP70), which is also phosphorylated by Lck. Activated Zap70 will eventually induce multiple downstream signaling pathways, phospholipase CΥ1 (PLCΥ1), MAPK and JNK activation, that regulate T cell response (80). Normally, Lck is bound to the plasma membrane at its N-terminal structure. It contains Src homology 2 and 3 (SH2 and SH3) domains followed by a kinase domain and a short C-terminal region (80). Lck activity is strictly regulated by a combination of phosphatases and kinases. Phosphorylation of Lck at its C-terminus (Tyr505) by the C-terminal Src kinase (Csk) causes a molecular arrangement that locks the kinase domain in an inactive conformation (81). This inhibitory phosphorylation can be also dephosphorylated by the tyrosine phosphatase CD45. In contrast, phosphorylation of the active site (Tyr394) promotes an active conformation loop that allows Lck to interact with Zap70 and TCR (814). This activating phosphorylation is also subjected to dephosphorylation by the SH2 domain-containing phosphatase-1 (SHP-1). In an inactive state, CD45 predominantly downregulates Lck by increasing Tyr505, and upon TCR activation, Lck segregates from CD45 and favors dephosphorylation of the inhibitory tyrosine (Tyr505) (81).

Evidence suggests that PD1, after PD-L1 or PD-L2 binding, can, directly and indirectly, inhibit TCR signaling. PD1 recruits SHP2, and this directly dephosphorylates Zap70 and the co-stimulatory receptor CD28, which indirectly inactivates Lck (82). This indicates that Lck is required for efficient TCR signaling, and by suppressing it, T cell's immune response is lost (83). In preclinical studies, interferon-Υ (IFN-Υ) and IL-2 secretion, along with pLck expression, were markedly decreased in Lck inhibitor-treated T cells (84). In one study, the SFKs tyrosine kinase inhibitor dasatinib was used as a pharmacological control switch for chimeric antigen receptor (CAR) T cell therapy (85).

Mice harboring B16.OVA melanoma tumors and treated with dasatinib had increased PD1 expression on their CD8 T cells (86). Several clinical trials combining Src inhibitors with anti-PD1/L1 agents are undergoing for the treatment of different malignancies. Currently, Src inhibitors are clinically used for some hematological malignancies including lymphoid and myeloid leukemias, and being tested for other types of malignancies (87).

Role of Syk in regulating the macrophage inflammatory response

One of the main non-receptor kinases that orchestrate signaling transduction pathways in macrophages is the spleen tyrosine kinase (Syk) (88, 89). Syk is 72 kDa non-receptor tyrosine kinase that consists of two tandem repeat of SH2 and a kinase domain (89). Mammalian cells also express another Syk family kinase named Zap70 (89). While both members share the same structure, Zap70 shows low homology to Syk in the amino sequence and its expression is highly restricted in other adaptive immune cells (T cells and NK cells). Ten autophosphorylation sites have been reported in Syk. These different phosphorylation sites have been shown to differentially regulate Syk biological activities, among those that are critical for propagating its downstream signaling are the two phosphorylation sites located in the kinase domain (Tyr519 and Tyr520) (89).

Although functions of Syk have been widely investigated in adaptive immune cells, its functions in the innate immune system have also been shown. Syk plays an important role in macrophage-mediated inflammatory response (89). Macrophage, after recognition of pathogens by pathogen recognition receptors (such as TLRs), initiates a series of signaling cascades that begins with the recruitment of Syk to TLR4. Activation of Syk subsequently induces downstream signaling molecules, such as AKT, p85 and

NF-κB, resulting in the induction of inflammatory genes such as iNOS, COX2 and TNF-α (89). Syk also binds to the activated ITAMs, when phosphorylated by SFKs. This binding leads to conformational changes of Syk, resulting in consequent autophosphorylation of Syk and phosphorylation by the SFK Lyn (89). Activated Syk will then transduce its signaling cascades downstream by activating several substrate proteins involved in immune responses. The phagocytic function of macrophages derived from Syk-deficient mice was significantly abrogated (90). This indicates the importance of Syk in maintaining the macrophage's defense mechanisms and its tumoricidal effects.

Immunomodulatory roles of EGFR TKIs

Accumulating evidence suggests that tumor intrinsic oncogenic alterations can modulate the TME and negatively affect the anti-tumor immune response. For example, upregulation of Wnt-β-catenin signaling, loss of p53 and PTEN tumor suppressor's function, and overexpression of Myc were all shown to negatively impact the immune-mediated cell killing mechanisms (91). In lung cancer, EGFR signaling has been shown to mediate and stabilize PD-L1 expression. EGFR TKIs decrease PD-L1 expression in NSCLC cell lines (92). In a recent high-throughput screening study, EGFR inhibitors were identified as one of the potent molecules that enhance antigen-specific cytotoxic T cells tumor killing. The EGFR TKI erlotinib worked synergistically with the PD-1 inhibitor in EGFR-mutant lung cancer mouse model (93). EGFR targeted therapies have been extensively shown to upregulate MHC expression in tumor cells (95). However, these tyrosine kinase inhibitors often exhibit significant unintended effects on other

kinases such as SFKs and Syk that are important for immune cells function. In Jurkat cells (human T cells), gefitinib suppressed the Syk kinase ZAP70, Lck, MAPK and Akt (96). Erlotinib has been also shown to inhibit T cell proliferation and activity through downregulation of MAPK and Akt pathways. IL-2 and IFN-ϒ were significantly reduced by erlotinib treatment in a dose-dependent manner (97). Dacomitinib, besides targeting HERs, has also shown an inhibitory effect against Src and Lck in vitro assay (98). Collectively, these observations suggest that while EGFR TKIs potently inhibit oncogenic signaling in cancer cells, they might also have an immunomodulatory role by negatively affecting important kinases in immune cells.

Exploring new treatment strategies to tackle NSCLC

The landscape of lung cancer treatment has progressed rapidly in the past two decades. Advances in molecular studies helped to gain insights into the major oncogenic alterations in lung cancer. This led to the discovery of targeted agents that specifically counteract these oncogenic pathways. Lung cancer treatment is tailored based on the genetic makeup of the tumor. EGFR, ALK, and ROS1 mutant tumors are treated with targeted agents that specifically inhibit these oncogenic proteins. However, their efficacies are only limited to those with the mutations, missing the majority of lung cancer patients, who still show overexpression of some of those oncogenes. Other bypass mechanisms have been also shown to develop during the use of targeted therapy, such as MET or HER2 overactivation, indicating that inhibiting one pathway is more likely to be overcome by other oncogenic pathways. Combination strategies are the key to enhance therapeutic outcomes. In EGFR-mutant NSCLC, clinical trials evaluating the

combination of anti-VEGF with EGFR inhibitor did show an improved efficacy compared to EGFR inhibitor alone (99). In another clinical study, patients treated with chemotherapy plus EGFR inhibitor did better than EGFR alone (100). Several other studies are undergoing to evaluate the combination of MET targeted agents with EGFR inhibitors in NSCLC (24).

Another major breakthrough in treating lung cancer is the discovery of the immunotherapeutic agents PD1/L1 inhibitors. These agents provided durable responses and high anticancer activity in lung cancer patients, even in those with unknown mutations that weakly respond to targeted agents (71, 72). However, the response rate with PD1/L1 inhibitors, when used alone, is less than 29% in NSCLC patients (101). PD-L1 expression was identified as the major predictive biomarker for these agents. Patients with high PD-L1 are more likely to respond compared with low expression (29). Other important factors are tumor mutational burden and the tumor-infiltrating lymphocytes counts (102). To increase the response rate, different combination strategies have been explored, including combining Anti-PD1/L1 with anti-VEGF (which is a highly immunosuppressive growth factor expressed in TME), or with cytotoxic chemotherapeutic agents (which increase tumor immunogenicity). These combination strategies did increase the response rate, even among those who are insensitive to PD1 agents alone (low PD-L1) (103). This suggests that targeting multiple tumorigenic factors is better than one and will provide improved efficacy in a large subset of NSCLC patients.

Previous reports demonstrate that ER-HER network contributes to poor outcomes in NSCLC. These two pathways communicate with each other to provide sustainable

oncogenic signaling even when one of them was pharmacologically interrupted (61). Along with the effects on cancer cells, estrogen signaling has been shown to play a role in modulating the TME toward more immunosuppressive phenotypes in ovarian cancer, where ER signaling enhances MDSCs activity in vivo (104). E2 promotes M2 phenotype in macrophages in preclinical models of breast cancer (105). In lung cancer, a high throughput screening identified the estrogen antagonist fulvestrant as the top hit molecule that showed enhanced immune-mediated cell killing (106). However, broad-spectrum HER TKIs have shown several off-target effects that include critical tyrosine kinases in immune cells (SFKs and Syk). This could attenuate the immune response and promotes an immune exhaustion phenotype that could be reversed by anti-PD1. The antitumor effect mediated by targeting ER-HERs network in lung cancer cells can be further augmented by enhancing the antitumor immune response.

Focus of research

Our hypothesis is that targeting multiple aspects of tumorigenesis will produce better anticancer effects in lung cancer. Inhibiting the potent oncogenic ER-HERs network, using fulvestrant and dacomitinib, will have a significant anti-tumor effect. Due to the possible negative effects of the latter on kinases expressed on immune cells, stimulating immune response by anti-PD1 will further enhance the net antitumor effect in lung cancer. (**Figure 1**). This hypothesis was tested as follows:

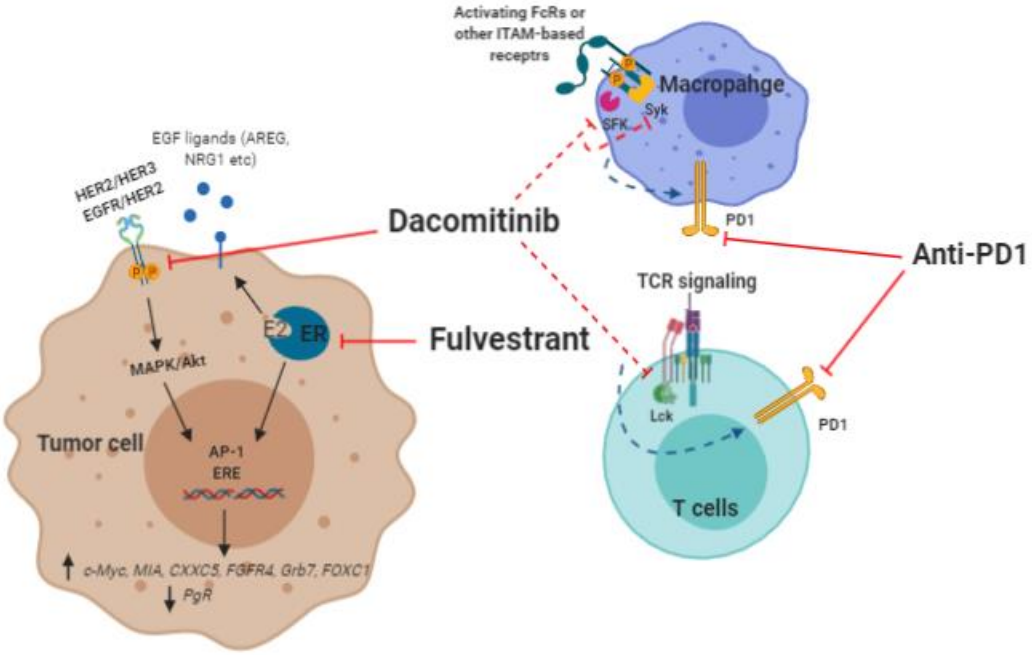

Figure 1: General model for combining anti-ER, pan-HERs with anti-PD1 agent. The bidirectional cross-talk between ER and HERs signaling confers aggressiveness of lung tumors. Blocking both pathways with fulvestrant and dacomitinib will have a potent anticancer effect and more likely to reverse the gene signature associated with poor prognosis. However, evidence suggest that dacomitinib, as a tyrosine kinase inhibitor, exhibits off-target effects against Src family kinases including Lck. This could be a limiting factor for immune-mediated tumor destruction of T cells and macrophages that can be overcome by using an immunotherapeutic agent

Chapter 3: Evaluating the anticancer effects of the anti-ER fulvestrant and the pan-HER TKI dacomitinib in human NSCLC models:

- To evaluate the antiproliferative effects of the combination of fulvestrant and dacomitinib in vitro models of NSCLC, (EGFR wild-type, EGFR-mutant and KRAS mutant), provide a mechanistic insight into the synergy, and analyze the modulation of the 7-gene model.
- To assess the antitumor effects of this combination in vivo models of NSCLC, and analyze the 7-gene model signature and HER dimerization using in situ proximity ligation technique (in situ PLA)
- To determine the survival benefits in EGFR-mutant NSCLC and analyze the development of common resistance mechanisms associated with EGFR TKIs in relapsed tumors.

Chapter 4: Assessing the immunomodulatory effects of fulvestrant–dacomitinib combination and evaluating the therapeutic potential of adding anti-PD1 to augment the antitumor effect:

- To assess the immunomodulatory effects of fulvestrant-dacomitinib on macrophage phagocytic activity and M2-phenotype induction, and assess the effects on CD8+ T cells activation and exhaustion phenotype in vitro.
- To evaluate the antitumor effects of combining fulvestrant and dacomitinib with anti-PD1 in vivo using a novel syngeneic lung cancer model FVBW17/FVB-N

Chapter 2: Materials and methods

Chemical reagents

Dacomitinib was purchased from Selleckchem (Houston, Texas). Fulvestrant was purchased form Tocris (Minneapolis, Minnesota). Both were dissolved in DMSO. Rat monoclonal blocking anti-mouse PD1 (clone RMP1.14) was purchased from BioXcell (West Lebanon, New Hampshire) prepared in InvivoPure ph 7.0 dilution buffer from BioXcell (Wes Lebanon, New Hampshire). The isotype control was rat IgG2a (clone 2A3) from BioXcell (West Lebanon, New Hampshire). Human AREG, human NRG1, mouse IFN-gamma, mouse TNF-alpha, and mouse VEGF ELISA kits were purchased from R&D Systems (Minneapolis, Minnesota). The CellTiter 96 one solution reagent (MTS reagent) was purchased from Promega (Madison, Wisconsin). Activated proetin-AP-1 and phospho-cyclic AMP response element binding (p-CREB) transcription factor ELISA kit were purchased from Active Motif (Carlsbad, California).

Cell culture

201T s human NSCLC previously derived from a patient with lung adenocarcinoma (EGFR and KRAS wild type). A549 is KRAS mutant lung adenocarcinoma cells and was purchased from American Type Culture Collection (ATCC). HCC827 is alung adenocarcinoma cell line with EGFR activating mutation (E746-A750 deletion). FBW-17 is a murine lung cancer cell line generated from FVB-N mouse with lung adenocarcinoma induced by the tobacco carcinogen (NNK), with KRAS and TP53 co-mutation. 201T and A549 were maintained in BME medium, HCC827 in RPMI medium and FVBW-17 in DMEM medium. Media were supplemented with 10% heat-inactivated

fetal bovine serum, 1X Strptomycin (Thermo Fisher) and 1X GlutaMax (Life Technologies).

Cell viability assay

Series of dose response experiments were conducted for fulvestrant and dacomitinib to assess the anti-cancer activity using CellTiter 96 reagent. Cells were plated in 96-well plates at 5000 cells/well. Increasing concentrations of dacomitinib with a fixed dose of fulvestrant (5μM)) were added to a serum starved cancer cells for 72hr. MTS reagent (5mg/ml) was added to each well and incubated for 30 minutes at 37ºC. The plates were read using Synergy microplate reader (BioTeck) at 490nm using Gene5 software. The synergy was determined by combination index (CI) using Chou-Talalay method (107) and CompuSyn software.

Isolation and culture of murine Bone Marrow-Derived macrophages

Femurs and tibia bones were obtained from a euthanized FVB-N mouse, rinsed with ethanol followed by DMEM medium. The ends of each bone were cut then flushed with DMEM medium and collected in 50mul tube. Single cell suspension was made by drawing media up and down using the syringe. Cells were centrifuged for 5 minutes at 4ºC. Supernatant was discarded and pellet containing the cells was resuspended in ACK lysis buffer (4.15g NH_4Cl, 0.5g $KHCO_3$, 0.1mM EDTA) for 1 minute. 10ml of culture medium DMEM10 medium (DMEM growth medium with 10%FBS, 1X Penicilling/Strptomycin, and 1X Glutamax). Cells then centrifuged at 1200rpm for 5 minutes and pellet was resuspended with DEME10 medium. $10X10^6$ cells were plated in 15 cm plates in a final volume of 30ml DMEM10 medium. Half of the culture medium

was replaced with a fresh DMEM10 medium on the 4th day. On day 6, the cells are confluent and ready for experiment.

Harvesting and activation of mouse CD8 T cells

CD8+ T cells were isolated from the FVB-N mouse's spleen. Spleen was cut in small parts and placed on a strainer attached to 50ml tube. The fragments were pressed through a strainer and washed by PBS. Collected cells were centrifuged for 10 minutes at 300 rcf.. Pellet was resuspended in ACK lysis buffer (2ml) for 10 minutes at 4°C. A 30ml PBS then centrifuged for 10 minutes at 300 rpm. Pellet was resuspended with culture media (RPMI + 10% FBS). CD8+ T cells were isolated using magnetic cell sorting by negative selection using CD8 T cell isolation kit (Miltenyi Biotec) following to the manufacture's protocol. CD8 T cells were activated using Dynabeads Mouse T-Activator CD3/CD28 beads (Thermos Fisher) using RPMI medium supplemented with 10% FBS for 24hr. Recombinant mouse IL-2 was added according to the manufacture's protocol for T cells expansion. Activation status was confirmed by measuring IFN-ϒ and TNF-α release by ELISA.

Immunoblotting

Cells were treated with inhibitors for indicated time points and cell lysates were prepared using cell lysis buffer plus protease and phosphatase inhibitors (1X PBS, 1% nonyl phenoxypolyethoxylethanol NP40, 0.5% sodiumdeoxylate, 0.1% sodium dodecyl sulfate and one tablet protease inhibitor/10 ml). This lysis buffer was used for cancer cells, macrophages, CD8 T cells, and tumor xenografts. Protein concentration was determined using DC assay reagent (Bio-Rad Laboratories). Cell lysates were electrophoresed on

7.5% or 12% sodium dodecyl sulfate polyacrylamide gels for 80 minutes at 100V. Then Gels were transferred into PVD membranes for 60 minutes at 100V. Membranes were blocked with 5% non-fat dry milk dissolved in TBST buffer (Tris buffered saline and polysorbate 20) for 60 minutes at room temperature. The membranes then were immunoblotted with primary antibodies overnight then washed with TBST three times (15 minutes each). Anti-rabbit IgG antibody (Cell Signaling Technology) was added for 1 hour at room temperature at 1:2000 dilution using 5% milk buffer. Blots were developed using super signal West Pico or Femto chemiluminescence substrate (Thermo Fisher). ImageJ software was used for densitometric quantifications.

Primary antibodies used for Western Blotting

Primary antibody	Dilution	Manufacture
p-EGFR (Tyr1068), Rabbit	1:1000	Cell Signaling Technology
p-HER2 (Tyr1221/1222), Rabbit	1:1000	Cell Signaling Technology
p-HER3 (Tyr1289), Rabbit	1:1000	Cell Signaling Technology
p-Akt (Ser473), Rabbit	1:1000	Cell Signaling Technology
p-MAPK (Tyr202/204), Rabbit	1:1000	Cell Signaling Technology
Cleaved caspase-3 (Asp175), Rabbit	1:1000	Cell Signaling Technology
p-c-Met (Tyr1234/1235), Rabbit	1:1000	Cell Signaling Technology

p-PTEN (Ser380), Rabbit	1:1000	Cell Signaling Technology
p-Syk (Tyr525/526), Rabbit	1:1000	Cell Signaling Technology
p-Src family (Tyr416), Rabbit	1:1000	Cell Signaling Technology

ELISA assays

For in vitro experiments, conditioned media for treated cells were collected at the indicated time points. Cell quantification was performed for normalization before samples were added to ELISA protocol. ELISA was performed according to the company's protocol. For in vivo experiments, three tumors per treatment group were harvested and lysed together in lysis buffer. Protein concentration was determined using DC assay reagent. A 100 μg per sample were used in triplicates for ELISA assay.

Macrophage phagocytic activity

Bone marrow derived macrophages (BMDMs) were cultured at a density of 8000 cells/well using 8-chamber slide. On the next day, BMDMs were treated with DMSO, fulvestrant, dacomitinib or combination for 6hr. The phagocytic activity was assessed using Phagocytosis Assay Kit (IgG FITC) from (Cayman chemical) according to the manufacture's protocol. Briefly, after 6hr treatment of treatment, latex beads (FITC complex) were added to each group at final dilution of 1:250 and incubated with the cells for 2 hours at 37ºC. Cells were washed with assay washing buffer followed by counterstaining with Hoechst 33342 staining (40μM) for 10 minutes. After two washes

with assay washing buffer, BMDMs were visualized at 20X magnification with a fluorescence microscope (Leica DM 4000B LED microscope) using LAS4.7 software.

Real Time Quantitative Polymerase Chain Reaction (RT-qPCR)

To analyze mRNA expression, Trizol reagent (Invitrogen) was used to extract RNA extraction following manufacturer's protocol for both in vitro and in vivo samples. RNA (1 µg) was reverse transcribed using cDNA synthesis kit from Quanta Biosciences following the company's protocol. A thermal cycler (Bio-Rad) was used to aid the cDNA synthesis. RT-qPCR was performed using SYBR Green Super Mix on CFX connect Real-Time System (Bio-Rad). Primers were synthesized at Biomedical Genomic Center at the University of Minnesota. The housekeeping gene Glyceraldehyde 3-phosphate dehydrogenase (*GAPDH*) and human 28S ribosomal RNA (*28S*) were used as internal controls for in vitro and in vivo mRNA expression and the ratio of normalized mRNA to the control gene was determined using comparative DCT method for analysis. Primer sequences are:

Target	**Forward**	**Reverse**
Human *28S*	5'-CAGTTCTCTTGGGAATCCAG-3'.	5'-TTCAGCAAAGGAGTCAATCCAC-3'.
Human *GAPDH*	5'-AGCCACATCGCTCAGACAC-3'	5'-GCCCAATACGACCAAATCC-3'.

Mouse *GAPDH*	5'GGAGCGAGATCCCTCCAAAAT-3'	5'GGCTGTTGTCATACTTCTCATGG-3'
NRG1-β1	5'-GCCAGGAATCGGCTGCAGGT-3'	5'AGCCAGTGATGCTTTGTTAATGCGA-3
AREG	5'GTGGTGCTGTCGCTCTTGATA-3'	5'ACTCACAGGGGAAATCTCACT -3'
c-Myc	5'AATGAAAAGGCCCCCAAGGTAGTTATCC-3',	5'GTCGTTTCCGCAACAAGTCCTCTTC-3'
CyclinD1	5'-GCTGCTAAGTGGAAACCATC-3'	5'CCTCCTTCTGCACACATTTGA -3'
FGFR4	5′CTGTGGCCGTCAAGATGCTCAA-3′	5′ATGTTCTTGTGTCGGCCGATCA-3′
CXXC5	5′CGGTGGACAAAAGCAACCCTAC-3′	5′CGCTTCAGCATCTCTGTGGACT-3′.
MIA	5′-CAT GCA TGC GGT CCT ATG CCC AAG CTG-3′	5′-GAT AAG CTT TCA CTG GCA GTA GAA ATC-3′
PgR	5'AGCTCATCAAGGCAATTGGTTT-3'	5'ACAAGATCATGCAAGTTATCA AGAAGTT -3'
Grb7	5′- AGGAAACTTCGAGAGGAGGA-3′	5′TTGGACTCGTTCACATCTGC-3′
FOXC1	5' GGCGAGCAGAGCTACTACC 3'	5'TGCGAGTACACGCTCATGG 3'

ERβ	5’-CCCTGCTGTGATGAATTACAG -3’	5’-CGGTTCCCACTAACCTTCC -3’
Aromatase	5’-CACATCCTCAATACCAGGTCC-3’	5’CAGAGATCCAGACTCGCATG -3’
IL-1β	5’TTCTTCGACACATTGGATAACG -3’	5’TGGAGAACACCACTTGTTGCT-3’
Mouse *IL-10*	5’-CTG GAC AAC ATA CTG CTA ACC G-3’	5’-GGG CAT CAC TTC TAC CAG GTA A-3’
Mouse *CD206*	5’CAGGTGTGGGCTCAGGTAGT 3’	5’TGTGGTGAGCTGAAAGGTGA 3’
Mouse *Pdcd1*	5’- ATGTGGGTCCGGCAGGTACC-3’	5’TCAAAGAGGCCAAGAACAATGTC3’
Mouse *PD-L1*	5’GACCAGCTTTTGAAGGGAAATG 3’,	5’CTGGTTGATTTTGCGGTATGG 3’
Mouse *IL-12*	5’-TGGTTTGCCATCGTTTTGCTG-3’	5’ACAGGTGAGGTTCACTGTTTCT-3’

Flow cytometry analysis

After treating macrophages and CD8 T Cells with fulvestrant and dacomitinib, cells were collected in FACS tube at $1X10^6$ in 100µl of PBS. Fc blocking antibody was added at 1µl/one million cells for 15 minutes at 4°C. Cells were then washed with FACS buffer (PBS + 2%FBS and 5mM EDTA). Cells were stained for 30 minutes on ice with viability dye (eFluor 780), anti-F4/80 BV785, anti-PD1 FITC and anti-CD8 APC. After incubation, cells were washed with FACS buffer and resuspended in FACS buffer

supplemented with 0.5% paraformaldehyde (PFA) at a final volume of 0.5ml. Cells were analyzed for cell surface markers expression using LSR Fortessa cell sorting machine and FACsDiva software.

For tumor and spleens flow cytometric analysis, we used Ficoll-Paque isolation media (Thermo Fisher) to separate mononuclear cells including lymphocytes and monocytes. Briefly, tumors and spleens of tumor bearing mice were collected from three individual mice per treatment group. Tumors were mechanically dissociated into small pieces using razor blades and incubated with 1x collagenase (Sigma Aldrich) and 1x DNase I (Invitrogen) for 30 minutes in the incubator at 37Cº 5% CO2, with periodic mixing. Spleens were only incubated with digestive enzymes buffer for 10 minutes. Tissues then were filtered through a filter strainer and washed with RPMI media containing 10% FBS. Cell count was performed and samples were separated to 2 FACS tubes with equal volume of FACS buffer (T cells and myeloid cells panels). Fc blocking was performed as described above and samples were stained with two panels:

T cells panel (CD45/CD3/CD8/PD1):

1- Anti-mouse CD45 APC-eFluor 780; eBiosciences
2- Anti-mouse CD3e PerCP-Cy5.5; BD Biosciences
3- Anti-mouse CD8a monoclonal antibody Super Bright 600; eBiosciences
4- Anti-mouse CD279 (PD1) FITC; Biolegend

Myeloid panel (CD45/CD11b/F480/CD206):

1- Anti-mouse CD45 APC-eFluor 780; eBiosciences
2- Anti-mouse CD11b APC; BD Biosciences

3- Anti-mouse F480 monoclonal antibody Alexa Fluor 700; Thermos Fisher

4- Anti-mouse CD206 PE; Biolegend

Fluorescence Minus One (FMO) tubes were used for data interpretation.

In vivo animal studies

For tumor xenografts, female nude mice (4 to 6 weeks old) were subcutaneously injected in the flank with $1X10^6$ cells (A549, 201T or HCC827) at 100µl volume with Maetrigel (1:1). After 2-3 weeks where the tumors reached 200 mm^3 in volume (calculated from the formula = (length x $width^2$)/2 by calipers. For syngeneic mode, female FVB-N mice were subcutaneously injected in the flank with $0.5x10^6$ FVBW-17 cells. After one week, mice were randomized into 4 groups; Isotype IgG control (250 µg intraperitoneal dose twice a week), fulvestrant (30 mg/kg subcutaneously twice a week)-dacomitinib (10 mg/kg daily through oral gavage), anti-PD1 (250 µg intraperitoneal dose twice a week), triple therapy. Mice were randomized into 4 groups; placebo, fulvestrant (30 mg/kg), dacomitinib (10 mg/kg) and combination. Mice were treated for 2-3 weeks. All experiments were approved by the University of Minnesota Institutional Animal Care and Use Committee. Mice were treated and sacrificed according to the institutional guidelines.

The synergy for drug combination was assessed by combination ratio method, as previously described (108). Fractional tumor volume (FTV) is defined as mean tumor volume of the treatment group divided by the mean in the control group. The combination ratio was calculated as: (FTV of fulvestrant x FTV of dacomitinib)/ FTV of combination. A ratio > 1 indicates synergy, < 1 indicates antagonism.

Immunohistochemistry (IHC) analysis

Resected tumors were prepared in blocks that were formalin-fixed and paraffin-embedded and cut in 5µm sections. Slides were deparaffinized and rehydrated with xylene and ethanol. Slides Antigen retrieval was performed in microwave for 20 minutes using sodium citrate based unmasking solution. Slides then were incubated with 3% hydrogen peroxide fort 15 minutes to block endogenous peroxidase. Sections then were blocked with the blocking buffer (1-10% goat serum in PBS) for one hour at room temperature. Slides then were incubated with primary antibodies overnight in cold room (4°C). The second day, slides were washed three times with PBS then a secondary antibody was added (anti-rabbit IgG Vector Laboratories). Sections were developed with 3,3'-diaminobenzidine solution (DAB) and counterstained with hematoxylin (Fisher chemicals). Staining was visualized using Leica DM 4000B LED microscope and LAS4.7 software. Three individual tumors per group were used for the analysis and blindly scored as low (< 30% of the fields stained positive), moderate (30-60% of the fields stained positive) or high (>60% of the fields stained positive).

Primary antibody	**Dilution**	**Manufacture**
Ki67, Rabbit	1:1000	Abcam
c-Myc, Rabbit	1:1000	Abcam
PR, Rabbit	1:1000	Abcam
p-EGFR, Rabbit	1:1000	Cell Signaling Technology
p-HER2, Rabbit	1:320	Cell Signaling Technology
p-HER3, Rabbit	1:1000	Cell Signaling Technology
p-c-Met	1:320	Cell Signaling Technology

In situ Proximity Ligation Assay (*in situ* PLA)

Detecting HER dimerization was performed on A549 FFPE blocks using Duolink kit (Sigma). After deparaffinization and rehydration process, slides were incubated with antigen retrieval solution in microwave for 20 minutes. Peroxidase activity was quenched using 3% of H2O2. Following the company's protocol, slides were blocked in a humid chamber for 30 minutes using the blocking buffer provided with the kit. Slides then incubated overnight in cold room with primary antibodies (mouse p-HER2, 1:1000; Themo Fisher) and (rabbit p-EGFR, 1:250; Cell Signaling Technology) or (rabbit p-HER3, 1:50; Cell Signaling Technology). PLA probes incubation, ligation and detection were performed per protocol. Slides were dehydrated and mounted with coverslip, then visualized using bright field microscope.

Statistical analysis

In vitro experiments were conducted at least twice. Data were reported as standard deviation (SD) or standard error of the mean (SEM). Significance was determined by two tailed Student's *t* test and ANOVA tests when p values < 0.05. IHC experiments were analyzed for statistical significance by Chi-square and Fisher's exact tests to compare the frequency of low, moderate and high staining scores.

Chapter 3: Evaluating the anticancer effects of combining fulvestrant and dacomitinib in NSCLC

Introduction

Preclinical and clinical studies support a role for the ER pathway in lung cancer progression (58). ERβ and aromatase expression were both overexpressed in lung tumor tissues compared to healthy tissues in more than 60% of NSCLC (58). High expression of both predicted worse survival in both female and male patients (58). Estrogen can be synthesized locally in lung tumor tissues via aromatase enzyme (CYP19A1) (58). Pro-tumorigenic effect of estrogen is largely mediated by the non-genomic pathway of the cytoplasmic ERβ compartment, where the cross-talk with growth factor receptors takes place (61). Bidirectional communication between ER and EGFR has been previously shown, and drugs that inhibit both pathways demonstrated preclinical and clinical efficacy (61).

In a recent report, genes contained in the prediction analysis of microarrays 50 (PAM50) have provided prognostic information in two large cohorts of NSCLC patients with high ERβ expression (65). The PAM50 signature is extensively used in breast cancer as a prognostic tool. In these two cohorts of NSCLC patients, ERβ expression was defined as having an Allred score of greater than 1 when analyzed by immunohistochemistry. Within the 50 genes, seven genes, when analyzed together, have demonstrated correlation with progression free survival. In high risk patients who have showed poor survival outcomes, six genes were upregulated (*c-Myc, MIA, CXC5, FGFR4, GRB7,* and *FOXC1*) and one gene was downregulated (*PgR*) (65). The 7-gene model predicted one interacting network that includes ERβ and HER2/HER3 signaling,

suggesting that these two pathways provide potent oncogenic signaling that confer poor outcomes in NSCLC. It also suggests that targeting both pathways might hold promise in treating lung cancer patients.

The first aim of the thesis is to evaluate the anticancer activity of combining the ER antagonist fulvestrant with the pan-HER TKI dacomitinib using in vitro and in vivo models of human NSCLC. Fulvestrant is currently approved for the treatment of ER-driven breast cancer and dacomitinib is approved for first-line treatment of EGFR-mutant NSCLC (48). While previous clinical trials comparing EGFR TKI (gefitinib or erlotinib) with or without fulvestrant have shown some clinical activities, neither of those TKIs strongly acts on HER2/HER3 signals. The outcomes could be further improved if a pan-HER TKI was used in combination with fulvestrant.

In this aim, we analyzed the synergy between fulvestrant and dacomitinib in three different models of NSCLC; EGFR-mutant, EGFR wild-type and KRAS mutant. The latter two models are intrinsically insensitive to EGFR TKI alone. The combination showed synergy in all the three models with combination index (CI) values > 0.5. in addition, only the combination reversed the gene signature associated with poor outcomes, suggesting both pathways are contributing to aggressive lung tumors. In vivo, the combination showed synergy, prolonged the survival of mice harboring the EGFR-mutant tumors, and prevented the development of two resistance mechanisms commonly associated with EGFR TKI in lung cancer. The data presented in this chapter have been published by Almotlak and colleagues in Journal of Thoracic Oncology (109).

Results

Fulvestrant plus Dacomitinib produced potent synergistic anticancer effects in NSCLC cell lines

In these in vitro studies, we sought to determine the antiproliferative effects of fulvestrant and dacomitinib in three different NSCLC cell lines that represent three different categories of NSCLC patients; EGFR wild-type (201T), EGFR-mutant (HCC827) and KRAS mutant (A549). We measured the cell growth of the three cell lines using MTS assay after single or double treatments. The combination of 5μM fulvestrant and 10μM dacomitinib (in A549 and 201T) and 10nM dacomitinib (in the HER inhibitor sensitive cell lines HCC827) significantly suppressed the percentage of viable cells compared to DMSO control of single treatment in all the three cell lines (**Figure 2 A**). The synergy between the two inhibitors was measured by determining combination index (CI), using Chou-Talalay method and calculated by CompuSyn software. Fulvestrant alone showed moderate anticancer effects. For this reason, we combined a fixed dose of fulvestarnt (5μM) with various concentrations of dacomitinib. The dual therapy showed potent synergistic effects in inhibiting cancer cell proliferation. The range of Ci values was 0.1 and 0.6. (**Figure 2 B, D, C**). Based on the Talalay's method, CI value < 1 indicates synergy, = 1 indicates additive effect, and > 1 indicates antagonism. These data suggest that inhibiting ER signaling could enhance pan-HER TKI activity in NSCLC. The bidirectional cross-talk between ER and HER could be an escaping mechanism for the cells to overcome the effect of either agent alone, supporting the notion of combining both inhibitors together for maximal anticancer effect.

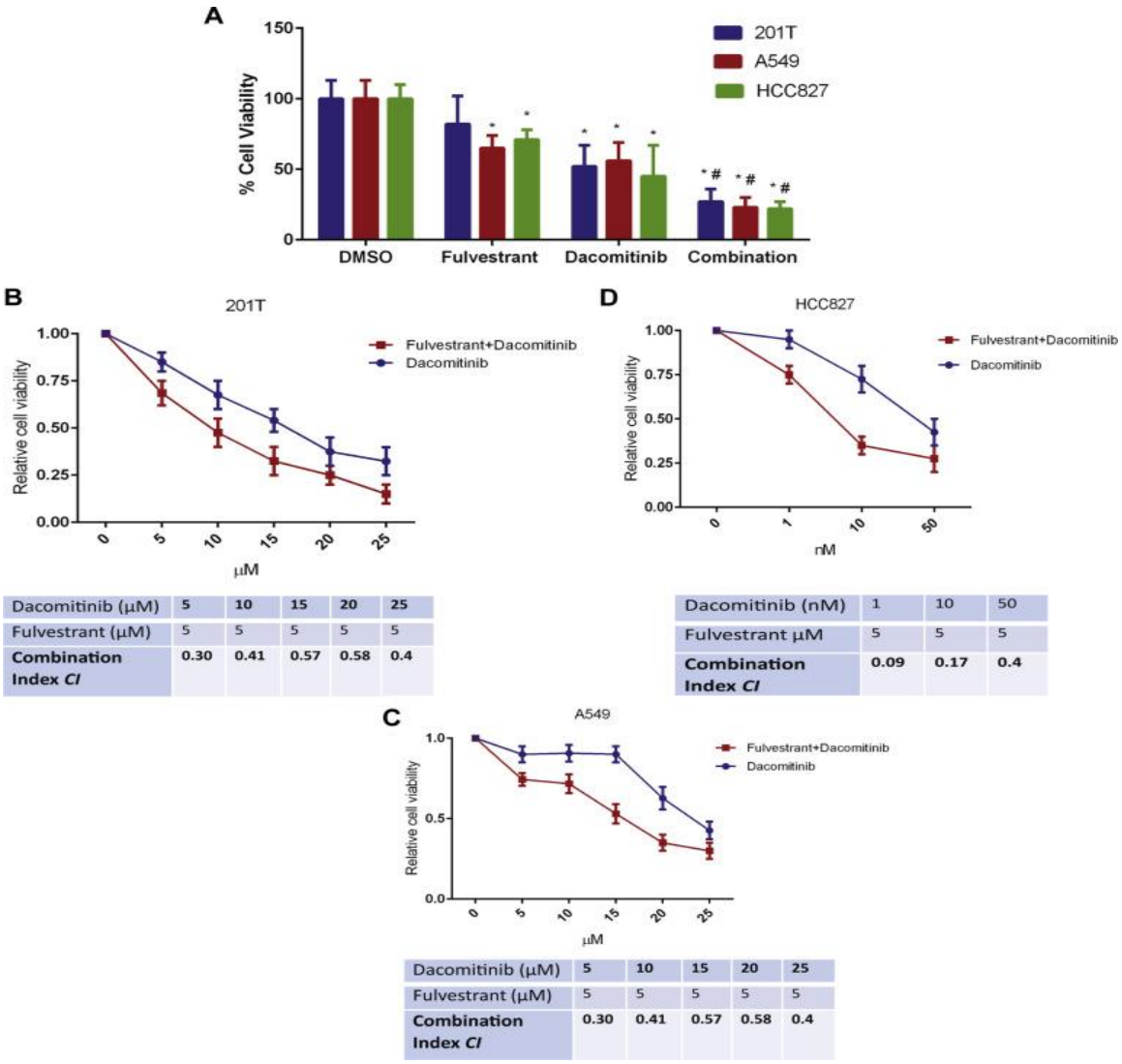

Dacomitinib (μM)	5	10	15	20	25
Fulvestrant (μM)	5	5	5	5	5
Combination Index *CI*	**0.30**	**0.41**	**0.57**	**0.58**	**0.4**

Dacomitinib (nM)	1	10	50
Fulvestrant μM	5	5	5
Combination Index *CI*	**0.09**	**0.17**	**0.4**

Dacomitinib (μM)	5	10	15	20	25
Fulvestrant (μM)	5	5	5	5	5
Combination Index *CI*	**0.30**	**0.41**	**0.57**	**0.58**	**0.4**

Figure 2. Effect of fulvestrant and dacomitinib on NSCLC cell proliferation. *A*, Cell viability examining the growth of 201T, A549, and HCC827 after single or dual treatment. Cell proliferation was measured using CellTiter96 Aqueous One Solution and results are presented with the mean SD of three individual experiments with eight samples per experiment. The statistical significance was determined by two-tailed Student's *t* test considering $p < 0.05$ as significant (* compared to DMSO and # to single treatments). *B-D*, Effect of fulvestrant (5 μM) on the antiproliferative activity of dacomitinib at various concentrations of dacomitinib in 201T, A549, and HCC827. Synergistic effect was measured by using combination index (CI) as indicated for each cell lines. CI < 1 is synergistic and CI > 1 is antagonistic. Statistical significance was considered when $p < 0.05$ (* compared to placebo, # to single treatments).

Combining fulvestrant with dacomitinib induced greater inhibition of HER signaling in NSCLC cells

Previously published observations demonstrate that the pro-tumorigenic effect of E2 is largely mediated by membrane-based estrogen signaling (non-genomic pathway) (61). E2 has been shown to induce EGF ligands that transactivate EGFR and subsequently MAPK in NSCLC cell lines (61). We showed that E2 can also induce HER2 and HER3 activation and promote AREG and NRG1-β1 release (**Figure 3 A, B, C**). The latter strongly binds to HER3. These rapid phosphorylation events mediated by E2 could lead to HER homo or heterodimerization. After treating the cells with dual inhibitors, we observed a significant decrease in HERs phosphorylation in all the three cell lines. These inhibitory effects were accompanied by decreased downstream activation of MAPK and Akt (**Figure 4 A**). These data suggest that part of HERs activity is mediated by E2, and inhibiting both pathways strongly downregulate HERs oncogenic signaling.

As previously described, inhibiting ER signaling with fulvestrant upregulated EGFR expression, and the EGFR TKI gefitinib induced ERβ expression in NSCLC cells (61). We observed a two-fold increase in NRG1-β1 and a more than three-fold increase in AREG in 201T and HCC827 cell lines after fulvestrant treatment (**Figure 4 B, C**). These compensatory effects were blocked by dacomitinib and were maintained with the combination. Measuring AREG in the conditioned media revealed a decrease in the amount of secreted AREG following the combination treatment in all the three cell lines (**Figure 4 D, E, F**). The induction of NRG1-β1 release was also blocked by dacomitinib in 201T cell lines (**Figure 4 G**). We observed also that dacomitinib induced ERβ mRNA

expression in 201T and A549 cells (**Figure 5, 6**). Fulvestrant was able to block this effect. Altogether, these data support the hypothesis that the two pathways communicate and compensate each other when one of them is blocked.

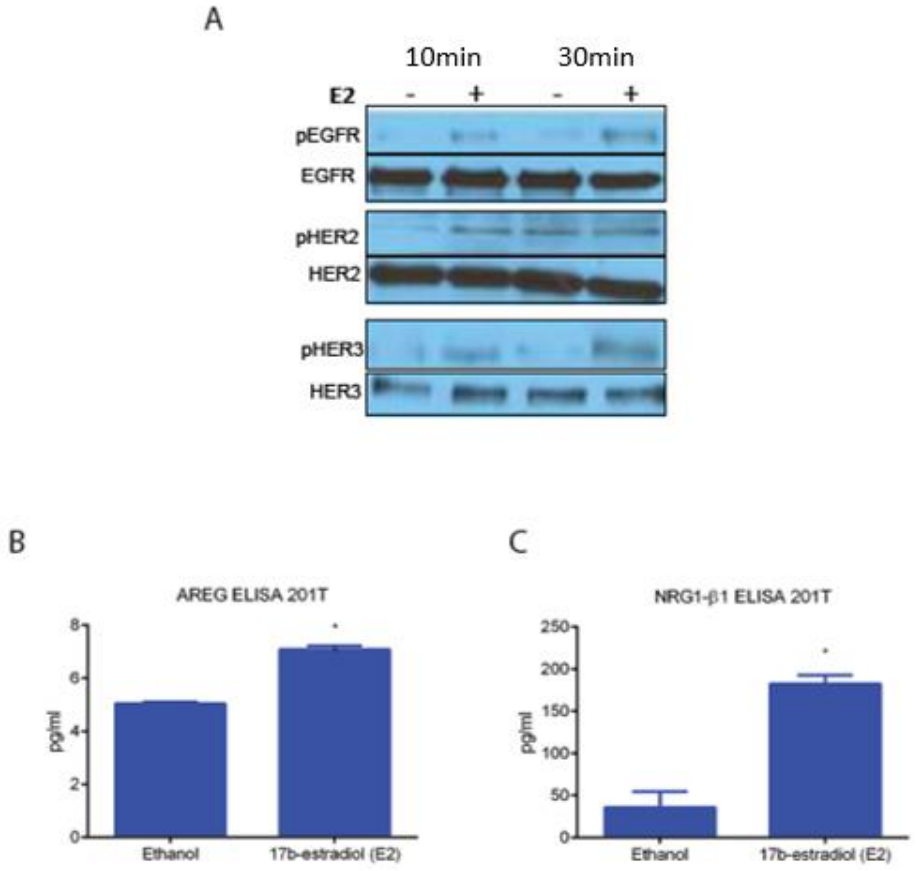

Figure 3. Estrogen rapidly induces HER activation in NSCLC cells in a ligand-dependent manner. **A**. Representative western blot showing rapid activation of phosphorylation of HER receptors following 10 and 30 minutes incubation with 17β-estradiol at 10nM. 201T cells were plated in 6-well plate for 24hr and serum starved for 48hr in phenol-red free and serum free media. Cell lysates were made and western blot was performed looking for p-EGFR, p-HER2 and p-HER3 signals and using total protein as a loading control for each one. **B**. ELISA measurement of AREG and NRG1-β1 in the conditioned media of 201T cells stimulated for 30 minutes with 17β-estradiol. A statistical significance was determined by two-tailed Student's t test and considered when $p < 0.05$ (* compared to placebo).

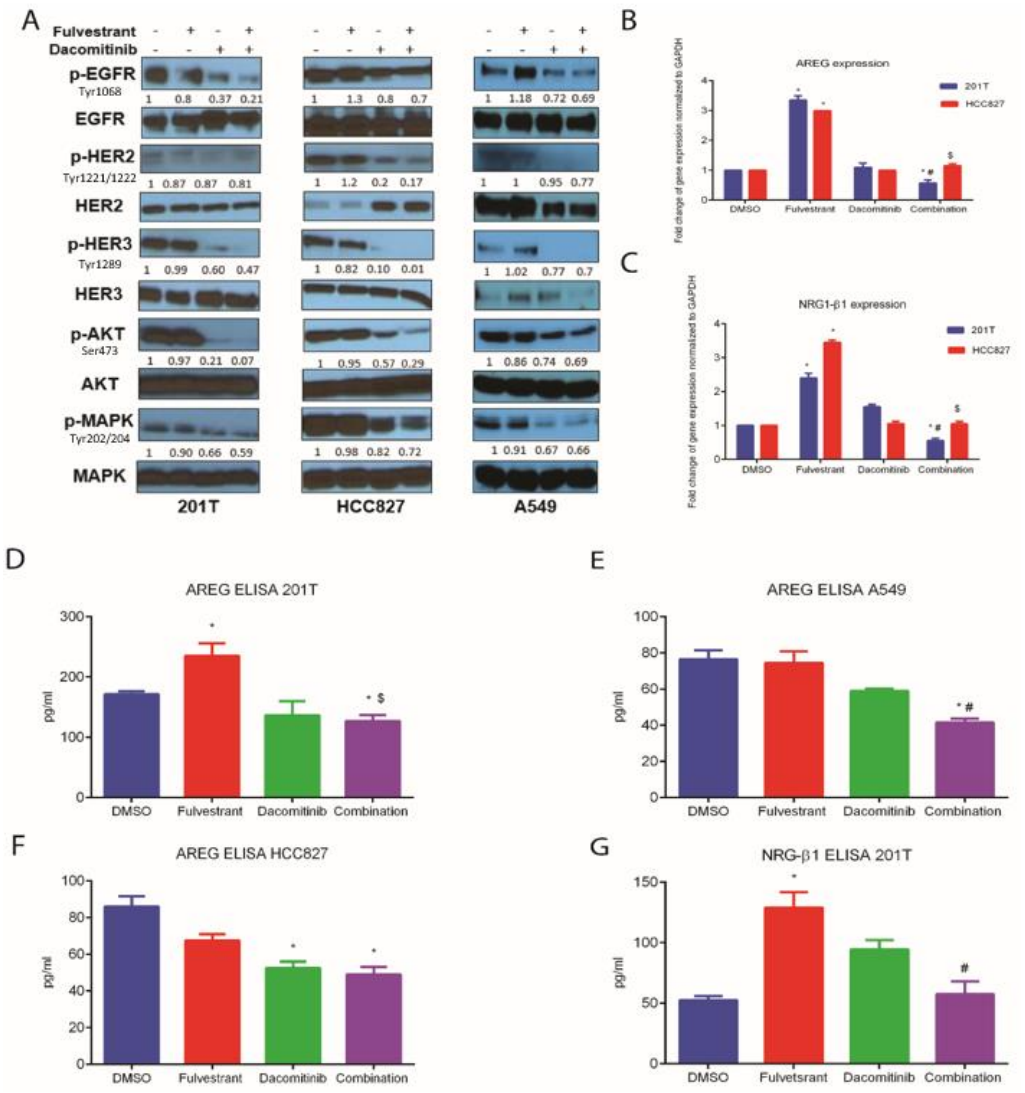

Figure 4. Effect of fulvestrant and dacomitinib on HER signaling. *A*, Immunoblotting data in 201T, HCC827, and A549 cells. Cells were treated for 6 hours with 5 μM of fulvestrant and 10 μM for dacomitinib (201T and A549) and 5 μM of fulvestrant and 10 nM of dacomitinib (HCC827). Cells lysates were immunoblotted for indicated antibodies. Densitometric measurements were corrected for the amount of total proteins as indicated. *B-G*, Effect of single or dual therapies on AREG and NRG1-β1 as detected by real-time quantitative polymerase (RT-qPCR) chain reaction and enzyme-linked immunosorbent assay (ELISA) in 201T, HCC827, and A549. Cells were treated with the inhibitors, and conditioned media and RNA were collected and subjected for ELISA and RT-qPCR to detect AREG and NRG1-β1 protein and mRNA levels. ELISA experiments were repeated twice and in triplicate for each experiment. The amount of conditioned media used was normalized to the amount of cells remained at the time of collection. The amount of mRNA was assessed by RT-qPCR using specific primers for AREG and NRG1-β1, and glyceraldehyde 3-phosphate dehydrogenase (GAPDH) was used as a control. Fold change is normalized to DMSO and statistical significance was determined by two-tailed Student's t test and considered when $p < 0.05$ (* compared to placebo, # to single treatments and $ to fulvestrant).

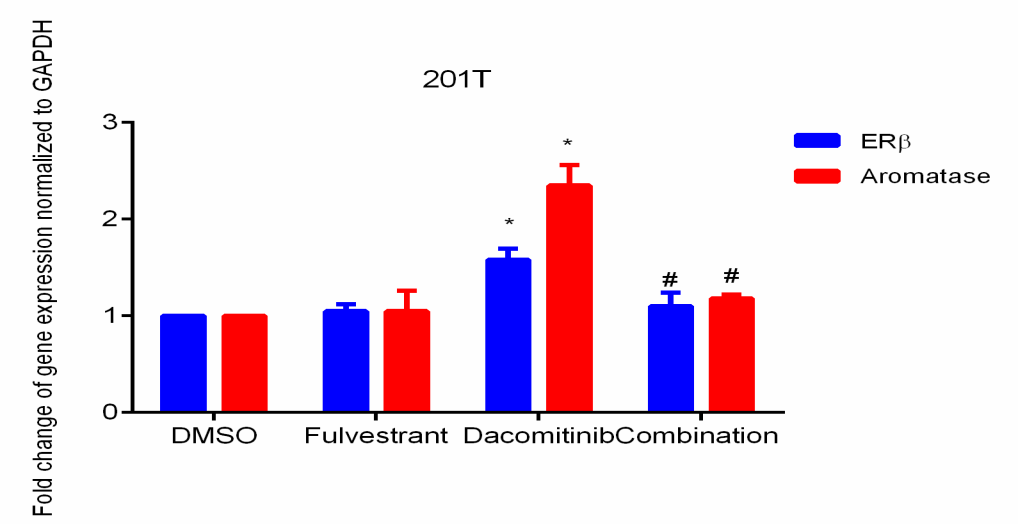

Figure 5. Targeting HER upregulates ERβ and aromatase mRNA expression in 201T. Cells were treated with fulvestrant (5μM) and dacomitinib (10μM) for 24hr. RNA was isolated using Trizol reagent and mRNA was assessed by RTq-PCR using specific primers for ER, aromatase, and GAPDH (which served as a control). Fold change is normalized to DMSO and statistical significance was determined by two-tiled Student's t test and considered when $p < 0.05$ (* compared to placebo and # compared to fulvestrant).

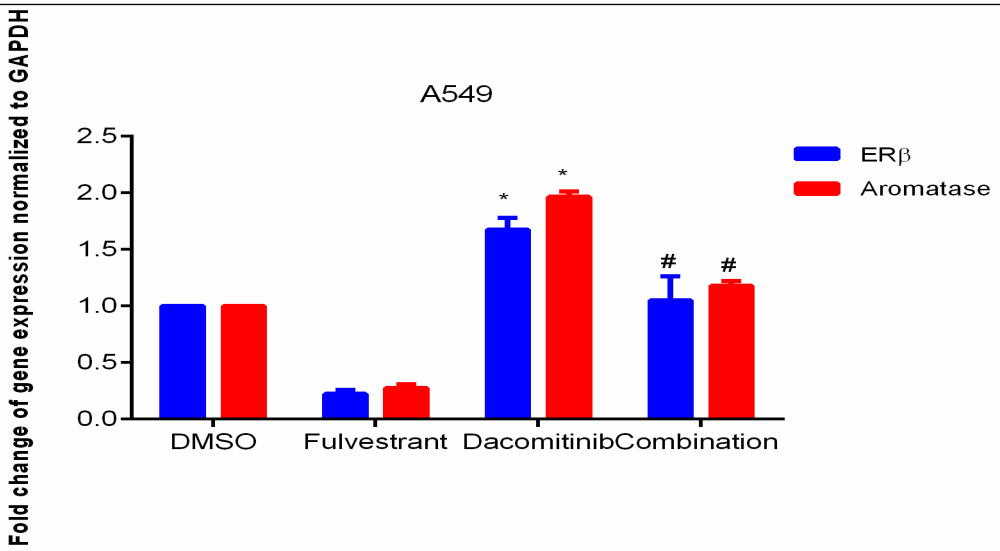

Figure 6. Targeting HER upregulates ERβ and aromatase mRNA expression in A549. Cells were treated with fulvestrant (5μM) and dacomitinib (10μM) for 24hr. RNA was isolated using Trizol reagent and mRNA was assessed by RTq-PCR using specific primers for ER, aromatase, and GAPDH (which served as a control). Fold change is normalized to DMSO and statistical significance was determined by two-tailed Student's t test and considered when $p < 0.05$ (* compared to placebo and # compared to fulvestrant).

The combination significantly downregulated AP-1/c-Fos transcription activity

AP-1 and phospho-cyclic adenosine monophosphate response element binding protein (p-CREB) are downstream effector molecules for HERs and ER. We sought to determine the effect of the combination treatment of the activity of these transcription factors in NSCLC cell lines. The combination of fulvestrant and dacomitinib significantly reduced JunB and c-Fos transcriptional activity in all the three cell lines compared to DMSO or fulvestrant alone (**Figure 7 A, B**). For p-CREB, the combination treatment slightly reduced p-CREB DNA binding (**Figure 8**). Consistent with AP-1 and p-CREB downregulation, the target genes *c-Myc* and *CyclinD1* were significantly reduced by the combination treatment in all the three cell lines (**Figure 7 C, D, E**).

The combination treatment was also effective in reversing the gene signature associated with poor outcome and aggressive disease in NSCLC patients. The combination, but not single agents, *downregulated c-Myc, MIA, CXXC5, FGFR4, GRB7,* and *FOXC1* expression, and upregulated *PgR* expression in all the three cell lines (*Grb7* and *FOXC1* were not detected in HCC827) (**Figure 7, F, G, H**). While some of the genes were modulated by single agents, only the combination reversed all the seven genes. For instance, MIA was induced by dacomitinib but inhibited by the combination treatment. To confirm this, we used two inhibitors for AP-1 and p-CREB activity to assess the changes in the 7-gene model. The c-Fos/Ap-1 (t-5224) paralleled the effect in reversing the gene signature (**Figure 7 F, G, H**), whereas the CBP-CREB (CAS92-78-4) partially affected the gene signature (**Figure 8**). These observations suggest that the combination treatment effect is largely mediated through suppression of AP-1 transcription activity.

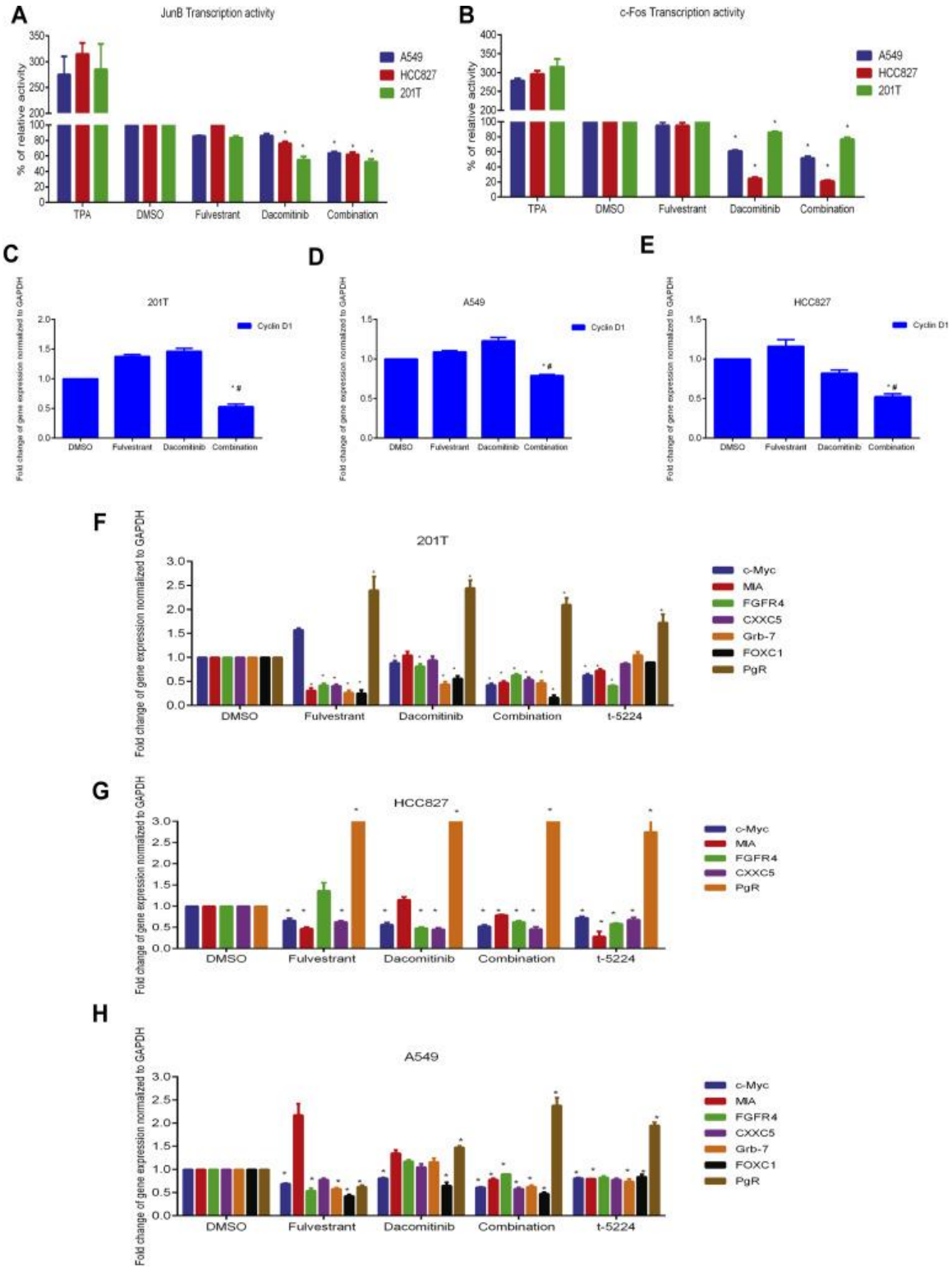
A
JunB Transcription activity
% of relative activity
A549
HCC827
201T
TPA
DMSO
Fulvestrant
Dacomitinib
Combination
B
c-Fos Transcription activity
C
201T
Cyclin D1
D
A549
E
HCC827
Fold change of gene expression normalized to GAPDH
F
201T
c-Myc
MIA
FGFR4
CXXC5
Grb-7
FOXC1
PgR
t-5224
G
HCC827
H
A549

Figure 7

Figure 7. Targeting ER and HER suppresses activator protein 1 (AP-1) transcription activity and reverses the gene signature associated with poor prognosis in NSCLC patients. The transcription activity of AP-1 was suppressed by the combination of fulvestrant and dacomitinib. *A*, *B*, The activity of c-Fos and JunB family was assessed using TransAM AP-1 kit (Active Motif) in an enzyme-linked immunosorbent assay (ELISA) – based assay. 201T and A549 cells were treated with fulvestrant (5 μM) and dacomitinib (10 μM), and HCC827 cells were treated with Fulvestrant (5 μM) and dacomitinib (10 nM) for 24 hours. Cells were harvested and nuclear extracts were isolated using Nuclear extract kit (Active Motif). Nuclear extracts (10 ug) from each treated groups were analyzed for c-Fos and JunB transcription activity. The percentage of activity is relative to DMSO (control group). The experiments were repeated twice with triplicates for each condition. Statistical significance was determined by two-tailed Student's t test and considered when *p < 0.05. *C-E*, Downregulation of *CyclinD1*mRNA expression in 201T, A549, and HCC827 cells treated with fulvestrant and dacomitinib. The mRNA levels was assessed by RT-qPCR using specific primers *Cyclin D1* and *GAPDH*. Fold change is normalized to DMSO and statistical significance was determined by Student's t test and considered when $p < 0.05$ (* compared to DMSO and # compared to single treatments). *F-H*, Targeting ER and HER pathways reversed the Prediction Analysis of Microarray 50 (PAM50) gene signature associated with worse survival in NSCLC cell lines. 201T (*F*), A549 (*G*), and HCC827 (*H*) cells were treated with fulvestrant (5 μM), dacomitinib 10 nM (HCC827), and 10 μM (201T and A549) or t-5224 (20 μM) for 24 hours. The mRNA levels were assessed by real-time quantitative polymerase chain reaction using specific primers for *c-Myc*, *MIA, CXXC5, FGFR4, FOXC1, Grb7, PgR*, and *GAPDH*. Fold change is normalized to DMSO and statistical significance was considered when *$p < 0.05$. The experiment repeated twice in duplicates.

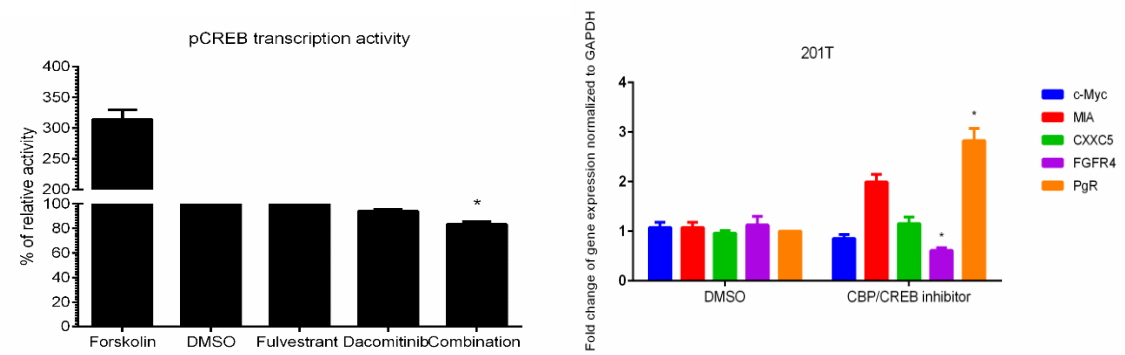

Figure 8. *Left*, Effect of the combination treatment on p-CREB activity on 201T using TransAM pCREB kit (Active motif). *Right*, Effect of the CREB/CBP inhibitor on the 7-gene model expression in 201T cell lines. The transcription activity was evaluated after 24hr treatment with fulvestrant, dacomitinib or combination. Cells were harvested and nuclear extracts were isolated. 10 μg of nuclear extracts from each treated groups were analyzed for pCREB transcriptional activity. For analyzing the 7-gene model, 201T cells were treated for 24hr with the CREB/CBP inhibitor then RNA were isolated using Trizol reagent and RT-qPCR was performed. GPADH was used as a housekeeping gene and data were normalized to DMSO for relative expression. Significance was determined by two-tailed Student's t test and considered when $p < 0.05$

The combination treatment induced tumor regression of NSCLC xenografts

We tested the combination of fulvestrant and dacomitinib in three xenografts using 201T, A549, and HCC827 cell lines. The cell lines were implemented subcutaneously in the flanks of female immunedeficient mice. Mice randomized into four groups: placebo, fulvestrant, dacomitinib, and combination and treated for 2-3 weeks. Tumors were measured by caliper three times a week. In 201T xenografts, single drugs were inhibitory, and we observed a potent antitumor effect in the combination treated group. The majority of the tumors were regressed, and when we consider any tumor volume smaller than the smallest tumor volume in the placebo group as a responder, we observed 100% response rate in the combination group, 50% in the dacomitinib group and 25% in the fulvestrant group (**Figure 9 A, B**). The average tumor volume in the combination treated group was significantly less dacomitinib ($p<0.002$), fulvestrant ($p<0.001$) or placebo ($p<0.001$).

In A549 xenografts, the combination completely suppressed tumor growth from baseline and some tumors exhibited regression up to 30% (**Figure 9 C, D**). The combination treatment antitumor effect was significantly better than dacomitinib ($p<0.012$), fulvestrant ($p<0.008$) and placebo ($p<0.0001$). In both xenografts studies, the combination treatment produced a synergistic effect as determined by combination ratio method (values > 1 indicates synergy, and < 1 indicates less than additive effects) (3.2 in 201T study and 1.27 in A549 study). Dacomitinib alone showed a potent anticancer effect in the KRAS mutant model A549. Both of the cell lines 201T and A549 with intrinsic resistance to EGFR TKIs showed enhanced sensitivity to dacomitinib when it is used in combination with fulvestrant. In HCC827 (EGFR-mutant model), both the

dacomitinib and combination treatment induced complete tumor regression (**Figure 9 E, F**). Based on tumor volume alone, the effect of the combination treatment was similar to dacomitinib alone.

After 2-3 weeks of treatment, xenografts from 201T study were resected and subjected to immunohistochemistry (IHC) analysis for the proliferation marker Ki67. We observed a marked decrease in Ki67 nuclear staining in the combination treatment group compared to single drugs or placebo. (**Figure 9 G**). The IHC scoring was defined by the percentage of tumor cells stained positive in the examined field. A Low score indicates < 30% of the field stained positive, a moderate score indicates 30-60% stained positive and a high score indicates > 60% stained positive. The Ki67 staining was low in 60% of the examined fields in the combination treatment group compared to 23% or less in the single treatment or placebo groups (**Figure 9 H**). The modulation in Ki67 was statistically significant compared to placebo or single agents as determined by a Chi square test.

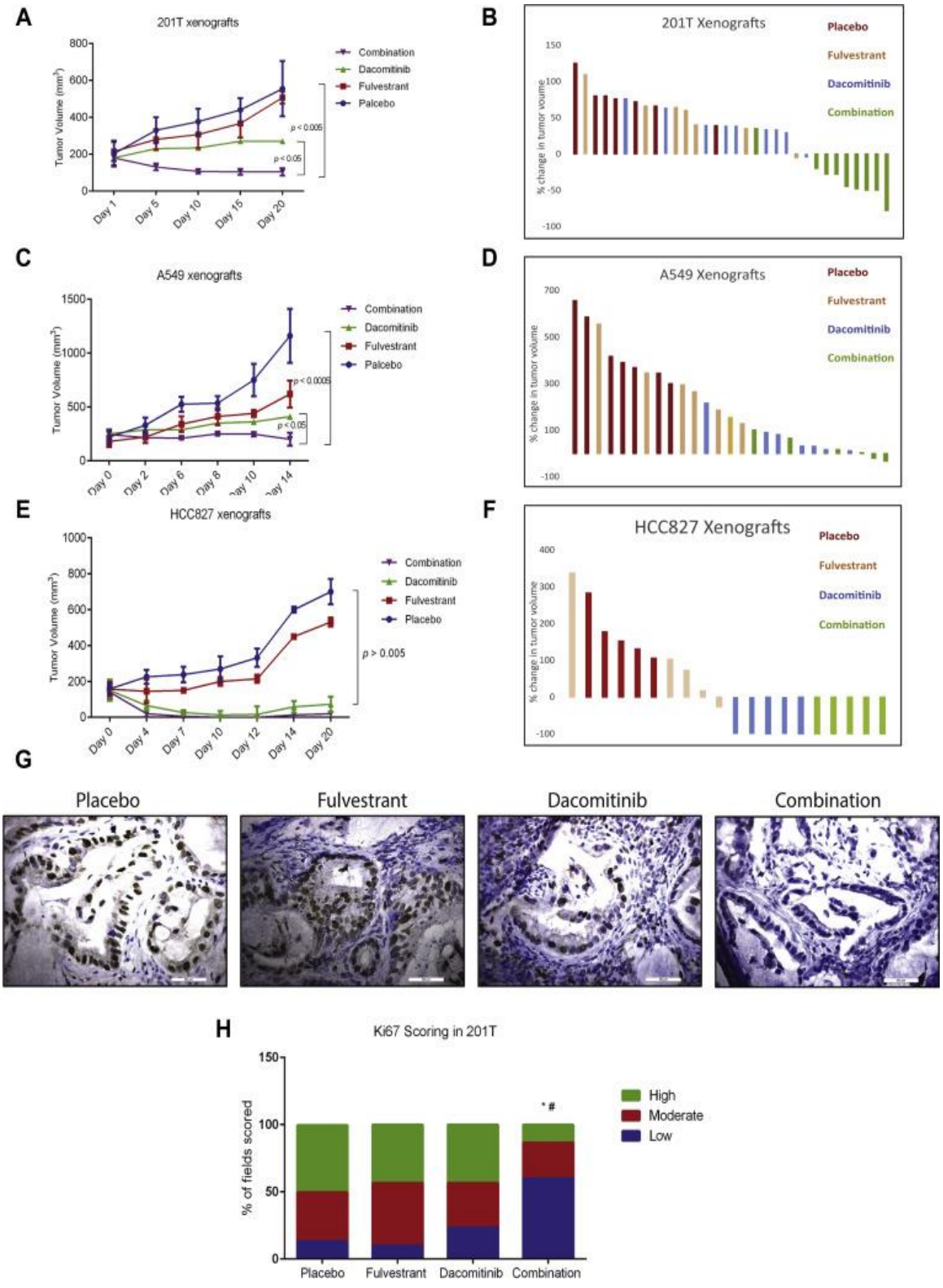
A
201T xenografts
Tumor Volume (mm³)
Combination
Dacomitinib
Fulvestrant
Palcebo
p < 0.005
p < 0.05
Day 1
Day 5
Day 10
Day 15
Day 20
B
201T Xenografts
Placebo
Fulvestrant
Dacomitinib
Combination
% change in tumor volume
C
A549 xenografts
p < 0.0005
p < 0.05
Day 0
Day 2
Day 6
Day 8
Day 10
Day 14
D
A549 Xenografts
E
HCC827 xenografts
p > 0.005
Day 0
Day 4
Day 7
Day 10
Day 12
Day 14
Day 20
F
HCC827 Xenografts
G
Placebo
Fulvestrant
Dacomitinib
Combination
H
Ki67 Scoring in 201T
% of fields scored
High
Moderate
Low
* #

Figure 9

Figure 9. The combination induces potent antitumor effect in vivo models of ERβ+ NSCLC. The combination of fulvestrant and dacomitinib induces tumor regression in vivo models of NSCLC. *A*, *C*, and *E*, Tumor volume curve showing the change in tumor size over the course of the treatment in 201T, A549, and HCC827 xenografts following the treatment with placebo, fulvestrant (30 mg/kg twice a week through subcutaneous injection), dacomitinib (10 mg/kg daily through oral gavage), or the combination for 14 to 20 days. Results represent relative mean tumor volume ± SEM of five to nine tumors per group and statistical significance was determined by two-tailed Student's t test when $p < 0.05$. *B*, *D*, and *F*, Waterfall plot showing the percentage of change in tumor volume after the initiation of treatment. *G*, Representative sections of 201T xenografts from different treatments groups stained for Ki67. Positive cells were counted in 40X magnification per fields/per tumor with low scoring (if less than 30% of tumor cells in each field stained positive), moderate (if 30% to 60% were positive), or high (if greater than 60% of the tumor cell in each field were positive). (Scale bar = 50 μM). The distribution of number of fields with each score was plotted for each treatment group. *p* values were analyzed by chi-square followed by Fisher's exact test, and values less than 0.05 were considered significant. *H*, Quantification of Ki67 labeling was performed in three individual tumors per group (* compared to placebo and # to single treatments)

To confirm the HERs downregulation observed in vitro, we analyzed tumor lysates prepared from the xenografts by immunoblotting. We observed a stronger downregulation of p-EGFR in three different tumors in the combination treated group compared to single or place groups (**Figure 10 A**), as quantified by densitometry. As a compensatory mechanism, Fulvestrant alone induced an overall increase in p-EGFR. This effect was inhibited by dacomitinib. For HER2 and HER3, we observed a downregulation of the total receptors, as quantified by densitometry relative to the loading control GAPDH (**Figure 10 A**). As a result, low levels of p-HER2 and p-HER3 were observed (**Figure 11**). Downregulation of HERs activity was also observed in A549 tumor lysates (**Figure 12**). HER4 was undetected in both studies. The combination treatment and dacomitinib treatment significantly downregulated ERβ expression (**Figure 10 A**). Interestingly, we observed a higher level of p-Akt in dacomitinib treated group compared to placebo, and the combination treatment was able to prevent this compensatory

mechanism. Both the combination treatment and dacomitinib alone decreased p-MAPK levels, with a trend of more downregulation seen in the combination group. The apoptosis marker cleaved caspase-3 was higher in the treatment group compared to single or placebo groups (**Figure 10 A**). Consistent with HERs downregulation, levels of AREG in 201T tumors, as detected by ELISA, were significantly lower in the combination treatment group compared to placebo ($p<0.003$), fulvestrant ($p<0.0032$) and dacomitinib ($p<0.004$). NRG1-β1 was not detected in 201T. In A549 tumors, AREG was not changed, but NRG1-β1 was significantly lower in the combination treatment group compared to placebo ($p<0.01$), fulvestrant ($p=0.013$) or dacomitinib ($p=0.03$) (**Figure 10 B, C**).

HER2 heterodimers are the most potent activators of HER oncogenic signaling. We assess the effect of the combination treatment on the formation of HER2 heterodimers by in situ proximity ligation technique (in situ PLA) in formalin fixed paraffin embedded (FFPE) sections. This technique has been used in breast cancer tissues to detect HER heterodimers (110). In A549 tumors, we observed a significant decrease in p-HER2/p-HER3 and p-HER2/p-EGFR heterodimers with the combination treatment compared to placebo or fulvestrant treated groups (**Figure 10 D, E**). Although both dacomitinib and the combination treated-groups have similar effect in downregulating pHER2/p-EGFR, the p-HER2/p-HER3 effect was significantly lower in the combination treated-group compared to dacomitinib in which 88% of the fields were negative (score 1) in the combination treatment compared to 33% in dacomitinib and less than 15% in placebo. These observations were confirmed when we stained the FFPE sections with p-HER2 and p-HER3 antibodies individually and observed the lowest p-HER2 and p-HER3 in the combination treated-xenografts (**Figure 13 A, B**). This potent suppression of

HER2/HER3 dimers may explain the potent antitumor effects observed with the combination treatment in vivo.

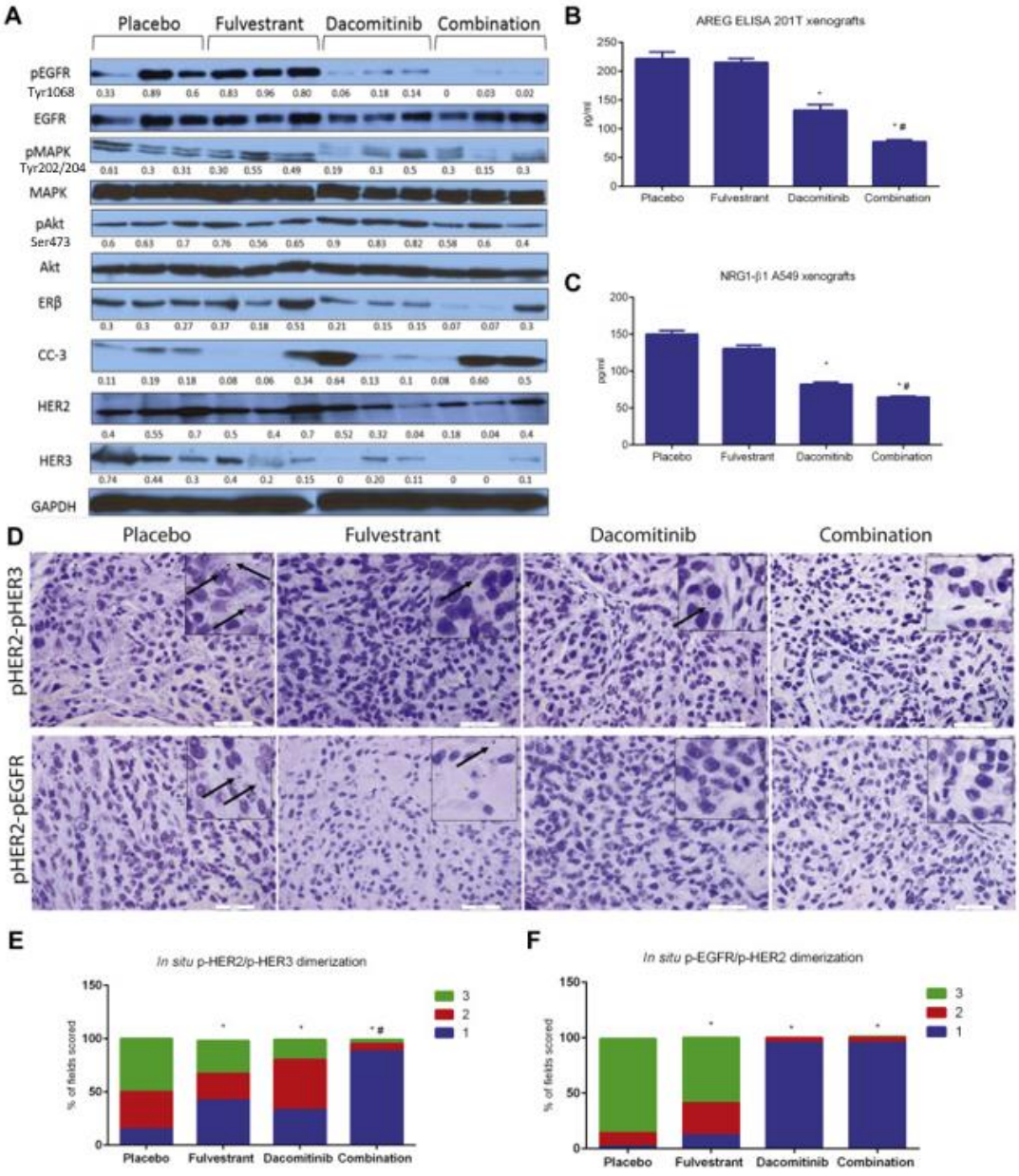

Figure 10

Figure 10. Downregulation of HER activity in 201T tumor xenografts treated with combination therapy. The combination induces global downregulation of HER signaling in 201T tumor lysates. *A*, Western blot analysis of three individual tumors per group that were harvested at the end of the study probed for different antibodies as indicated using glyceraldehyde 3-phosphate dehydrogenase (GAPDH) as a loading control and 50 μg of protein/sample. The combination treatment strongly suppresses HERs family, p-Akt, p-MAPK, and ERβ expression, and induces apoptosis though cleavage of caspase-3. *B* and *C*, The combination suppresses amphiregulin (AREG) and neuregulin beta 1 (NRG1-β1) protein expression in vivo as measured by enzyme-linked immunosorbent assay (ELISA). Protein (100 μg) from three individual tumors/per treatment group was used for AREG ELISA detection. two-tailed Student's *t* test was performed to determine significance between combination treatments; single and placebo group $p < 0.05$ was considered significant. (* compared to placebo, # compared to single treatments). *D-F*, Representative sections of A549 xenografts stained with p-HER2/p-HER3 and p-HER2/p-EGFR for detecting dimerization by in situ proximity ligation assay. Dimers (*red dots*) were counted in 40X magnification per field/per tumor. Tumors were scored 1 (negative), 2 (<15 dimers/field) or 3 (>15 dimers/field). The distribution of number of fields with each score was plotted for each treatment group. *P* values were analyzed by chi-square and Fisher's exact test, and values less than 0.05 were considered significant (* compared to placebo and # to single treatments)

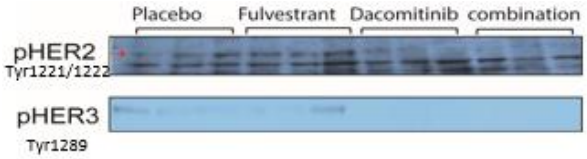

Figure 11. The combination treatment suppresses p-HER2 and p-HER3 in 201T xenografts. Representative western blotting data of three individual tumors per treatment groups.

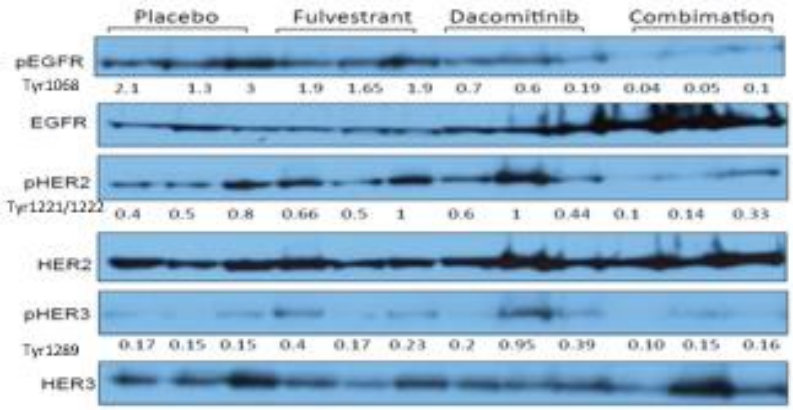

Figure 12. The combination treatment suppresses p-EGFR, p-HER2 and p-HER3 in A549 xenografts. Representative western blotting data of three individual tumors per treatment groups.

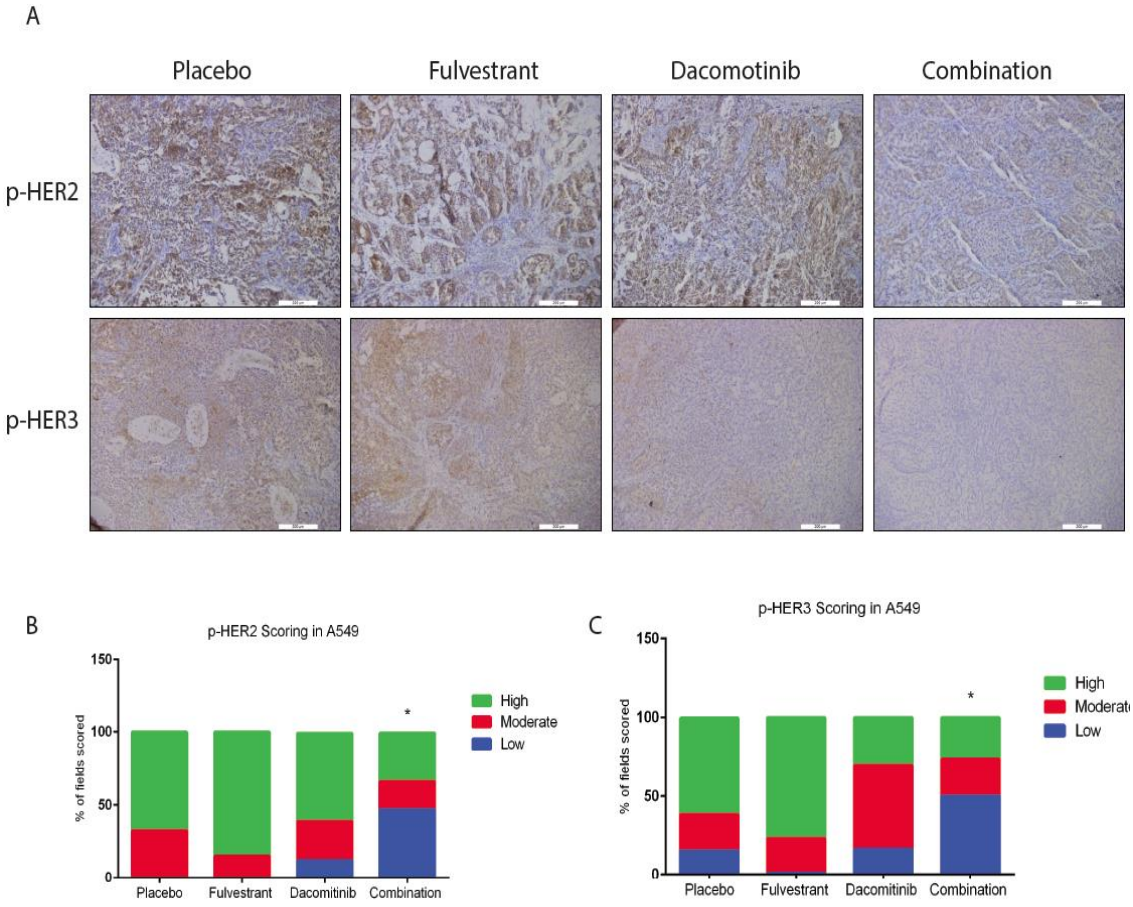

Figure 13. The combination treatment strongly suppresses p-HER2 and p-HER3 in A549 tumors. A, representative sections of A549 stained with p-HER2 and p-HER3 antibody. Quantification of p-HER2 staining (B) and p-HER3 (C) was performed in three individual tumors per group and scored to low, moderate or high scoring. * $p < 0.05$ was considered significant as measured by Chi square and Fisher test.

The combination treatment reversed the gene signature associated with poor outcome in NSCLC in tumor xenografts.

The 7- gene model signature that responded to the combination treatment in vitro was also modulated by the treatment in tumor lysates. Real-time quantitative PCR (RT-qPCR) data revealed that combination treatment produced a gene signature associated with favorable outcomes. In both 201T and A549 studies, the combination therapy but

not single agents, downregulated *c-Myc, MIA, CXXC5, FGFR4, Grb7* (detectable only in A549), and *FOXC1*, and upregulated *PgR* expression (**Figure 14 A, B**). The reversal of the gene signature was more complete with the combination treatment compared to single treatments, suggesting that both pathways are involved in modulating the gene signature.

To validate the change in mRNA, we performed IHC in 201T and A549 xenografts to analyze c-Myc and PR protein expression. Consistent with mRNA data, we observed a significant decrease in c-Myc protein expression and marked increase in PR expression (**Figure 14 C, D, E**). For example, in 201T tumors, the combination treatment significantly suppressed c-Myc expression (8.1% of fields scored high) compared to placebo (48% of the fields scored high; $p<0.005$), fulvestrant (43% of fields scored high; $p<0.005$), and dacomitinib (30.5% of the fields scored high; $p<0.02$). Higher expression of total PR was also observed in fulvestrant and combination treatment. The same observation was seen in A549 tumors (**Figure 15 A, B**) and (**Figure 16 A, B**).

Combination treatment in mice bearing HCC827 tumors altered the development of two resistance mechanisms commonly associated with EGFR TKIs in NSCLC

In HCC827 study, both dacomitinib and combination treatment induced complete tumor regression (**Figure 9 E, F**). We evaluated survival as an alternative endpoint. Treatments were stopped at two weeks and mice in each group were monitored for tumor recurrence and death. Death occurred when a mouse with a tumor reached a volume of $1000mm^3$ was sacrificed (following IACUC guidelines). Kaplan-Meier survival analysis showed an increase in survival rate in both dacomitinib (54 days) and combination treatment (59 days) compared to 9 days in placebo group ($p<0.008$ for combination; $p<0.01$ for dacomitinib) (**Figure 17 A**). However, the tumors in the combination

treatment group were necrotic, filled with fluid and composed of stromal tissue as indicated by hematoxylin/eosin, EpCam and alpha-smooth muscle actin staining (**Figure 17 B**). Tumors in the combination treatment group were less aggressive as determined by Ki67 staining (14.5% of the fields scored high) compared to placebo (55.8% of the fields scored high), fulvestrant (62.5% of the fields scored high) and dacomitinib (45.7% of the fields scored high) (**Figure 17 E**). The mRNA expression of the stem cell markers *Sox2*, *Oct4* and *Nanog* were significantly downregulated in the combination treatment group whereas fulvestrant and dacomitinib produced partial effects (**Figure 17 C**). Since HCC827 xenografts harbor EGFR activating mutation, we analyzed p-EGFR activity in the recurred tumors and found that combination treatment showed less p-EGFR staining compared to all other groups (**Figure 17 B**). We examined two major resistance mechanisms to EGFR TKIs, mesenchymal-epithelial transition tyrosine kinase receptor (c-Met) and phosphatase tensin homolog (PTEN) expression. Using IHC, we observed less p-cMet expression in the combination treatment group but not with single treatment (**Figure 17 B**). We also detected less PTEN phosphorylation (Ser380) in tumor lysates with the combination group but was slightly elevated in fulvestrant and dacomitinib (**Figure 17 D**). This phosphorylation site regulates PTEN stability and tumor suppressor function. Reduced ERβ expression was only seen in the combination treatment group (**Figure 17 D**). Along with producing a gene signature that predicts favorable outcomes, markers associated with two common resistance mechanisms were altered by the combination treatment.

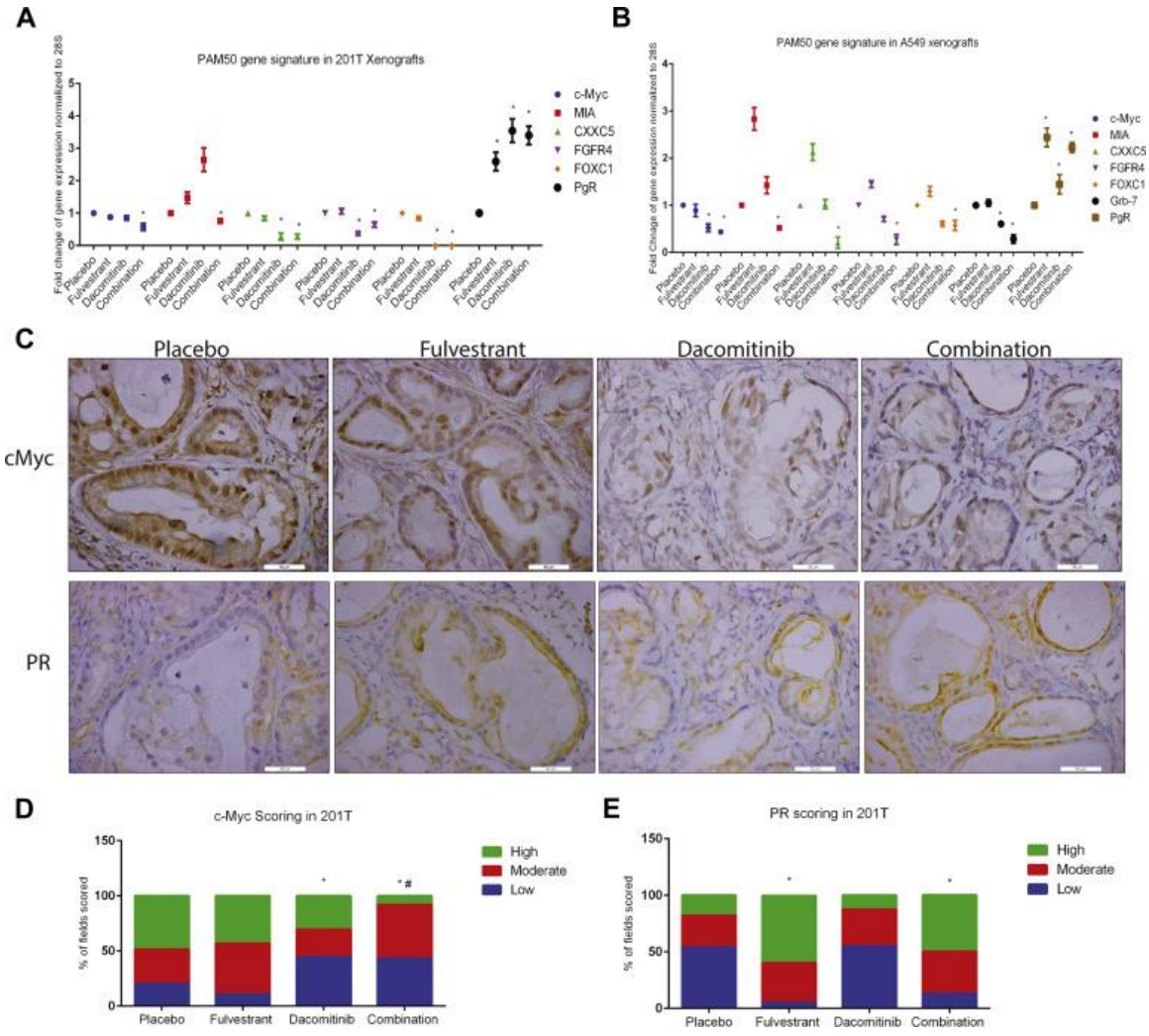

Figure 14. Targeting estrogen receptor (ER) and HER signaling produces a gene signature that predicts better clinical outcomes in vivo models ERβ+ NSCLC. Targeting ER and HER pathways promote a gene signature associated with good prognosis and better clinical outcomes. *A* and *B*, The combination treatment reversed the gene signature associated with better survival, with *c-Myc*, *MIA, CXXC5*, *FGFR4*, *FOXC1*, and *Grb7* being downregulated and *PgR* was upregulated in 201T (*A*) and A549 (*B*) tumor xenografts. Three individual tumors/group were harvested at the end of both studies and RNA was extracted using Trizol reagent. The mRNA expression was assessed by real-time quantitative polymerase chain reaction, and fold change was normalized to human *28S* ribosomal RNA (as internal control) and relative to placebo. Statistical significance was determined by two-tailed Student's t test and considered when $p < 0.05$ (* compared to placebo). *C*, Modulation of c-Myc and progesterone receptor (PR) protein expression in 201T tumor xenografts. Representative sections from each study were formalin-fixed, paraffin-embedded, and stained for c-Myc and PR (scale bar = 50 μM). *D* and *E*, Quantification of c-Myc and PR staining and statistical analysis were performed in three individual tumors per group as described in Figure 9 (* compared to placebo and # to single treatments). PAM50, Production Analysis of Microarray 50.

A

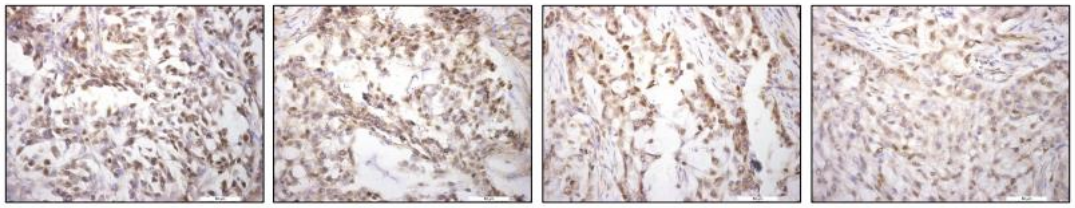

B

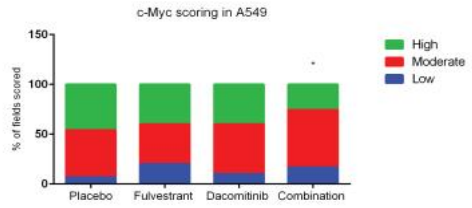

Figure 15. The combination treatment reduces c-Myc protein expression in A549 tumor xenografts. A, Representative sections of A549 tumors stained with c-Myc antibody showing a decrease in the number of positive cells labeled with c-Myc. B, Quantification of c-Myc labeling was performed in three individual tumors per group and scored to low, moderate or high scoring. * $p < 0.05$ was considered significant as measured by Chi square and Fisher test.

A

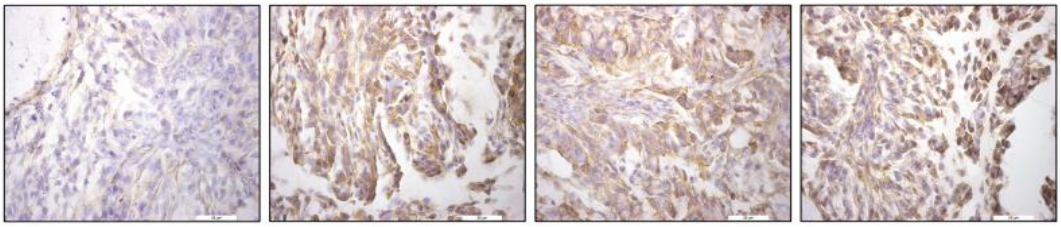

B

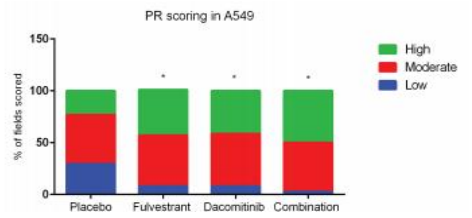

Figure 16. The combination treatment increases PR protein expression in A549 tumor xenografts. A, Representative sections of A549 tumors stained with c-Myc antibody showing a decrease in the number of positive cells labeled with c-Myc. B, Quantification of c-Myc labeling was performed in three individual tumors per group and scored to low, moderate or high scoring. * $p < 0.05$ was considered significant as measured by Chi square and Fisher test.

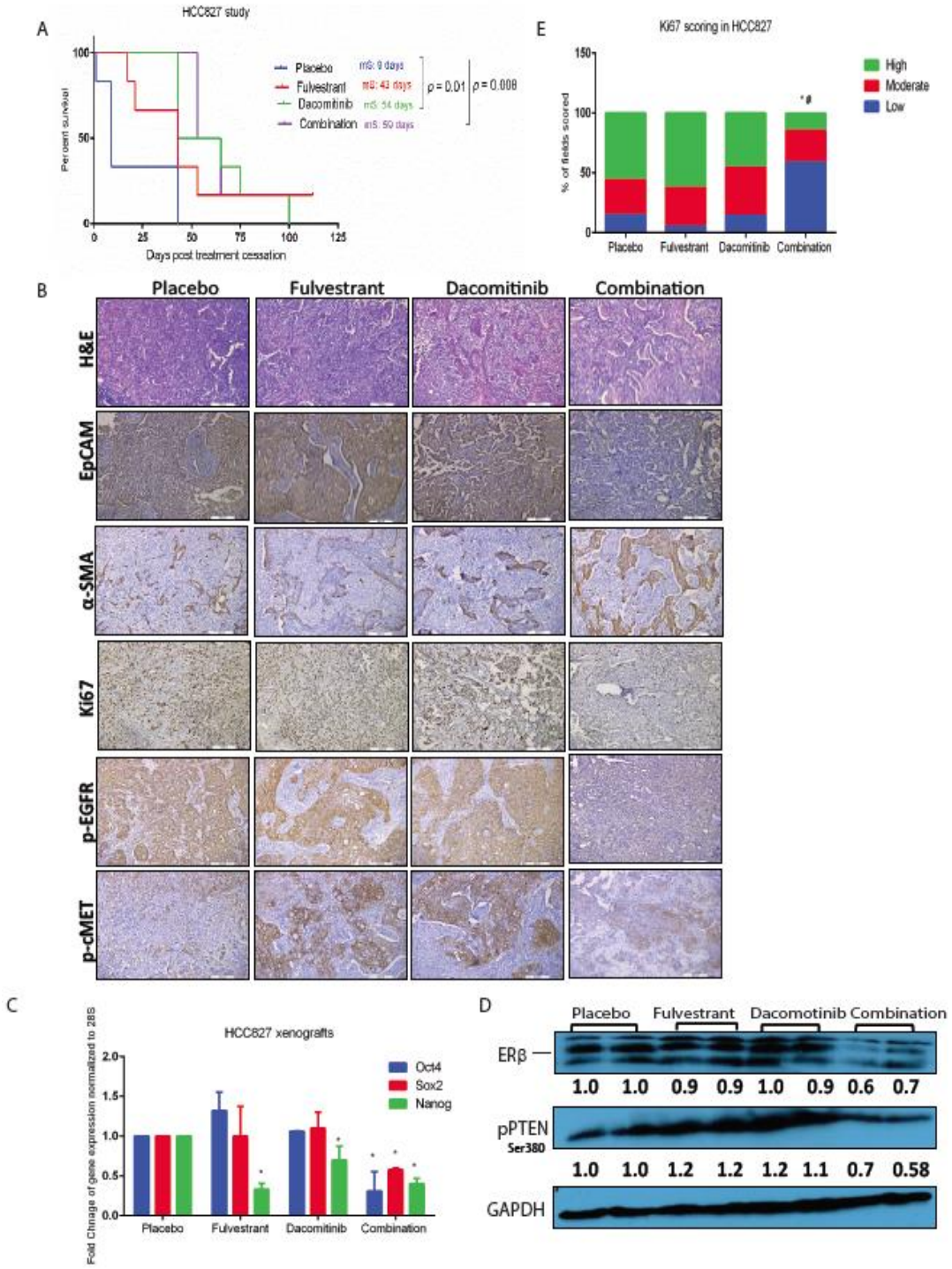
A
HCC827 study
Placebo
Fulvestrant
Dacomitinib
Combination
p = 0.01
p = 0.008
Days post treatment cessation
E
Ki67 scoring in HCC827
High
Moderate
Low
% of fields scored
Placebo
Fulvestrant
Dacomitinib
Combination
B
Placebo
Fulvestrant
Dacomitinib
Combination
H&E
EpCAM
α-SMA
Ki67
p-EGFR
p-cMET
C
HCC827 xenografts
Oct4
Sox2
Nanog
Fold Chnage of gene expression normalized to 28S
Placebo
Fulvestrant
Dacomitinib
Combination
D
Placebo
Fulvestrant
Dacomotinib
Combination
ERβ
1.0 1.0 0.9 0.9 1.0 0.9 0.6 0.7
pPTEN
Ser380
1.0 1.0 1.2 1.2 1.2 1.1 0.7 0.58
GAPDH

Figure 17

Figure 17. The combination treatment prolonged the survival of mice bearing HCC827 tumors and altered the development of two common resistance mechanisms to HER tyrosine kinase inhibitors. The combination treatment significantly reduced tumor burden and improved survival in animals engrafted with HCC827 tumor. *A*, The Kaplan Meier survival curve of HCC827 bearing mice showing significant survival advantage compared to placebo ($p < 0.008$). *B*, Representative immunohistochemistry staining for α-SMA, Ki67, hematoxylin/eosin stain (H&E), EpCAM, p-EGFR, and p-c-Met showing significant differences between combination group and single or placebo groups (scale bar = 200 μM). *D*, Western blot analysis of ERβ and p-PTEN expression in two different HCC827 tumor lysates per group showing significant downregulation of ERβ receptors and PTEN phosphorylation only in the combination treatment group. Densitometry was performed using GAPDH as a loading control. *C*, The combination treatment significantly downregulate the mRNA expression of the cancer stem cell markers *Sox2*, *Oct4*, and *Nanog* as detected by real-time quantitative polymerase chain reaction. The mRNA analysis was conducted on a mixture of cDNA of three different tumors per group and the fold change in expression was normalized to human *28S* ribosomal RNA, and statistical significance was determined by two-tailed Student's t test and considered when $*p < 0.05$. *E*, Quantification of Ki67 labeling was performed in three individual tumors per group (* compared

Conclusion

The role of estrogen signaling in lung cancer progression has been extensively studied. Preclinical studies suggested that ER pathway contributes to lung tumorigenesis through activating EGFR pathway (61). Combining EGFR inhibitor with fulvestrant showed enhanced anticancer effect in vitro and in vivo models of NSCLC (61). Clinically, a phase II clinical study showed that the combination of erlotinib and fulvestrant showed an improvement in median overall survival among all subgroups (64). The clinical outcomes could be further improved if HER2/HER3 signaling was also effectively inhibited. Our data indicate that targeting HERs with the pan-HER TKI dacomitinib in combination with fulvestrant has a better antitumor effect in preclinical models. More importantly, the potent antitumor effect is accompanied by the ability of the combination to produce a gene signature that predicts better clinical outcomes.

The cross-talk between ER and EGFR pathways is consistent with previous reports in breast cancer. Fulvestrant has been shown to modulate EGFR ligands activity in breast cancer cells (112). HER2/HER3 overactivation is one of the major mechanisms of resistance to endocrine therapy in breast cancer (63, 113). Our data indicate that fulvestrant upregulates NRG1-β1 and AREG ligands in NSCLC cells. This was abrogated by dacomitinib. In fact, the combination treatment induced significant downregulation in the AREG and NRG1-β1 expression. Clinically, higher expression of HER ligands is associated with poor outcomes in NSCLC patients receiving EGFR TKIs (114). As a result, a significant decrease in HER activity was observed in vitro and in

vivo. The marked decrease in HER2/HER3 active dimers observed with the combination treatment may explain the strong antitumor effects observed in vitro and in vivo.

EGFR TKIs are approved for first-line therapy for EGFR-mutant NSCLC. Although EGFR is overexpressed in the majority of NSCLC patients, only patients with activating mutations will respond to EGFR TKIs (34). KRAS mutation is one of the major predictors of resistance to EGFR TKIs (115). Our data suggest that combining fulvestrant with dacomitinib has a significant enhanced antitumor effect compared to dacomitinib or fulvestrant alone in EGFR wild-type and KRAS mutant NSCLC models. Recent preclinical studies demonstrated that HER2/3/4, along with EGFR, are required in KRAS mutant lung cancer, and pan-HER inhibitor could provide clinical benefit in this subset of NSCLC patients (116, 117).

As many other targeted approaches, tumors treated with EGFR inhibitors eventually develop acquired resistance via various mechanisms. Overactivation of c-Met signal is one of the major mechanisms, which rescues the cells from apoptosis induced by EGFR TKIs by transactivating other oncogenic pathways (25, 118). Evidence suggests that estrogen can induce HGF release from lung fibroblasts, which makes a positive regulator for c-Met activity (119). The bidirectional cross-talk between ER and HERs predicts that c-Met activity will be reduced by the combination of fulvestrant and dacomitinib. PTEN, the negative regulator of PI3K pathways, has been also shown to be attenuated in lung cancer (120). Phosphorylation of PTEN at its c-terminal site has been shown to negatively regulate its tumor suppressor function (120). The phosphorylation in c-tail could lock PTEN structure in a closed conformation and attenuate its catalytic activity (121). Our data showed that the combination treatment, in addition to less c-Met

phosphorylation, maintained less PTEN phosphorylation at the c-terminal residue Ser380. Recurred tumors in dacomitinib-treated group showed signs of increased c-Met activity and lower PTEN tumor suppressor function. This was similar to the observation of increased p-Akt in 201T xenografts treated with dacomitinib alone. The combination of fulvestrant and dacomitinib altered the development of both these resistance mechanisms in vivo studies.

Chapter 4: Assessing the immunomodulatory effects of fulvestrant–dacomitinib and exploring the therapeutic potential of adding anti-PD1 to augment the antitumor effects.

Introduction

Tumor microenvironment (TME) is a key determinant for tumor progression and the response to treatment. While oncogene activation and tumor suppressor gene inactivation are considered the main driving mechanisms of tumorigenesis, the reciprocal communication between tumor cells and immune cells in the TME also plays an important role in controlling tumor fate and patient outcome. In lung cancer, the immune cells comprising the TME harbor both pro-tumorigenic and anti-tumorigenic activities, and certain components of the TME may predict a patient's prognosis. It has been widely recognized that cancer oncogenic signaling and TME act together to drive tumorigenesis. Therefore, disturbing this reciprocal interaction by targeting the oncogenic network in the cancer cells and switching the TME from an immunosuppressive phenotype towards an immunostimulatory phenotype can be a powerful therapeutic strategy to treat cancer.

In lung cancer, macrophages are abundant components of the lung cancer infiltrate. They are highly plastic and display different phenotypic and functional patterns during lung tumorigenesis. Besides the tissue resident macrophages, macrophages mostly originate in the bone marrow, circulate in the blood as monocytes, and can be recruited and differentiated by the TME (77). The polarization of macrophages can be broadly categorized as classically activated macrophages, M1, with pro-inflammatory and anti-tumor functions, and alternatively activated macrophages, M2, with pro-tumorigenic functions. During lung tumorigenesis, tumor associated macrophages (TAMs) are

educated to exhibit an immunosuppressive phenotype and pro-tumorigenic properties that resemble M2 macrophages (122, 123). High expression of M2 markers such as Arginase1, CD206, PD-L1, IL-10 and PD1 is associated with reduced phagocytic and tumoricidal functions, and worse prognosis in lung cancer patients compared to M1 markers (79).

The adaptive immune cells are another major component of the TME that are critical in mediating the immune response against tumor cells. The antitumor immune response mediated by T lymphocytes, particularly CD4 and CD8 T cells, is often attenuated by the factors and cytokines secreted from the tumor that shape the TME to be more immunosuppressive (124). T cells are either excluded from infiltrating the TME, due to hypoxia and loss of tumor antigens, or they become nonfunctional exhausted infiltrates characterized by high expression of inhibitory receptors, such as PD1, and inability to produce effector cytokines, IFN-ϒ, TNF-α, and granzyme B. Additionally, recruitment of other immunosuppressive immune cells, such as MDSC or M2 macrophages, can directly or indirectly inactivate antitumor immune response mediated by T cells (125). This indicates the importance of determining the effect of any proposed therapeutic strategy on the immune cells comprising the TME.

Different pharmacological approaches targeting different mechanisms of immunosuppression have been investigated with the aim to reverse immunosuppression and restore T cell immune-mediated antitumor effects. Among these approaches is targeting PD1/L1 axis, and this approach has shown great efficacy in stimulating the antitumor immune response in various types of cancer including lung cancer. However, the efficacy of this approach as a monotherapy is limited to less than 29% of NSCLC

(101), and different combination approaches have been proposed to improve their therapeutic effects. Recently, a cocktail of two cytotoxic agents (carboplatin and paclitaxel), PD-L1 inhibitor (atezolizumab) and anti-VEGF (bevacizumab) have shown an improved efficacy and clinical outcome over PD-L1 inhibitor alone in lung cancer, and now is approved as a first-line treatment of NSCLC regardless of PD-L1 expression (100). This suggests that a combination approach that targets different drivers of oncogenesis is a key to achieve a better clinical outcome in lung cancer treatment. Additionally, new treatment approaches are desperately needed.

Our previous data showed that the targeting ER-HER network produces a potent anti-cancer effect in different models of NSCLC. The combination of fulvestrant and dacomitinib synergistically inhibits tumor growth in NSCLC models that are sensitive and insensitive to EGFR TKI, and induce a gene signature that predicts favorable outcome. While this has been tested in an immunocompromised mouse model, the effect of this combination on immune cells and the TME is unknown. Evidence suggests that EGFR TKIs have dual immunomodulatory effects and may either enhance or suppress the antitumor immune response (95, 96, 97, 98). EGFR inhibitors have been extensively shown to increase major histocompatibility complex I and II (MHC I and II) on tumor cells (95). However, broad spectrum TKIs, such as dacomitinib, may possess unwanted effects by targeting essential tyrosine kinases in immune cells, which will possibly have a negative impact on the antitumor immune response (98).

In this study, we sought to evaluate the effect of the fulvestrant-dacomitinib combination on macrophages polarization states and their phagocytic activity, and CD8+ T cell functionality. Apart from its potent anticancer effect directly on tumor cells, we

found that the combination treatment inhibited Syk activity, decreased macrophages phagocytic function, and induced M2 markers, including IL-10, CD206 and PD1. Additionally, the combination treatment downregulated Src activity, induced high PD1 expression on CD8 T+ cells, and suppressed IFN-ϒ and TNF-α secretion. These effects produce immunosuppression, which could attenuate the positive antitumor effects of the fulvestrant-dacomitinib combination. However, in a highly aggressive lung cancer syngeneic mouse model, the cocktail of fulvestrant, dacomitinib and anti-PD1 antibody potently suppressed tumor growth. The antitumor effect was better than fulvestrant-dacomitinib or anti-PD1 antibody alone and was associated with a TME with low M2 macrophages and high CD8+ T cells with low PD1, especially when checkpoint blockade was given sequentially, after fulvestrant-dacomitinib. The data suggest that amalgamation of different anticancer agents that target multiple aspects of lung tumorigenesis enhances therapeutic efficacy and is better than monotherapy approach. In particular, the ability of the fulvestrant-dacomitinib combination to enhance PD1 expression may provide a means to enhance the anti-tumor activity of anti-PD1 antibodies. Sequential triple therapy was synergistic and superior to triple therapy given together, which could also limit toxicity of multiple agents.

Results

Fulvestrant-dacomitinib combination synergistically inhibited the growth of FVBW17 murine lung cancer cell line

To study the impact of the combination treatment on immune cells either alone or co-cultured with conditioned media for cancer cells, we utilized a novel murine cancer cell line (FVBW17) generated from FVB-N mice treated with the lung specific carcinogen (NNK), as previously described (126). Genomic analysis confirmed the presence of KRAS (G12D) and TP53 co-mutations, suggesting that it is a very aggressive and highly immunogenic cell line (confirmed by Laura Stabile, PhD at University of Pittsburgh). We first confirmed the expression of ERβ and HER 1,2, and 3 receptors in this cell line (**Figure 18**). As expected, dacomitinib alone or combined with fulvestrant potently inhibits phosphorylation of EGFR, HER2, HER3, MAPK1/2 and Akt kinases (**Figure 18**). Additionally, the combination treatment synergistically suppressed the growth of FVBW17 in vitro (**Figure 19**) and produced a combination index (CI) that ranges between 0.12-0.5, indicating strong synergy, demonstrating that murine FVBW17 cells recapitulate the effects we previously published using human NSCLC cell lines.

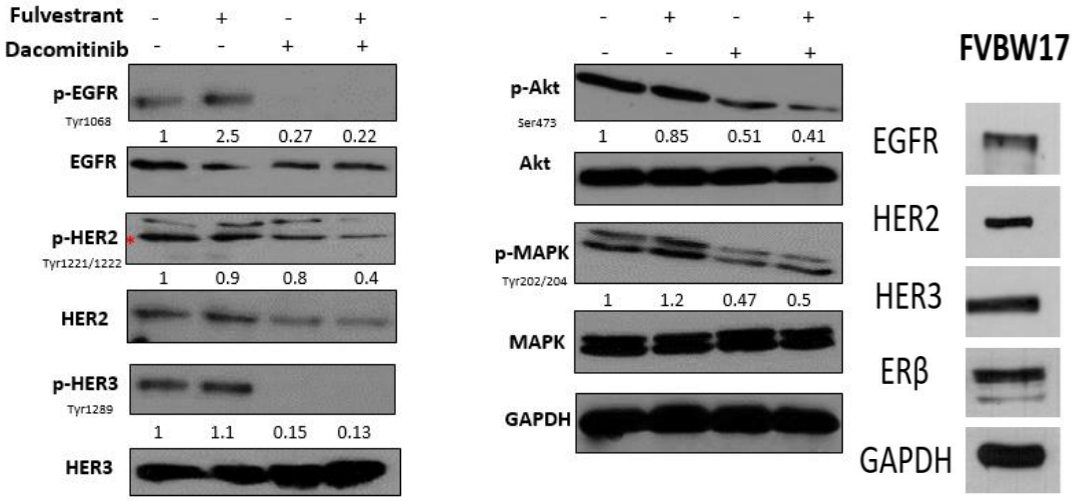

Figure 18. The combination treatment potently suppressed HERs phosphorylation in the murrain lung cancer cells FVBW17. FVBW17 cells were treated fulvestrant (5μM), dacomitinib (10μM) or combination for 24 hours. Lysates were immunoblotted with indicated antibodies, as described in chapter 2.

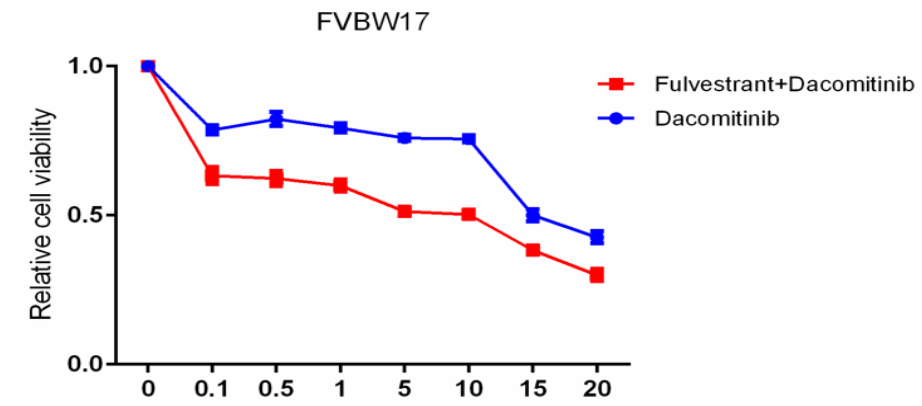

Dacomitinib (μM)	0.1	0.5	1	5	10	15	20
Fulvestrant (μM)	5	5	5	5	5	5	5
Combination index CI	0.5	0.46	0.48	0.38	0.40	0.16	0.12

Figure 19. The combination treatment synergistically reduces FVBW17 cell viability. The FVBW17 cells viability were examined using CellTiter 96 reagent after 72 hours incubation with fulvestrant (5 μM) combined with at various concentrations of dacomitinib. Combination index was calculated as described in chapter 2. CI < 1 indicates synergy.

The fulvestrant-dacomitinib treatment induced expression of M2 markers in primary murine macrophages differentiated from bone-marrow derived monocytes.

We next assessed the effect of fulvestrant-dacomitinib combination on resting state macrophages. Primary murine macrophages were differentiated from bone marrow derived monocytes as described in Chapter 2. We chose to analyze the effect of the combination on resting state macrophages (M0) to see how they will behave following treatment. M0 were treated for 6 hours with fulvestrant, dacomitinib or the combination with the same concentrations used in cancer cells. RT-qPCR showed a marked increase in PD1, CD206, and PD-L1 compared to placebo, fulvestrant or dacomitinib (**Figure 20**). We observed an 8-fold increase in PD1 expression following combination treatment compared to a 2-fold increase with dacomitinib, and 3-fold with fulvestrant. CD206 and PD-L1 were both only upregulated following the combination treatment. We then investigated how the conditioned media from FVBW17 cells treated with the combination treatment will reinstruct M0 macrophages. FVBW17 cells were treated for 6 hours with fulvestrant, dacomitinib, or combination. After 6 hours, the conditioned media containing the drugs were replaced with serum free media for 18 hours. After 24 hours, the conditioned media were added to M0 macrophages for 24 hours. Analyzing the conditioned media for immunosuppressive factors, we found that the combination treatment significantly induced VEGF release both after 24 hours of treating FVBW17 cells or in the serum free media 18 hours after 6 hours of treatment (**Figure 21**). The conditioned media from the combination treatment significantly induced PD1, CD206 and IL-10 mRNA expression (**Figure 22**). A 7-fold increase in PD1 expression was observed with combination treatment compared to a 3-fold increase in single treatment

groups. To confirm the upregulation of PD1 at the mRNA level, we double stained macrophages with F4/80 and PD1 and analyzed them by flow cytometry. The combination treatment increased the percentage of PD1 positive macrophages from 11.2% (DMSO treated) to 18.8%, while dacomitinib alone increased it to 15.8% and fulvestrant slightly increased it (12.8%) (**Figure 23**). These data suggest that macrophages treated directly with the combination treatment or with conditioned media from cancer cells show high levels of PD1 expression and evidence of enhanced M2 function and release of a pro-angiogenic growth factor, which may impair their anti-tumor function.

Phagocytosis is one of the main functions of macrophages to destroy and clear up pathogens and diseased cells. We sought to assess the phagocytic activity of macrophages treated directly with the combination treatment. Using IgG latex beads, and after 6 hours of treatment, dacomitinib alone or in combination with fulvestrant impaired the phagocytic activity of M0 macrophages (**Figure 24**). Although fulvestrant alone significantly enhanced the phagocytic activity, this effect was overcome by the addition of dacomitinib. Mechanistically, dacomitinib is known to have off-targets effects on other tyrosine kinases including Src family of kinases (98). We found also that dacomitinib alone or in combination with fulvestrant significantly reduced p-Syk (Tyr520), which is another essential kinase for macrophage immune function (**Figure 25**). These data suggest that while the combination treatment strongly suppresses the growth of cancer cells, dacomitinib may have unwanted effects on macrophages by suppressing essential kinases in macrophages, which cannot be overcome by fulvestrant.

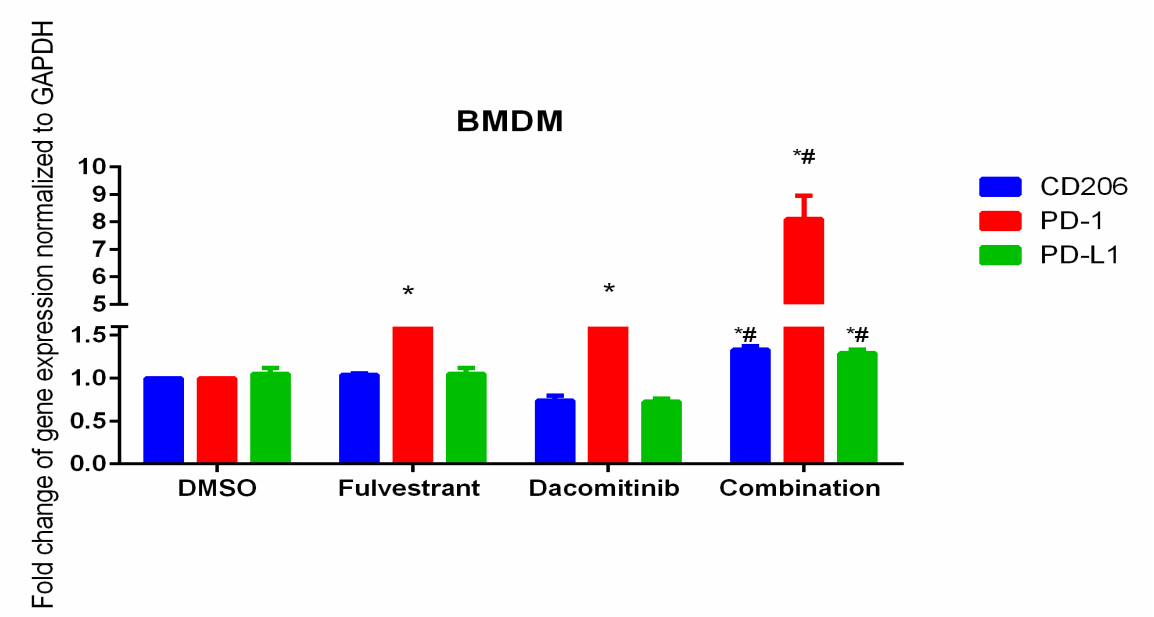

Figure 20. The combination treatment upregulates M2 markers in BMDMs. BMDMs, on resting state, were treated for 6 hours with fulvestrant (5µM), dacomitinib (10µM), or combination and RNA were isolated using Trizol reagent for RT-qPCR analysis. GPADH was used as a housekeeping gene and data were normalized to DMSO for relative expression. Significance was assessed by two-tailed Student's t test and considered when $p < 0.05$. * compared to DMSO, # compared to single treatment group.

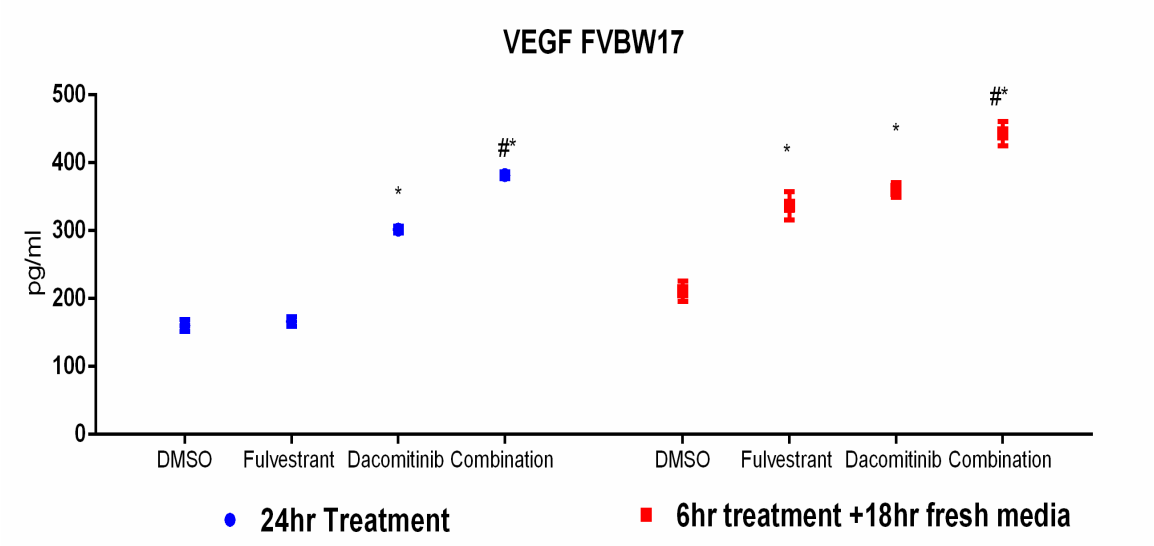

Figure 21. The combination treatment induces VEGF expression in FVBW17 cells. The conditioned media from FVBW17 that were treated with fulvestrant (5µM), dacomitinib (10µM), or combination, were analyzed by ELISA for VEGF expression at the indicated time points. Significance was assessed by two-tailed Student's t test and considered when $p < 0.05$. * compared to DMSO, # compared to single treatment group.

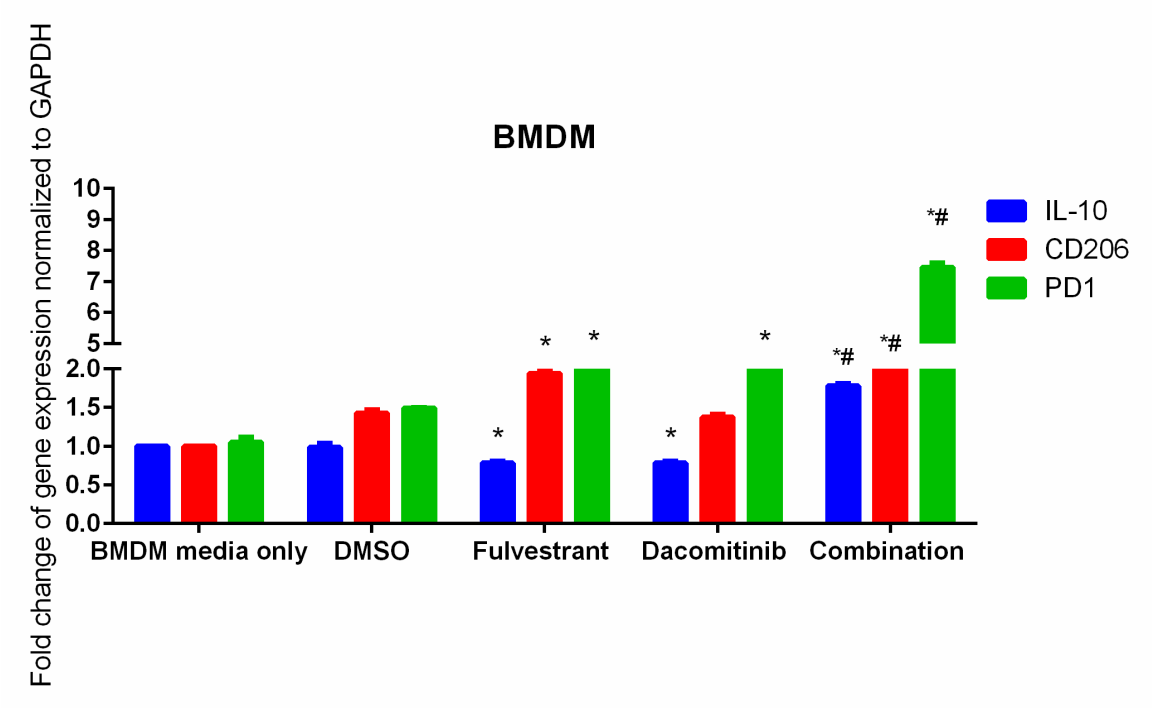

Figure 22. The effect of the conditioned media of FVBW17 treated with the combination treatment significantly induces M2 markers in BMDMs. BMDMs, on resting state, were treated for 24 hours with FVBW17 conditioned media. FVBW17 cells were treated with fulvestrant (5µM), dacomitinib (10µM), or combination for 6 hours, then the media were replaced with serum free media for 18 hours. The media collected after 24 hours were added to macrophages for 24 hours. RNA were isolated using Trizol reagent for RT-qPCR analysis. GPADH was used as a housekeeping gene and data were normalized to BMDM media only (not exposed to media from FVBW17) for relative expression. Significance was assessed by two-tailed Student's t test and considered when $p < 0.05$. * compared to DMSO, # compared to single treatment group.

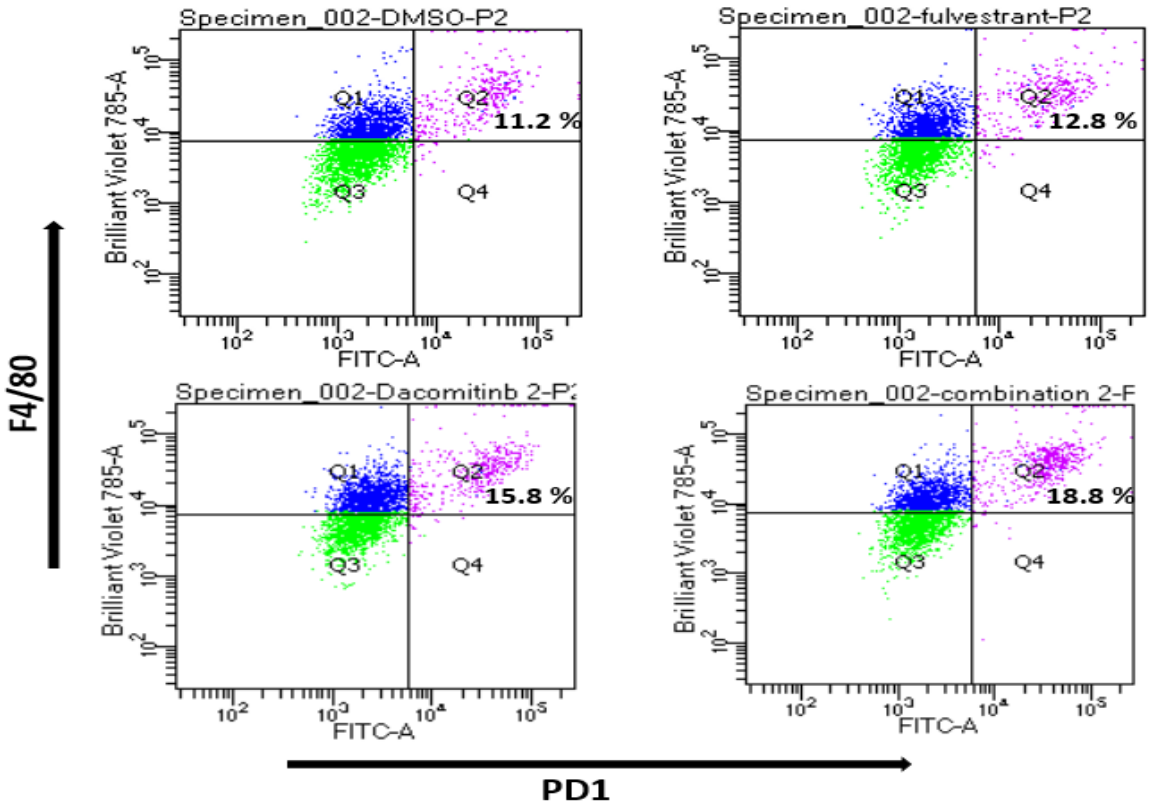

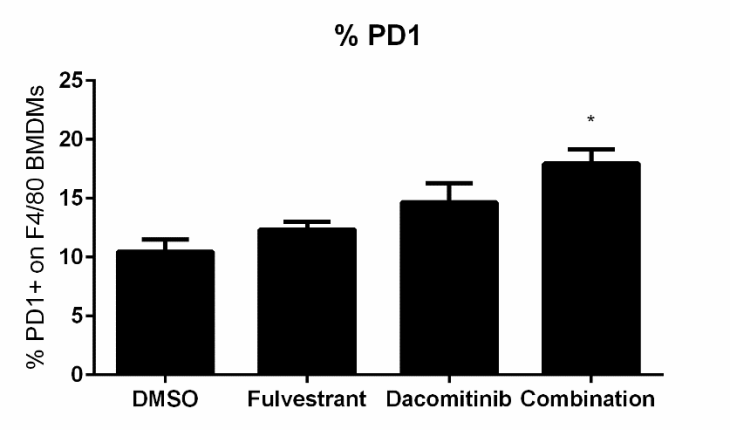

Figure 23. *Top*: A representative example of PD1 flow cytometric analysis performed on BMDMs treated with the combination. BMDMs were treated for 6 hours with fulvestrant (5μM), dacomitinib (10μM), or combination. Cells were double stained with cell surface markers for macrophages F4/80 and PD1 antibodies. Q2 represents double positive population (F4/80+/PD1+). Top left: DMSO, top right: fulvestrant, bottom left: dacomitinib, and bottom right: combination. *Bottom*; the data are represented as mean ± SD of two experiments. Significance was determined by two-tailed Student's t test and considered when $p < 0.05$ * and determined by Student's t test.

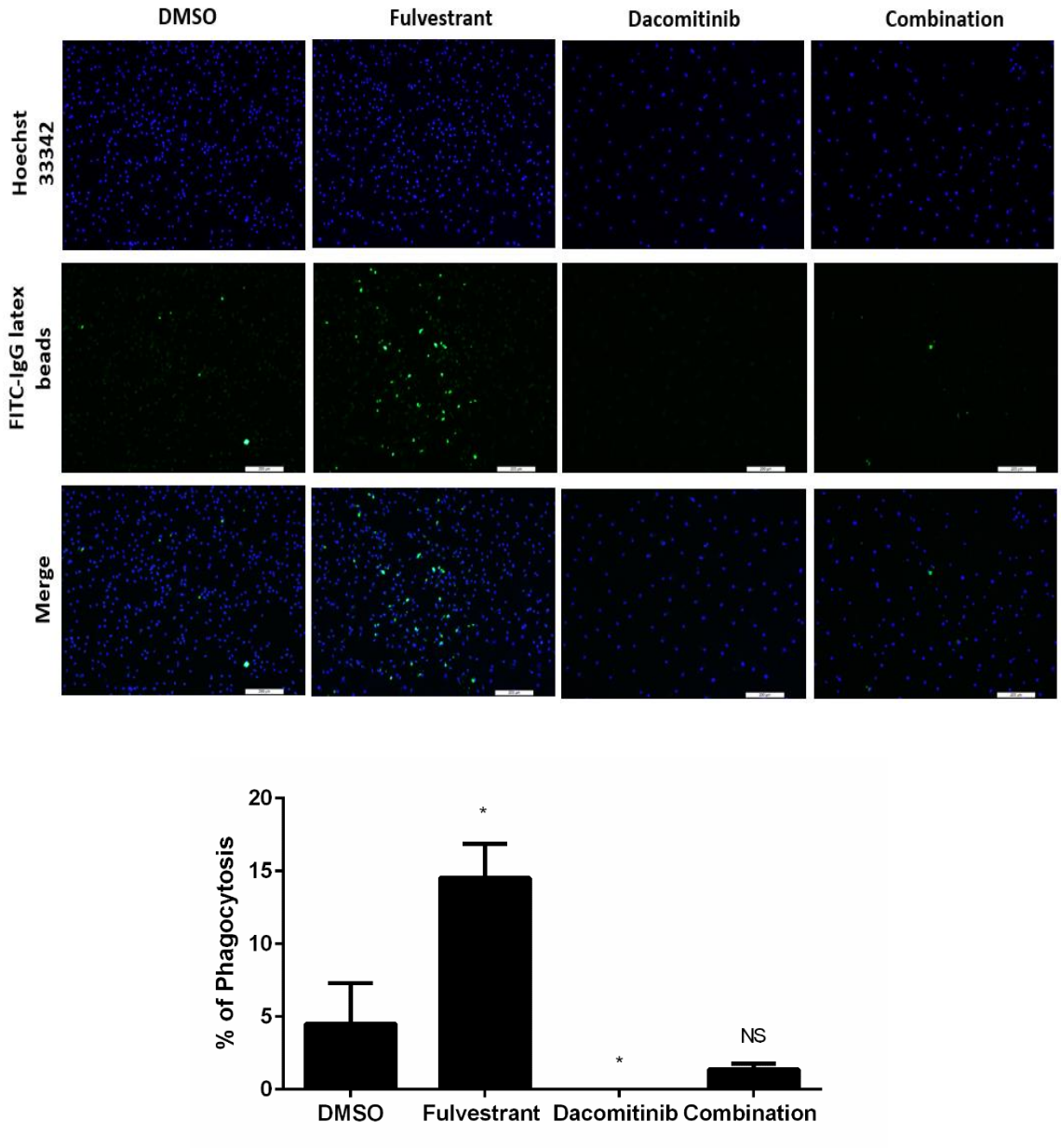

Figure 24. *Top*: A representative example of phagocytosis assay performed on BMDMs following the combination treatment. BMDMs were treated for 6 hours with fulvestrant (5µM), dacomitinib (10µM), or combination. FITC-IgG beads were added directly to the cells for 2 hours. Washing was performed before counterstaining with Hoechst 33342 blue staining as described in chapter 2. Images were captured by fluorescence microscope at 10X. (Scale= 200 µM). *Bottom*: Quantification of phagocytic macrophages normalized to the total number of macrophages. Data represented ± SD of two independent experiments. Significance was considered when $p < 0.05$ * and determined by two-tailed Student's t test.

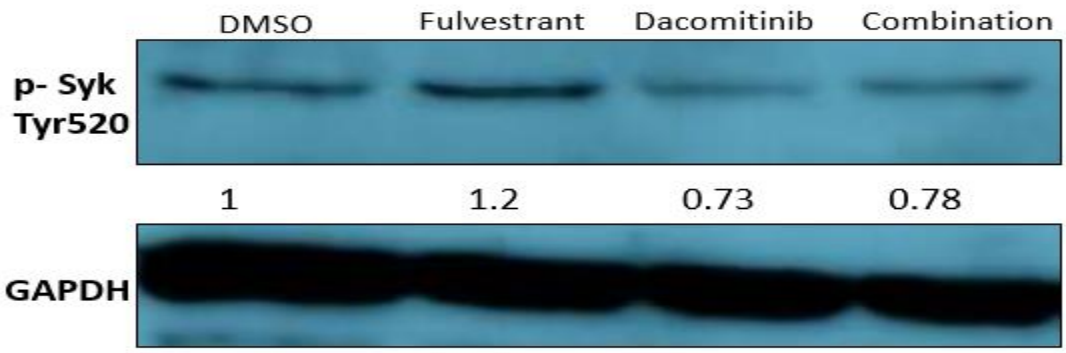

Figure 25. Effect of the combination treatment on BMDMs phosphor-Syk kinase activity. BMDMs were treated for 6 hours with fulvestrant (5μM), dacomitinib (10μM), or combination. Densitometric quantification was performed using GAPDH as a loading control.

The combination treatment inhibited CD8+ T cell activation and highly induced PD1 expression

We then sought to investigate the immunomodulatory effects of the fulvestrant-dacomitinib combination on the activity of T cells. We isolated primary cytotoxic T cells (CD8+ T cells) from the spleen of FVB-N mouse. The stimulation with anti-CD28 and CD3 beads and IL-2 treatment was confirmed by measuring IFN-ϒ and TNF-α release by ELISA. The combination treatment completely suppressed the secretion of IFN-ϒ and TNF-α from stimulated mouse CD8 T cells, while fulvestrant slightly reduced TNF-α and had no effect on IFN-ϒ release, and dacomitinib significantly reduced both IFN-ϒ and TNF-α (**Figure 26**). To gain mechanistic insights, we investigated the effect of the combination treatment on the Src family kinases, which are essential tyrosine kinases involved in mediating TCR signaling. Dacomitinib alone or in combination with fulvestrant significantly reduced the phosphorylation of Tyr416, which is located in the activation loop of Src family kinases, while fulvestrant alone had no effect. (**Figure 27**). The same inhibitory effect was observed in human T cells (Jurkat cells) (**Figure 28**).

To further assess the activity of CD8 T cells, we analyzed the expression of PD1 as a marker for exhaustion, following combination treatment. As in macrophages, the combination treatment significantly induced PD1 mRNA expression on CD8 T cells and this effect was entirely mediated by dacomitinib (**Figure 29**). Analyzing PD1 protein expression by flow cytometry on stimulated CD8 T cells, we found that 61.3% of CD8+ T cells were also positive for PD1, while 51.8% in dacomitinib, 22.8% in fulvestrant, and 26.4% in DMSO treated group (**Figure 30**). Altogether, these data suggest that the combination treatment, largely driven by dacomitinib, impairs T cell function. The increase expression of PD1 on both macrophage and CD8+ T cells provides a rationale for adding anti-PD1 immunotherapeutic agent to the fulvestrant/dacomitinib combination to treat lung cancer.

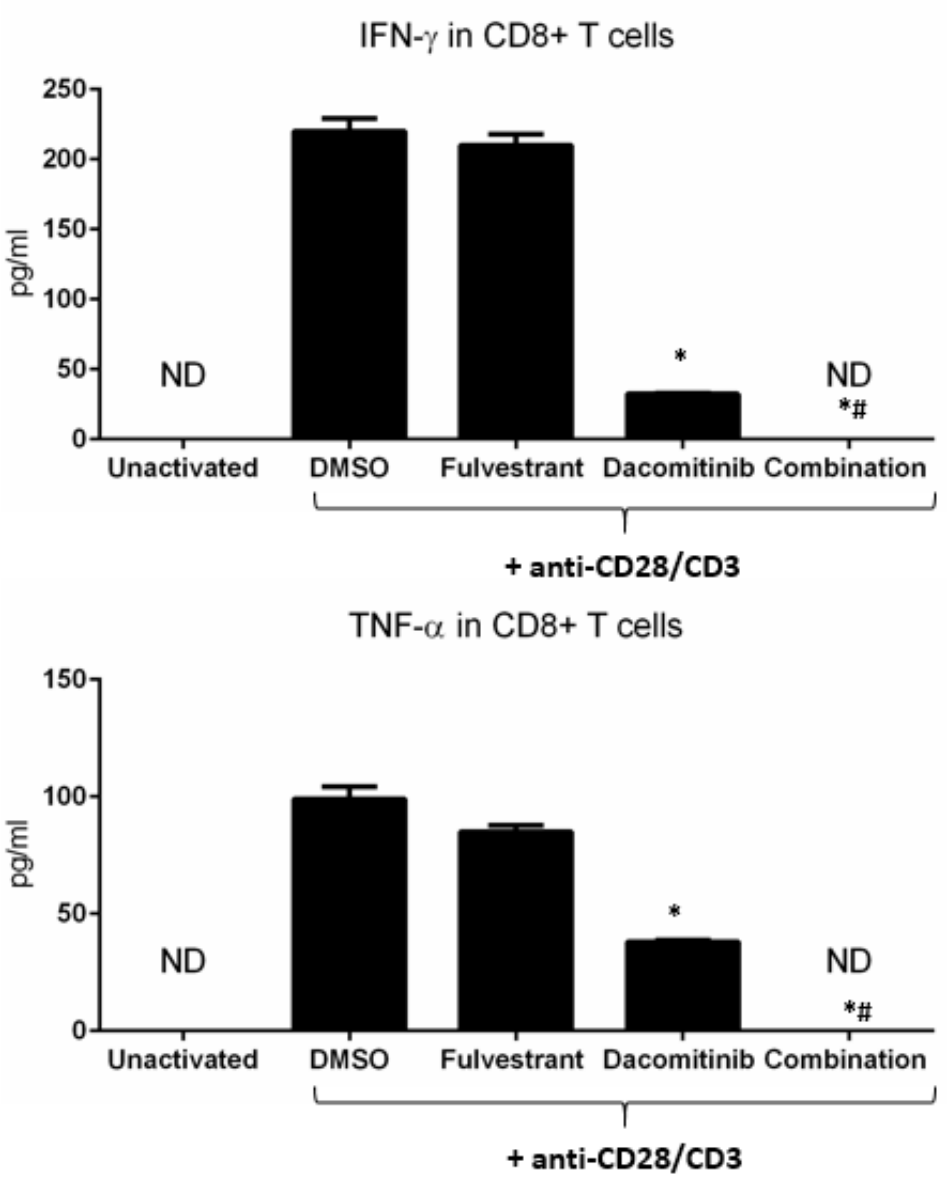

Figure 26. Effect of the combination treatment on cytokine release on mouse CD8+ T cells. T cells isolated from mouse's spleen were activated with anti-CD28/CD3 before treatment with fulvestrant (5μM), dacomitinib (10μM), or combination for 6 hours. Media were collected for ELISA analysis. Significance was assessed by two-tailed Student's t test and considered when $p < 0.05$. * compared to DMSO, # compared to single treatment.

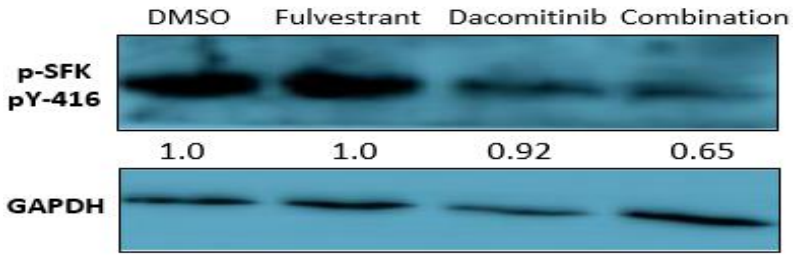

Figure 27. Effect of the combination treatment on Src kinase activity in mouse CD8+ T cells. CD* T cells were isolated and activated with anti-CD28/CD3 for 24 hr, then treated for 6 hours with fulvestrant (5µM), dacomitinib (10µM), or combination. Lysates were immunoblotted with phospho-Src family kinase (Tyr 416) antibody. Densitometric quantification was performed using GAPDH as a loading control.

Figure 28. Effect of the combination treatment on Src kinase activity in Jurkat cells (human T cells). Jurkat cells were stimulated using PMA/PHA mixture for 24 hours then treated for 6 hours with fulvestrant (5µM), dacomitinib (10µM), or combination. Lysates were immunoblotted with phospho-Src family kinase (Tyr 416) antibody. Densitometric quantification was performed using β-Actin as a loading control.

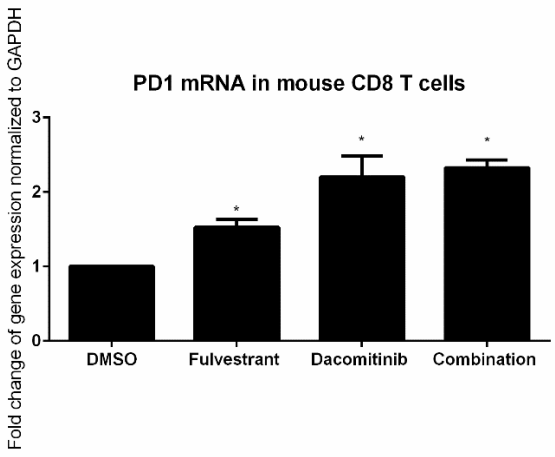

Figure 29. PD1 mRNA expression on mouse CD8+ T cells following the combination treatment. CD8 T cells were treated for 6 hours with fulvestrant (5µM), dacomitinib (10µM), or combination. mRNA expression was analyzed by RT-qPCR using GAPDH as a housekeeping gene. The fold change is relative to DMSO treated group. significance was assessed by two-tailed Student's t test and considered when $p < 0.05$.

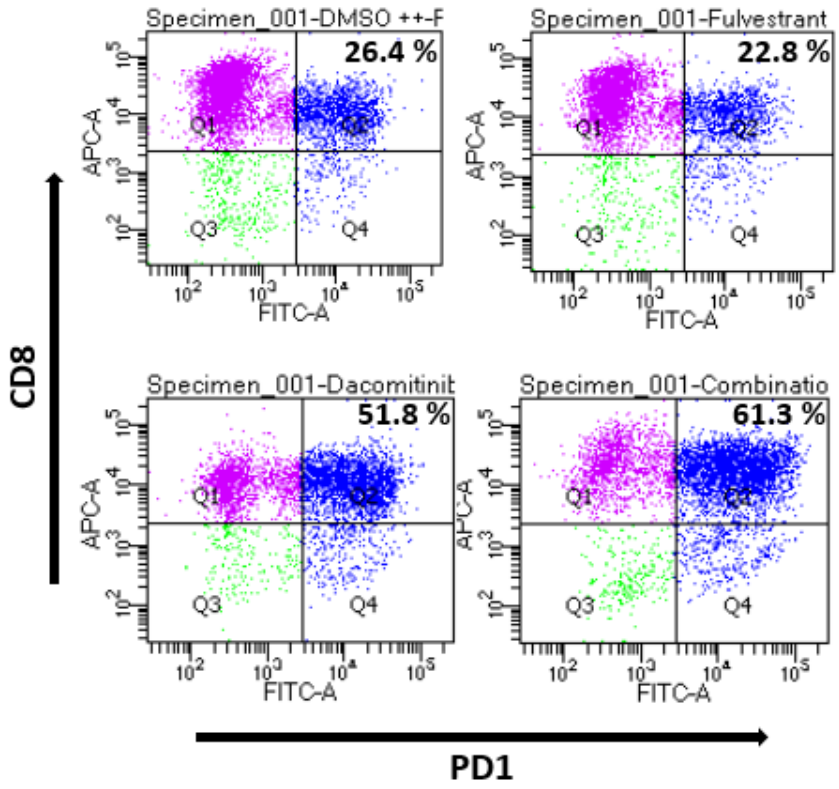

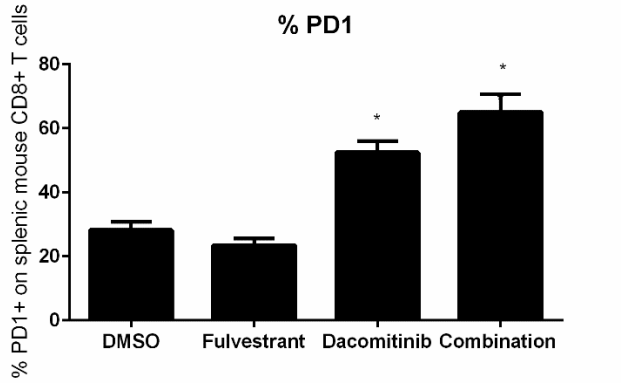

Figure 30. *Top*: A representative flow cytometric analysis of PD1 expression on mouse CD8+ T cell following the combination treatment. CD8 T cells were stimulated with anti-CD28/CD3 for 24 hours then treated for 24 hours with fulvestrant (5μM), dacomitinib (10μM), or combination. Cells were double stained with cell surface markers for CD8 T cells anti-CD8 and anti-PD1 antibodies. Q2 represents double positive population (CD8+/PD1+). Top left: DMSO, top right: fulvestrant, bottom left: dacomitinib, and bottom right: combination. *Bottom*: Data are represented as mean ± SD of two experiments. Significance was determined by two-tailed Student's t test and considered when $p < 0.05$ *.

The triple therapy modulates the tumor microenvironment by increasing cytotoxic CD8+ T lymphocytes and reducing M2 macrophages infiltration

To assess the effects of adding anti-PD1 to the combination of fulvestrant and dacomitinib on the tumor microenvironment, FVB-N mice were engrafted subcutaneously with FVBW17 lung cancer cells. Mice were then randomized to receive fulvestrant, dacomitinib, anti-PD1 antibody, dual therapy or the triple agents concomitantly for one week. We chose a rat monoclonal blocking anti-mouse PD1 antibody (clone RMP1-14 from BioXcell). This antibody has shown great efficacy in different solid tumor models, including lung cancer (101). The goal was to assess the immediate effects of these agents on the TME and on the spleens of tumor-bearing mice, as spleen is one of the major reservoirs of lymphocyte and inflammatory cells. We subjected three tumors and spleens of tumor-bearing mice from each group for flow cytometric analysis after one week of treatment. Two flow cytometric panels were followed: TheT cells panel (CD45+/CD3+/CD8+/PD1+) and the macrophage panel (CD45+/CD11b+/F480+/CD206+). An example of the gating strategy for both panels is shown in (**Figure 31, 32**).

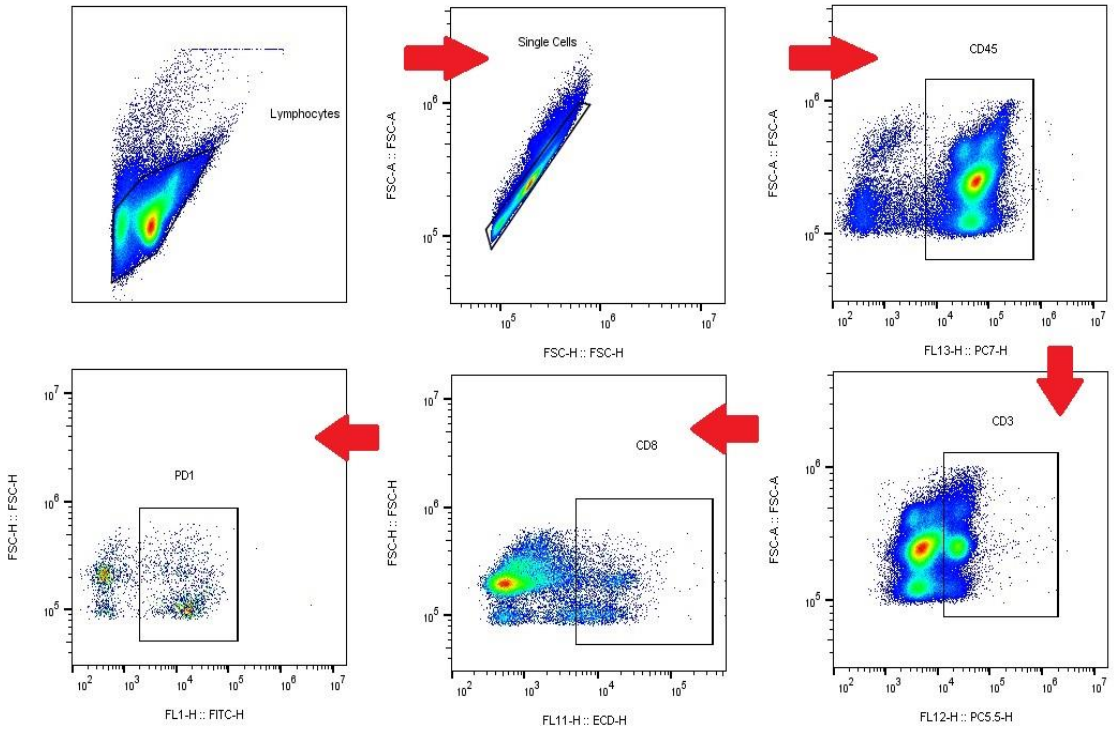

Figure 31. An example for the gating strategy applied to evaluate the CD8+/PD1+ population in the placebo control group.

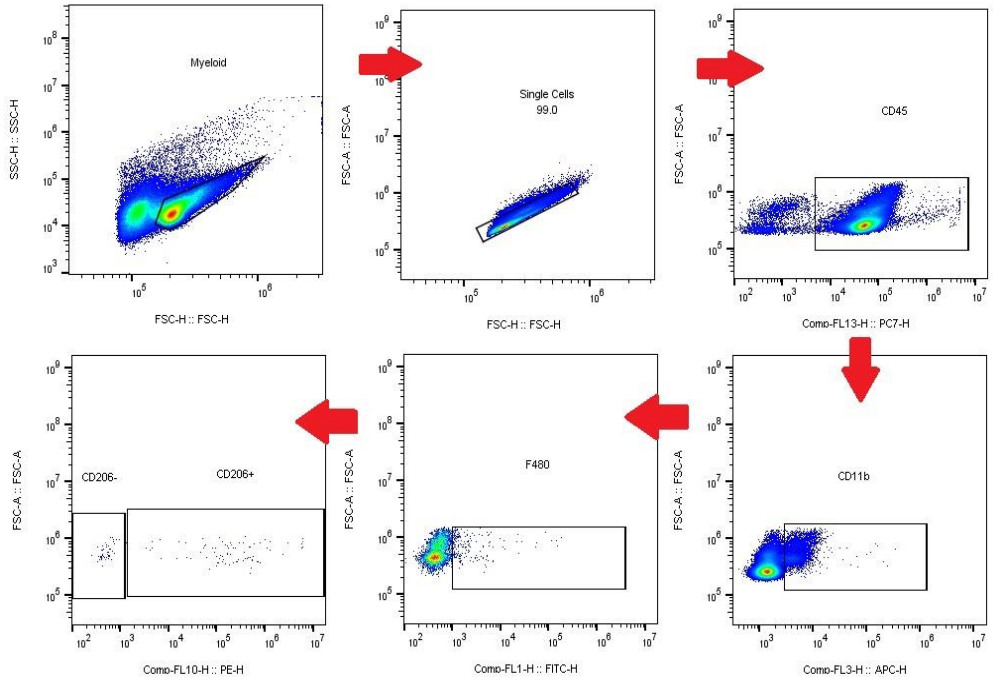

Figure 32. An example for the gating strategy applied to evaluate the F480+/CD206+ population in the placebo control group.

After one week of treatment, three tumors and spleens were pooled together and subjected to flow cytometric analysis. The combination of fulvestrant and dacomitinib significantly increased CD11b+ myeloid cells tumor infiltration (P=0.01), while triple therapy showed a slight but not significant decrease (**Figure 33**). F4/80 macrophages were also significantly higher in fulvestrant (p=0.022) and fulvestrant-dacomitinib groups (p=0.04), but lower in fulvestrant-anti-PD1 group (p=0.038) (**Figure 34**). Importantly, CD8+ T cells were significantly increased in the tumors of mice treated with single drugs, dual treatment or the triple therapy groups (**Figure 35**)**.** The triple therapy, fulvestrant-dacomitinib and dacomitinib-anti-PD1 groups showed a three-fold increase in CD8+ T cells at the tumor bed (p=0.0004, p=0.02, and p=0.0005, respectively) compared to placebo.

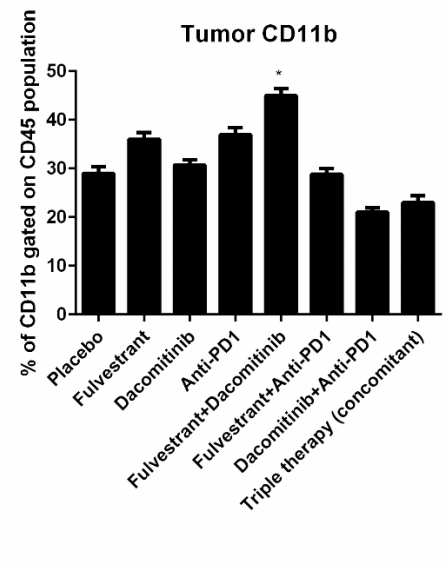

Figure 33. The proportion of CD11b+ gated on CD45 population in FVBW17 tumors following the treatment with fulvestrant, dacomitinib, anti-PD1 or the triple therapy. A pool of three tumors/group were subjected for flow cytometric analysis as described in chapter 2. Significance was tested by ANOVA and considered when p value < 0.05 * compared to placebo group. The data are represented as mean ± SEM.

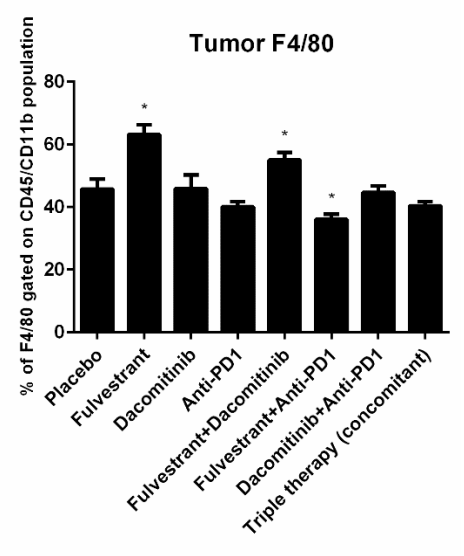

Figure 34. The proportion of F4/80+ gated on CD45/CD11b+ population in FVBW17 tumors following the treatment with fulvestrant, dacomitinib, anti-PD1 or the triple therapy. A pool of three tumors/group were subjected for flow cytometric analysis as described in chapter 2. Significance was tested by ANOVA and considered when p value < 0.05 * compared to placebo group. The data are represented as mean ± SEM.

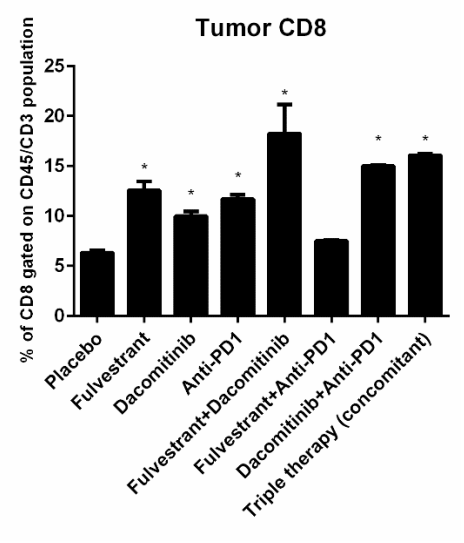

Figure 35. The proportion of CD8+ gated on CD45/CD3 population in FVBW17 tumors following the treatment with fulvestrant, dacomitinib, anti-PD1 or the triple therapy. A pool of three tumors/group were subjected for flow cytometric analysis as described in chapter 2. Significance was tested by ANOVA and considered when p value < 0.05 * compared to placebo group. The data are represented as mean ± SEM.

To assess the phenotypic changes among CD8+ T cell populations both at the tumor site or the spleen of tumor bearing mice, we assessed CD8+ T cells based on the expression of PD1, as a marker of T cell exhaustion. We observed that the PD1 expression on CD8+ T cells in the tumors was significantly reduced in fulvestrant-anti-PD1 (p=0.03), dacomitinib-anti-PD1 (p=0.005) or the triple therapy groups (p=0.002) compared to placebo (**Figure 36**). The triple therapy was significantly lower than dacomitinib-anti-PD1 group (p=0.03) and fulvestrant-anti-PD1 group (p=0.0044).

Neither anti-PD1 alone nor other single drugs showed an effect on PD1 expression on the tumoral CD8+ T cells. The triple therapy also significantly reduced PD1 expression on splenic CD8+ T cells of tumor bearing mice compared to placebo (p=0.008) and compared to dacomitinib-anti-PD1 (p=0.034) (**Figure 37**). A lower PD1 expression was also observed in fulvestrant group (p=0.037). However, fulvestrant-dacomitinib group showed a higher PD1 expression on splenic CD8+ T cells compared to placebo (p=0.031), which confirms our in vitro findings (**Figure 37**).

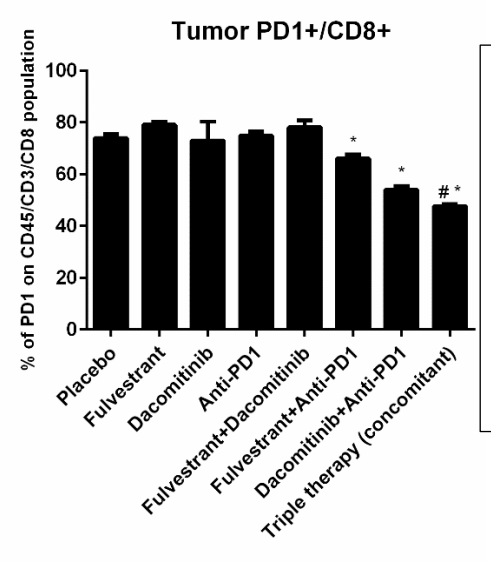

Figure 36. The proportion of PD1+ gated on CD45/CD3/CD8 population in FVBW17 tumors following the treatment with fulvestrant, dacomitinib, anti-PD1 or the triple therapy. A pool of three tumors/group were subjected for flow cytometric analysis as described in chapter 2. Significance was tested by ANOVA and considered when p value < 0.05 * compared to placebo group. The data are represented as mean ± SEM.

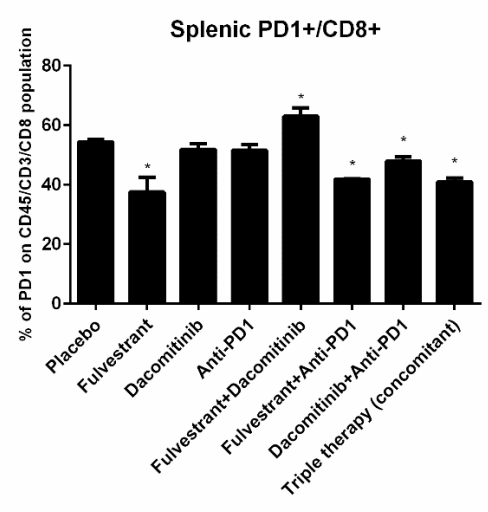

Figure 37. The proportion of PD1+ gated on CD45/CD3/CD8 population in the spleens of FVBW17 tumor-bearing mice following the treatment with fulvestrant, dacomitinib, anti-PD1 or the triple therapy. A pool of three spleens/group were subjected for flow cytometric analysis as described in chapter 2. Significance was tested by ANOVA and considered when p value < 0.05 * compared to placebo group. The data are represented as mean ± SEM.

Macrophages, both at the tumor bed and spleens of tumor bearing mice were stratified based on the expression of M2 marker CD206. As expected, we observed an overall high expression of CD206 on tumor F4/80+ macrophages compared to splenic F4/80 macrophages across all the treatment groups. Only the triple therapy group showed a significant decrease in CD206 expression both on tumoral and splenic macrophages compared to the placebo group (tumoral; p=0.026 and splenic; p=0.0028) (**Figure 38, 39**). Anti-PD1 antibody and dual treatment demonstrated less CD206 expression only in the splenic compartment (**Figure 39**). However, fulvestrant-dacomitinib treatment slightly induced CD206 expression on splenic macrophages but it was not significant. Altogether, these data suggest that fulvestrant-dacomitinib can induce an inflamed tumor microenvironment by increasing the infiltration of CD11b+ myeloid cells, including macrophages, and cytotoxic T cells. This inflamed TME facilitates the response to checkpoint blockade, as mounting evidence suggests that inflamed TME is a highly predictive factor for response to immune-checkpoint blockade therapy. We believe that these effects could potentiate the checkpoint blockade therapy if the anti-PD1 was given after fulvestrant and dacomitinib in a sequential approach.

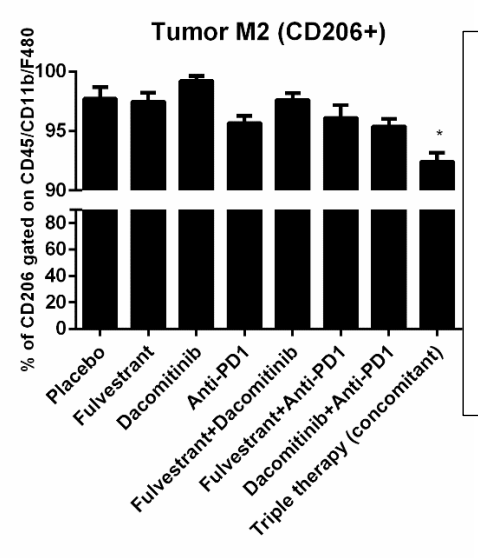

Figure 38. The proportion of CD206+ gated on CD45/CD11b/F480 population in FVBW17 tumors following the treatment with fulvestrant, dacomitinib, anti-PD1 or the triple therapy. A pool of three tumors/group were subjected for flow cytometric analysis as described in chapter 2. Significance was tested by ANOVA and considered when p value < 0.05 * compared to placebo group. The data are represented as mean ± SEM.

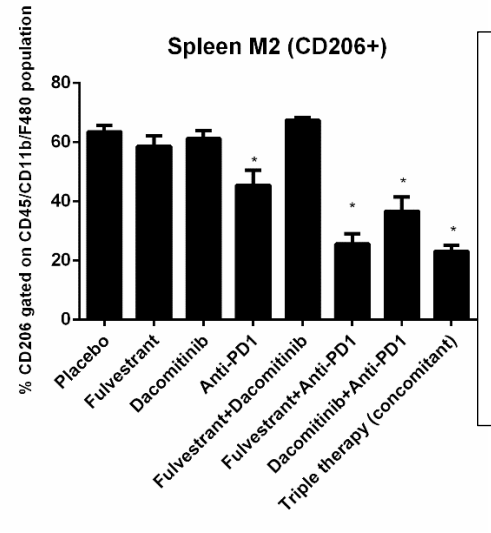

Figure 39. The proportion of CD206+ gated on CD45/CD11b/F480 population in the spleens of FVBW17 tumor-bearing mice following the treatment with fulvestrant, dacomitinib, anti-PD1 or the triple therapy. A pool of three spleens/group were subjected for flow cytometric analysis as described in chapter 2. Significance was tested by ANOVA and considered when p value < 0.05 * compared to placebo group. The data are represented as mean ± SEM.

We then investigated the effects of the triple treatment on the expression of PAM50 gene signature. We chose to analyze c-Myc and PR protein expression by IHC on anti-PD1, fulvestrant-dacomitinib, and triple therapy. As expected, fulvestrant-dacomitinib was effective in downregulating c-Myc expression. This effect was maintained but it was not significantly different in the triple therapy group (**Figure 41**). Both fulvestrant-dacomitinib and triple therapy groups demonstrated low scoring in 22% of the fields compared to 0% in placebo and anti-PD1 groups. Additionally, PR was

significantly elevated in all the three treatment groups compared to placebo. 70% of the fields scored high in the triple treatment group compared to 50% in fulvestrant-dacomitinib and anti-PD1 groups, and 25% in the placebo group (**Figure 42**). Collectively, these data suggest that the triple therapy improved a gene signature that predicts better clinical outcomes while exhibiting a robust antitumor effect.

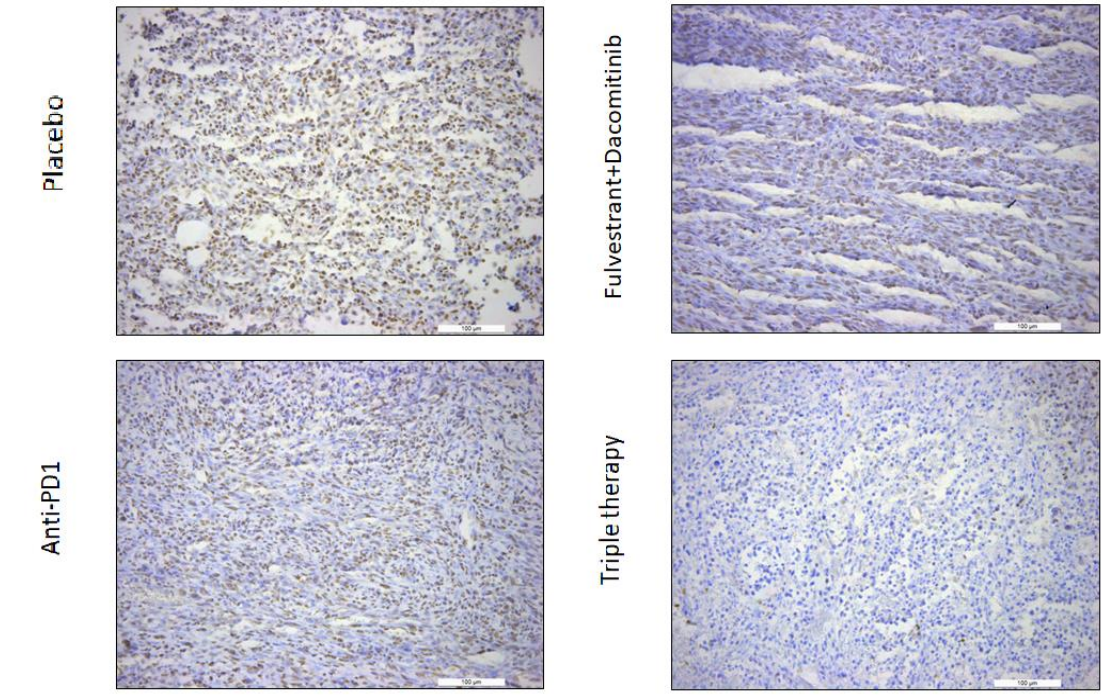

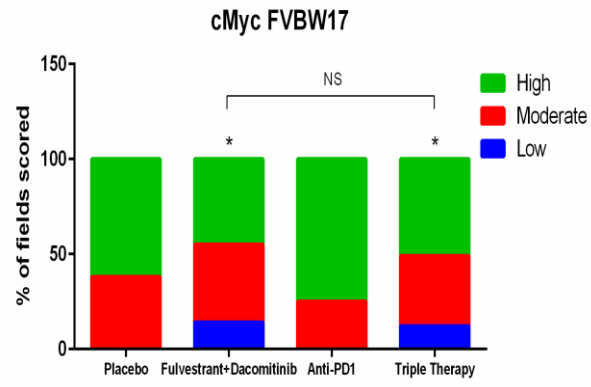

Figure 40. Downregulation of c-Myc protein expression following two weeks of fulvestrant-dacomitinib, anti-PD1 and triple therapy. *Upper*, Representative sections of FVBW17 tumors stained with c-Myc antibody showing a decrease in the number of positive cells labeled with c-Myc. *Left*, Quantification of c-Myc labeling was performed in three individual tumors per group and scored to low, moderate or high scoring. $p < 0.05$ was considered significant as measured by Chi square and Fisher test. * compared to placebo.

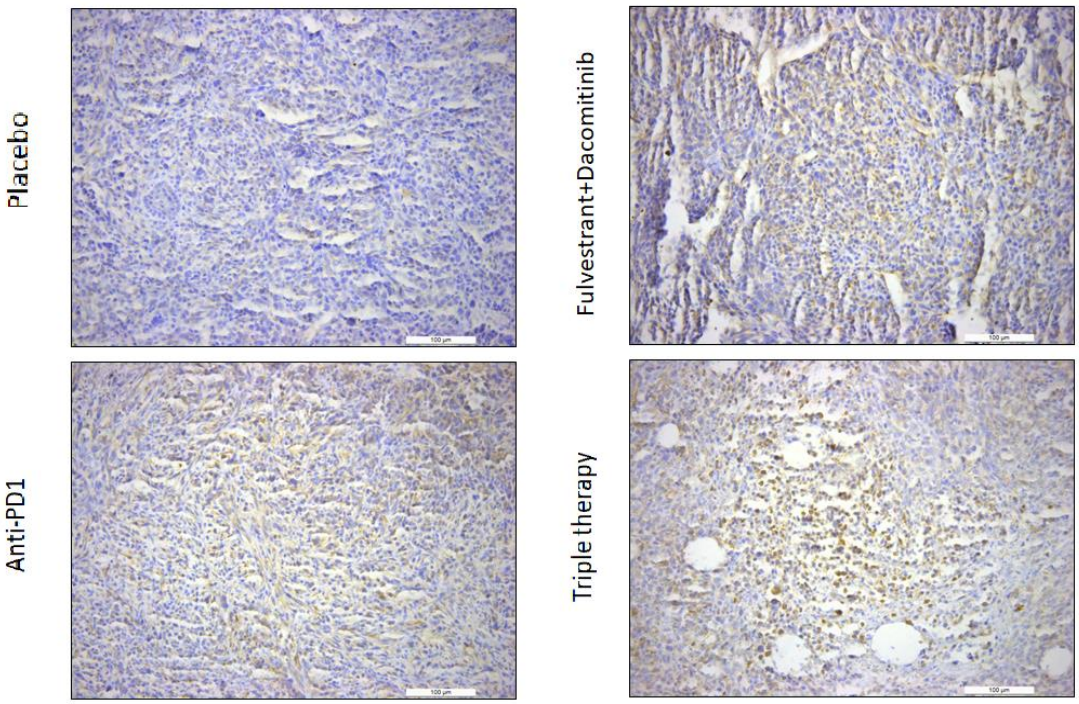

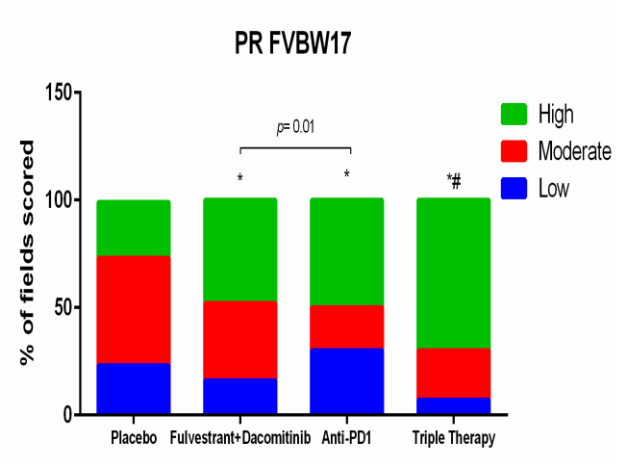

Figure 41. Upregulation of PR protein expression following two weeks of fulvestrant-dacomitinib, anti-PD1 and triple therapy. *Upper*, Representative sections of FVBW17 tumors stained with c-Myc antibody showing a decrease in the number of positive cells labeled with c-Myc. *Left*, Quantification of c-Myc labeling was performed in three individual tumors per group and scored to low, moderate or high scoring. $P < 0.05$ was considered significant as measured by Chi square and Fisher test. * is compared to placebo and # compared to fulvestrant-dacomitinib or anti-PD1

Adding anti-PD1 antibody to the combination of fulvestrant and dacomitinib in a sequential approach significantly improved the antitumor effect in FVBW17/FVB-N model

To determine whether these changes on the TME will translate into better antitumor effects, we assessed the tumor volume over two weeks of treatment using the

same syngeneic mouse model FVB-N/FVBW17. The mice were randomized to receive fulvestrant, dacomitinib, anti-PD1 antibody, dual therapy and triple therapy (concomitantly or sequentially) for two weeks of treatment. In the sequential group, mice were treated first with the fulvestrant-dacomitinib combination for 7 days, then anti-PD1 was added for another week. We also examined the effect of dual therapy including fulvestrant-dacomitinib, fulvestrant-anti-PD1, and dacomitinib-anti-PD1 using the same model. Over two weeks, the triple therapy was significantly better than single agents or any of the dual therapy groups, with the sequential approach being the most effective regimen (**Figure 42**). Within one week of treatment, the fulvestrant-dacomitinib combination showed a strong antitumor effect that deteriorated by the beginning of the second week. However, switching to anti-PD1 in the second week (sequential) was able to maintain that antitumor effect and inhibit the tumor outgrowth. The average tumor volume in the sequential group was four-fold less than the placebo group ($p< 0.00005$) and two-fold less than the concomitant group ($p< 0.005$). The concomitant group showed two fold decrease in tumor growth compared to placebo ($p<0.05$). Surprisingly, the immunotherapeutic agent did not show any sign of activity when given alone, suggesting this model is resistant to checkpoint blockade. The combination given sequentially but not concomitantly demonstrated a synergistic effect with a combination ratio of 1.35 (>1 indicates strong synergy and <1 less than additive effects).

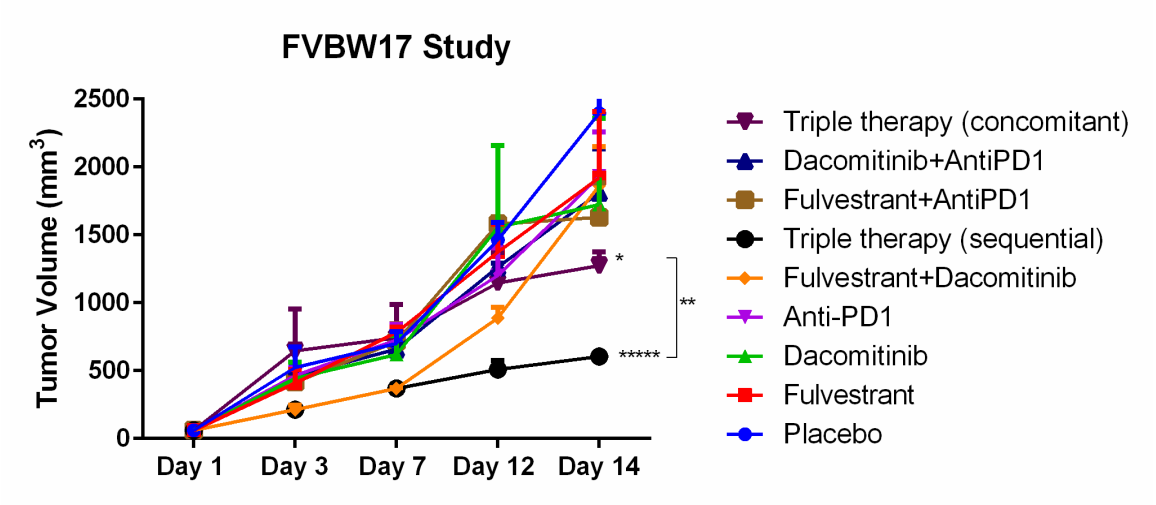

Figure 42.The antitumor effect of the triple therapy on FVBW17 syngeneic model. Five mice per group were randomized to receive; placebo (isotype IgG control 250µg/twice a week intraperitoneal), fulvestrant (30mg/kg twice a week subcutaneously), dacomitinib (10mg/kg daily through oral gavage) or mouse anti-PD1 (250µg/twice a week intraperitoneally). In sequential group, mice were treated from day 1 to 7 with fulvestrant and dacomitinib then switched to anti-PD1 on day 7 to day 14. Results represent relative mean tumor volume ± SEM of five tumors per group. Significance was assessed by ANOVA and considered when p value < 0.05 * compared to placebo group was considered when p value < 0.05. * < 0.05, ** < 0.005, **** < 0.00005.

Conclusion

In this study, we investigated the immunomodulatory effects of fulvestrant and dacomitinib as a combination treatment that showed greater efficacy in preclinical models of NSCLC in cell culture and in a xenograft model in immunosuppressed mice. We described the ability of the fulvestrant-dacomitinib combination to modulate the tumor microenvironment by increasing the immune cell infiltrate, but with evidence of increased immunosuppression. However, using a novel syngeneic lung cancer model, fulvestrant plus dacomitinib could still synergize with the checkpoint blocker anti-PD1. The combination of fulvestrant and dacomitinib induced tumor immune cell infiltration with a relatively higher rate of exhaustion characterized by increasing both the M2 marker CD206 and PD1 expression on T cells. Adding an anti-PD1 antibody to the combination of fulvestrant-dacomitinib improved the immune response and produced a significant antitumor effect. The triple therapy demonstrated a high CD8+ T cell infiltrate that expresses low PD1 and has a low number of M2 macrophages. Our data provide a rationale for using this triple regimen to treat NSCLC with a very aggressive phenotype and with a highly unresponsive to checkpoint blockade therapy.

The increase in tumor infiltration of immune cells following fulvestrant-dacomitinib treatment was also associated with a potent constraining of the oncogenic network ER/HERs. Preclinical evidence suggests that extensive cancer cell death following TKI treatment in EGFR-mutant lung cancer models can induce high immune infiltration that includes dendritic cells, macrophages and cytotoxic lymphocytes (127). In a recent clinical observations, Najagawa and colleagues showed that patients who relapsed on first-line EGFR TKI experienced a change in the tumor microenvironment

that tend to be highly immunosuppressive (128). PD-L1 and tumor mutational burden (TMB) were significantly elevated, which both manifest a durable response to subsequent anti-PD1 therapy. While we did not evaluate both of these factors in our in vivo model, we now know that besides the potent oncolytic effect, the combination of fulvestrant-dacomitinib unwantedly counteracts essential signaling pathways in immune cells. This strongly supports the notion of combining fulvestrant-dacomitinib sequentially with the anti-PD1 immunotherapeutic agent.

The recruitment of immune cells to the tumor site does not necessarily indicate the activation of their responses. Dying cells release neoantigens and pro-inflammatory factors that recruit antigen-presenting cells (APCs), which in turn will facilitate the tumor infiltration of CD8+ T cells and other immune cells. MHC I and II expressed by tumor cells has been extensively shown to be upregulated by EGFR targeted therapy (95), which is one of the first stages of initiating the cancer-immune cycle (66). Recently, high throughput screening of 2000 FDA-approved agents identified fulvestrant as one of the top enhancers of the lung carcinoma cells sensitivity to the cytotoxic effects of T cells and natural killer (NK) cells (106). While dacomitinib can upregulates MHC II on tumor cells, as it has been shown previously by Kobayashi and colleagues (129), it also inhibits Syk and Src kinases on macrophages and T cells. Syk and Src kinases play a pivotal role in regulating innate and adaptive immune response, and drugs that target these kinases have a wide range of anti-inflammatory effects and are being used for some hematological malignancies (130, 131). Dacomitinib impaired macrophages' phagocytic activity and CD8+ T cells' cytokine production and significantly increased PD1 expression on both cells in vitro. Unleashing the immune response with an

immunostimulatory strategy, such as anti-PD1 antibody, is a key to overcome these side effects. Indeed, anti-PD1 antibodies have been extensively shown to reprogram the TME and reverse the exhausted phenotype of T cells (132, 133). These agents also promote an M1-like phenotype and restore the phagocytic functions of PD1+ macrophages (79). However, to work, these agents require an inflamed TME and high expression of PD1/L1 pathways (134). Therefore, these observations collectively could explain the better antitumor effect of the sequential treatment approach over the concomitant strategy of combining fulvestrant, dacomitinib and anti-PD1 to treat lung cancer.

A sequential treatment approach is not a new treatment strategy. Clinically, most treatment regimens are given in cycles where drugs are often given sequentially. This is important for maximal efficacy and minimal toxicity. The off-target effects of dacomitinib that inhibits kinases essential for immune cell functions have prompted us to test the sequential approach of adding an immunotherapeutic agent after administrating fulvestrant-dacomitinib. A sequential treatment approach has been proposed previously with the aim to potentiate tumors to respond to immune checkpoint blockade treatment. It is well-known that a lack of immune cell infiltration and low tumor immunogenicity are the most predictive factors for response to immune checkpoint inhibitors. Treatment strategies that enhance immune cell infiltration or tumor immunogenicity could enhance the efficacy of PD1/L1 inhibitors. For instance, turning tumors from ‘cold’ to ‘hot’ or from immune-excluded to immune-infiltrated tumors by a vaccination strategy have been extensively shown to work synergistically with anti-PD1/L1 agents in different solid tumors (135, 136, 137). Kalos and colleagues also showed that cyclin-dependent kinase 4/6 (CDK4/6) inhibitors could synergize with checkpoint blockade in breast cancer

models only when CDK4/6 inhibitor is given before immunotherapy (138). They demonstrated that CDK4/6 inhibitor upregulated MHC I and II on tumor cells and induced inflamed tumor microenvironment, which both potentiate the effects of immunotherapy. Here, fulvestrant-dacomitinib's potent antitumor effect is also potentiating the effect of PD1 inhibitor in lung cancer, largely by inducing changes in the tumor microenvironment and very likely by upregulating MHC on tumor cells as it has been shown previously (95, 129).

In lung cancer, the majority of EGFR-mutant tumors express high PD-L1. EGFR TKI, the standard of care, showed improved efficacy when combined with PD1 inhibitors in preclinical models of EGFR-mutant NSCLC tumors (94). However, the effectiveness of this approach has not been confirmed in a clinical setting. In fact, preliminary analysis of some of the ongoing clinical trials suggest a lack of improvement with a significant increase in toxicities when both agents were used concomitantly (139). There are many explanations for this but one important one is that EGFR-mutant tumors are generally considered cold tumors with very low immunogenicity unlike KRAS-mutant tumors that tend to be highly immunogenic (140). That being said, concomitant use of both drugs might not be effective at the beginning of treatment as the tumor lacks immune infiltration and requires time for efficient immune response. Additionally, the effects of other EGFR TKIs on immune cell signaling are not completely understood, and they might exhibit off-target effects as dacomitinib, which makes concomitant treatment strategy less effective. In fact, anti-PD1/L1 agents are approved for EGFR-mutant diseases only after progression on EGFR TKIs, suggesting a favorable impact of EGFR inhibition on modulating the TME with regard to immune checkpoint inhibitor efficacy

(128). However, combining pan-HER TKI with a checkpoint inhibitor in other than EGFR-mutant models has never been extensively studied, and it is worth exploring clinically given the fact that KRAS mutant tumors are highly dependent on HER pathways (116, 117).

The complexity of TME and the heterogeneity of NSCLC tumors argue for the need for new treatment approaches that consider different aspects of tumorigenesis. Clinically, chemo-immunotherapy strategy has shown greater efficacy than immunotherapy or chemotherapy alone and with an acceptable toxicity profile. A cocktail of fours drugs that includes two cytotoxic drugs, a checkpoint blocker and an anti-VEGF are clinically used for advanced stage NSCLC (100). While we did not observe any major signs of toxicities over the two weeks of treatment with the triple therapy, future studies should focus on confirming the long-term safety of this regimen. In clinical sitting, several of the EGFR TKIs demonstrated a high rate of severe toxicities when concomitantly combined with checkpoint blockers in EGFR-mutant tumors (141). However, sequential use of checkpoint blockers after the TKIs showed improved efficacy with an acceptable toxicity profile (128). In animal models, sequential use of TKIs and anti-PD1/L1 is less toxic compared to giving them together at the same time (142). Although we used here a different model (KRAS-mutant) than the model used clinically (EGFR-mutant) for combining EGFR TKI with checkpoint blocker, we are proposing to use the triple therapy in a sequential manner for greater efficacy (synergistic antitumor effect) and for better tolerability and for its toxicity profile. Future studies should focus on assessing the immune-contexture in both the concomitant and sequential treatment approaches by looking at the activation states of these immune cells and analyzing other

important immune subsets, such as MDSCs and regulatory T cells. Lastly, the survival rate and long-term safety using an orthotopic model should be assessed as well in all the treatment groups.

Chapter 5: Discussion

Lung carcinomas are the leading cause of cancer mortality in both sexes. Historically, lung cancer prognosis has been bleak. However, over the past two decades, there have been important advances in understanding the biology and the underlying genetic causes of lung cancer that led to the discovery of new effective therapies. Investigation has mainly focused on identifying important molecular targets that are essential for tumor cell viability and immune escape. To date, several molecularly targeted agents and immunotherapeutics have revolutionized the systemic management of NSCLC. While patient clinical outcomes have greatly improved with the introduction of these options, the emergence of drug resistance with molecularly targeted agents and the low response rate with immunocheckpoint inhibitors- when used alone- have remained to be addressed. Several combination treatments are being tested with the goal to increase the response rate among patients receiving immunotherapy. We have focused here on testing a cocktail of targeted agents to treat lung cancer that effectively hinders two mechanisms of lung tumorigenesis. We were able to show that combining ER blocker and pan-HER TKI with anti-PD1 demonstrates a very potent antitumor effect in a lung cancer model with aggressive biology.

ERβ and HERs pathways are known individually to play an important role in lung cancer tumorigenesis. The mutual regulation between these two pathways was discovered two decades ago, in which ERβ has been shown to mediates EGFR activation and EGF ligands were shown to upregulate ERβ activity (61). This also involves HER2/HER3 pathway, where E2 can rapidly activate HER2 and HER3 in NSCLC cells, suggesting that the interaction is more than just an EGFR receptor but also involves HER2 and

HER3. Consistent with previous reports in breast cancer, blocking ER with the anti-estrogen fulvestrant activates HER receptors differentially and regulates HER ligands (112). In fact, HER2/HER3 overactivation is one of the major resistance factors associated with endocrine therapy in treating ER-driven breast cancer (113). This compensatory mechanism could be the underlying reason for the moderate antiproliferative effect observed with anti-ERs when used alone to treat lung cancer cells (61). In fact, analysis of the PAM50 genes in ERβ+ NSCLC patients revealed a gene signature (7-gene model) with prognostic value comprising of one interacting network that includes ERβ and HER2/HER3, suggesting both pathways are contributing for poor clinical outcome in ERβ+ NSCLC (65).

The striking antitumor effect of the fulvestrant-dacomitinib seen in different NSCLC models was accompanied by producing a gene signature that predicts a better prognosis. We showed that the 7-gene model identified from the steroid hormone genes signature PAM50 is regulated the AP-1 family of transcription factors. In fact, some of the genes contained in the PAM50 signature have been shown previously and in different cancer models to be regulated by members of the AP-1 family. For instance, c-Myc and CyclinD1 were both found to be tightly controlled by AP-1 transcription machinery (143), and both EGF and estrogen signaling upregulate c-Myc expression in an AP-1-dependent mechanism (144). PgR expression is induced by estrogen signaling in breast cancer, and AP-1 was shown to limit this induction (145). In lymphoma cases, FOXC1 expression was found to be potently suppressed by Jun knockdown, suggesting that FOXC1 is a target gene for AP-1 (146). These cases provide some evidence aligning with our findings that AP-1 is an important orchestrator in regulating the 7-gene model, and

the effect of fulvestrant-dacomitinib is mainly dependent on AP-1 downregulation. Although dacomitinib and the combination showed the same extent of AP-1 suppression, only the combination completely reversed the gene signature. This potentially occurs by further attenuation of ER and CREB transcription activity that both cannot be achieved by dacomitinib alone. It is well-established that AP-1, CREB and ER work together to control gene expression, and the mutual upregulation between ER and HERs suggests that blocking both pathways will achieve a maximal reversal of the gene signature.

The second aim of this project is to understand the effects of fulvestrant-dacomitinib on the tumor microenvironment and explore the therapeutic potential of adding a checkpoint inhibitor to further improve the efficacy. It is becoming well-known that the bidirectional interplay between cancer cells and immune cells is strongly affecting tumor progression. We found that dacomitinib-besides its potent anti-HERs activity- also inhibits Src family kinases (SFKs) and spleen tyrosine kinase (Syk). Both of these non-receptor kinases play pivotal roles in orchestrating immune cell functions. These suppressive effects provide a rationale for adding an immunotherapeutic agent that will be able to unleash the immune response and further maximizes the antitumor response. Initially, a week of fulvestrant-dacomitinib treatment showed a good response on suppressing tumor growth compared to placebo; however, this effect did not last as tumors started to show signs of immunosuppression. Spleen is one of the major reservoirs for recruiting immune cells to the tumor bed. In the spleens of tumor-bearing mice treated with fulvestrant-dacomitinib, markers of immunosuppression were elevated characterized by high PD1 CD8+ T cells and M2 macrophages. The reverse effect was observed with the triple combination, in which both tumor and splenic compartment showed less PD1

expression on CD8+ T cells and less M2 macrophages, suggesting an enhanced immune response.

Checkpoint blockade therapy has altered the landscape of NSCLC treatment and agents that target the inhibitory checkpoint pathway PD1/L1 are now approved for first and second-line treatment (139, 140). While the reported response rate to these agents are relatively small that less than 29%, patients, however, tend to have durable effects and longer survival rates when responding. Surprisingly, we did not observe any signs of activity with the anti-PD1 agent when used alone, despite the fact that FVBW17 cells were driven from the tobacco carcinogen NNK and the preliminary analysis suggests a high mutation rate. FVBW17 (conducted by Laura Stabile, PhD at University of Pittsburgh). Clinically, smokers tend to respond to checkpoint blockade therapy better than never-smokers, as smoking creates a highly inflamed lung microenvironment with a high rate of mutations (147). The dose and schedule of dosing were the same as others have previously reported with great efficacy (101). This suggests that FVBW17 cells are intrinsically resistant to checkpoint blockade, at least in the subcutaneous model. Studies on orthotopic models will confirm the sensitivity of these cells to this treatment approach. Nevertheless, the potent antitumor effect observed with the triple regimen was not seen with either agents alone or the dual treatment groups, indicating that targeting multiple facets of tumorigenesis synergistically improves the antitumor response.

The flow cytometric analysis clearly showed a change in the tumor microenvironment after one week of treatment. CD11b+ immune cells were highly increased following fulvestrant-dacomitinib treatment. CD45+/CD11b+ cells are a very heterogeneous groups of cells that could be expressed on different subpopulations

including but not limited to; macrophages, myeloid derived suppressor cells (MDSC) or dendritic cells with antigen presenting properties or even natural killer cells (NK cells) (148, 149). We only subcategorized this population for the expression of macrophage markers F4/80 and CD206. While we did see a great response in terms of less M2 polarization after the triple combination treatment, we did not look at MDSCs or NK cells infiltration and activities. We also did not investigate regulatory T cells (Tregs) population, which are considered to be major drivers of immunosuppression and their accumulation in the tumor correlates with poor prognosis (66, 67). These are other caveats to be explored in future studies.

Preclinical evidence suggest that fulvestrant can sensitize lung tumor cells to T cells and NK cells immune-mediated cytotoxicity (106). In fact, estrogen signaling was found to be an important enhancer of MDSCs mobilization and activity, and antiestrogens have been proposed to synergize with immunotherapy (104). Additionally, a recent rigorous study led by Nishikawa and colleagues showed that EGFR signaling in lung cancer is an important mediator for Treg recruitment and activity, and the EGFR TKI erlotinib significantly suppressed Tregs tumor infiltration and synergized with immunotherapy (94). Based on these observations, it is very likely that the triple therapy will modulate Tregs, MDSCs and NK cells activities to be more immunostimulatory and less immunosuppressive. While this remains to be proven, we think that the increase in CD8+ T cells infiltration and the decrease in PD1+ and M2 macrophages following the triple therapy strongly support the use of this treatment strategy to treat aggressive lung cancer. The immunosuppressive effects of pan-HER TKI could be a limiting factor in using this approach concomitantly. The reinvigorating effect of PD1 inhibitor on T cell

functionality will not be achieved if TCR signaling is interrupted by dacomitinib. Dasatinib, the other Src inhibitor, has been shown to acts as an on/off switch for CAR T cell therapy to control the excessive activity of CAR T cells and minimize its lethal toxicities. In fact, CAR T cell activities were restored after discontinuation of dasatinib, suggesting the effect is transient (85). It is very likely the effects will be the same with dacomitinib. As a result, the sequential approach could be more effective in boosting the antitumor immune response than the concomitant approach of combining fulvestrant and dacomitinib with anti-PD1 agents. Future studies should be directed to compare the activity of immune cells in the TME between the sequential and the concomitant approach.

References

1- SEER Cancer Stat Facts: Lung and bronchus cancer. National Cancer Institute, Bethesda, MD. https://seer.cancer.gov/statfacts/html/lungb.html. Accessed on May 15, 2019.

2- Lu T, Yang X, Huang Y, et al. Trends in the incidence, treatment, and survival of patients with lung cancer in the last four decades. *Cancer Manag Res*. 2019;11:943–953. Published 2019 Jan 21. doi:10.2147/CMAR.S187317

3- Siegel RL, Miller KD, Jemal A. Cancer statistics, 2018. *CA Cancer J Clin* 2018; **68**: 7-30

4- De Groot PM, Wu CC, Carter BW, Munden RF. The epidemiology of lung cancer. *Translational Lung Cancer Research* 2018; **7**: 220-233

5- American Cancer Society. Lung Cancer Risk Factors. https://www.cancer.org/cancer/lung-cancer/prevention-and-earlydetection/risk-factors.html (accessed 2020 March 31).

6- Dela Cruz CS, Tanoue LT, Matthay RA. Lung cancer: epidemiology, etiology, and prevention. Clin Chest Med. 2011;32(4):605–644.

7- Coté ML, Liu M, Bonassi S, et al. Increased risk of lung cancer in individuals with a family history of the disease: a pooled analysis from the International Lung Cancer Consortium. *Eur J Cancer*. 2012;48(13):1957–1968. doi:10.1016/j.ejca.2012.01.038

8- Landi MT, Chatterjee N, Yu K, et al. A genomewide association study of lung cancer identifies a region of chromosome 5p15 associated with risk for adenocarcinoma. *Am J Hum Genet* 2009; **85**: 679-91

9- 9. Yokota J, Shiraishi K, Kohno T. Genetic basis for susceptibility to lung cancer: Recent progress and future directions. *Adv Cancer Res* 2010; **109**: 51-72

10- 10. Herbst RS, Heymach JV, Lippman SM. Lung cancer. *N Engl J Med* 2008; **359**: 1367-80

11- Pelosof L, Ahn C, Gao A, Horn L, Madrigales A, Cox J, McGavic D, Minna JD, Gazdar AF, Schiller J. Proportion of Never-Smoker Non-Small Cell Lung Cancer Patients at Three Diverse Institutions. J *Natl Cancer Inst* 2017; 109(7)

12- 12. Wakelee HA, Chang ET, Gomez SL, et al. Lung cancer incidence in never smokers. *J Clin Oncol* 2007; **25**: 472-8

13- 13. Sun S, Schiller JH, Gazdar AF. Lung cancer in never smokers--a different disease. *Nat Rev Cancer* 2007; **7**: 778-90

14- Hanna JM, Onaitis MW. Cell of origin of lung cancer. *Journal of Carcinogenesis* 2013; **12**: 6

15- Ou SH, Zell JA. Carcinoma NOS is a common histologic diagnosis and is increasing in proportion among non-small cell lung cancer histologies. J Thorac Oncol. 2009;4:1202–1211

16- Alexandrov LB, Nik-Zainal S, Wedge DC, et al. Signatures of mutational processes in human cancer [published correction appears in Nature. 2013 Oct 10;502(7470):258. Imielinsk, Marcin [corrected to Imielinski, Marcin]]. *Nature*. 2013;500(7463):415–421. doi:10.1038/nature12477

17- Quintanal-Villalonga A, Paz-Ares L, Ferrer I, Molina-Pinelo S. Tyrosine Kinase Receptor Landscape in Lung Cancer: Therapeutical Implications [published correction appears in Dis Markers. 2018 Jul 19;2018:3714684]. *Dis Markers*. 2016;2016:9214056. doi:10.1155/2016/9214056
18- El-Telbany A, Ma PC. Cancer genes in lung cancer: racial disparities: are there any?. *Genes Cancer*. 2012;3(7-8):467–480. doi:10.1177/1947601912465177
19- Prior IA, Lewis PD, Mattos C. A comprehensive survey of Ras mutations in cancer. *Cancer Res*. 2012;72(10):2457–2467. doi:10.1158/0008-5472.CAN-11-2612
20- Dearden S, Stevens J, Wu YL, Blowers D. Mutation incidence and coincidence in non small-cell lung cancer: meta-analyses by ethnicity and histology (mutMap). *Ann Oncol.* (2013) 24:2371–6. doi: 10.1093/annonc/mdt205
21- Jacqueline V. Aredo, Sukhmani K. Padda, Christian A. Kunder, Summer S. Han, Joel W. Neal, Joseph B. Shrager and Heather A. Wakelee. Impact of KRAS mutation subtype and concurrent pathogenic mutations on non-small cell lung cancer outcomes. Lung Cancer. 2019;133:144-150
22- Canon, J., Rex, K., Saiki, A.Y. *et al.* The clinical KRAS(G12C) inhibitor AMG 510 drives anti-tumour immunity. *Nature* **575,** 217–223 (2019). https://doi.org/10.1038/s41586-019-1694-1
23- Janes MR, Zhang J, Li LS, Hansen R, Liu Y, et al. Targeting KRAS mutant cancers with a covalent G12C-specific inhibitor. Cell. 2018;172(3):578-589
24- Miranda O, Farooqui M, Siegfried JM. Status of Agents Targeting the HGF/c-Met Axis in Lung Cancer. *Cancers (Basel)*. 2018;10(9):280. Published 2018 Aug 21. doi:10.3390/cancers10090280
25- Remon J, Morán T, Majem M, Reguart N, Dalmau E, Márquez-Medina D, Lianes P. Acquired resistance to epidermal growth factor receptor tyrosine kinase inhibitors in EGFR-mutant non-small cell lung cancer: a new era begins. *Cancer Treat Rev. 2014 Feb; 40(1):93-101.*
26- Devarakonda S, Morgensztern D, Govindan R. Genomic alterations in lung adenocarcinoma. Lancet Oncol 2015; 16: E342–51
27- Halberg, R.H. Palmer. Mechanistic insight into ALK receptor tyrosine kinase in human cancer biology. Nat Rev Cancer. 2013(13):685-700
28- Ai X, Guo X, Wang J, et al. Targeted therapies for advanced non-small cell lung cancer. *Oncotarget*. 2018;9(101):37589–37607. Published 2018 Dec 25. doi:10.18632/oncotarget.26428
29- Arteaga CL, Engelman JA. ERBB receptors: from oncogene discovery to basic science to mechanism-based cancer therapeutics. *Cancer Cell*. 2014;25(3):282–303. doi:10.1016/j.ccr.2014.02.025
30- Singh B, Carpenter G, Coffey RJ. EGF receptor ligands: recent advances. *F1000Res*. 2016;5:F1000 Faculty Rev-2270. Published 2016 Sep 8. doi:10.12688/f1000research.9025.1
31- Alroy I, Yarden Y: The ErbB signaling network in embryogenesis and oncogenesis: Signal diversification through combinatorial ligand-receptor interactions. FEBS Lett 410::83,1997–86

32- Mishra R, Hanker AB, Garrett JT. Genomic alterations of ERBB receptors in cancer: clinical implications. *Oncotarget*. 2017;8(69):114371–114392. Published 2017 Nov 30. doi:10.18632/oncotarget.22825
33- Gupta R, Dastane AM, Forozan F, Riley-Portuguez A, Chung F, Lopategui J, Marchevsky AM. Evaluation of EGFR abnormalities in patients with pulmonary adenocarcinoma: the need to test neoplasms with more than one method. *Mod Pathol. 2009 Jan; 22(1):128-33.*
34- Shigematsu H, Gazdar AF. Somatic mutations of epidermal growth factor receptor signaling pathway in lung cancers. *Hum Pathol. 2005 Oct; 36(10):1127-34.*
35- Mitsudomi T, Kosaka T, Yatabe Y Biological and clinical implications of EGFR mutations in lung cancer. *Int J Clin Oncol. 2006 Jun; 11(3):190-8.*
36- Rosell R, Moran T, Queralt C, Porta R, Cardenal F, Camps C, Majem M, Lopez-Vivanco G, Isla D, Provencio M, Insa A, Massuti B, Gonzalez-Larriba JL, Paz-Ares L, Bover I, Garcia-Campelo R, Moreno MA, Catot S, Rolfo C, Reguart N, Palmero R, Sánchez JM, Bastus R, Mayo C, Bertran-Alamillo J, Molina MA, Sanchez JJ, Taron M, Spanish Lung Cancer Group. Screening for epidermal growth factor receptor mutations in lung cancer. *N Engl J Med. 2009 Sep 3; 361(10):958-67.*
37- Tam IY, Chung LP, Suen WS, Wang E, Wong MC, Ho KK, Lam WK, Chiu SW, Girard L, Minna JD, Gazdar AF, Wong MP. Distinct epidermal growth factor receptor and KRAS mutation patterns in non-small cell lung cancer patients with different tobacco exposure and clinicopathologic features. *Clin Cancer Res. 2006 Mar 1; 12(5):1647-53.*
38- Lara PN Jr, Laptalo L, Longmate J, Lau DH, Gandour-Edwards R, Gumerlock PH, Doroshow JH, Gandara DR, California Cancer Consortium. Trastuzumab plus docetaxel in HER2/neu-positive non-small-cell lung cancer: a California Cancer Consortium screening and phase II trial. *Clin Lung Cancer. 2004 Jan; 5(4):231-6.*
39- Stephens P, Hunter C, Bignell G, Edkins S, Davies H, Teague J, Stevens C, O'Meara S, Smith R, Parker A, Barthorpe A, Blow M, Brackenbury L, Butler A, Clarke O, Cole J, Dicks E, Dike A, Drozd A, Edwards K, Forbes S, Foster R, Gray K, Greenman C, Halliday K, Hills K, Kosmidou V, Lugg R, Menzies A, Perry J, Petty R, Raine K, Ratford L, Shepherd R, Small A, Stephens Y, Tofts C, Varian J, West S, Widaa S, Yates A, Brasseur F, Cooper CS, Flanagan AM, Knowles M, Leung SY, Louis DN, Looijenga LH, Malkowicz B, Pierotti MA, Teh B, Chenevix-Trench G, Weber BL, Yuen ST, Harris G, Goldstraw P, Nicholson AG, Futreal PA, Wooster R, Stratton MR. Lung cancer: intragenic ERBB2 kinase mutations in tumours. *Nature. 2004 Sep 30; 431(7008):525-6.*
40- Holbro T, Beerli RR, Maurer F, Koziczak M, Barbas CF 3rd, Hynes NE. The ErbB2/ErbB3 heterodimer functions as an oncogenic unit: ErbB2 requires ErbB3 to drive breast tumor cell proliferation. *Proc Natl Acad Sci U S A. 2003 Jul 22; 100(15):8933-8.*

41- Lee-Hoeflich S.T., Crocker L., Yao E., Pham T., Munroe X., Hoeflich K.P. A central role for HER3 in HER2-amplified breast cancer: implications for targeted therapy. Cancer Res. 2008;**68**:5878–5887

42- Scharpenseel, H., Hanssen, A., Loges, S. *et al.* EGFR and HER3 expression in circulating tumor cells and tumor tissue from non-small cell lung cancer patients. *Sci Rep* **9,** 7406 (2019). https://doi.org/10.1038/s41598-019-43678-6

43- Liu Q, Yu S, Zhao W, Qin S, Chu Q, Wu K. EGFR-TKIs resistance via EGFR-independent signaling pathways. *Mol Cancer*. 2018;17(1):53. Published 2018 Feb 19. doi:10.1186/s12943-018-0793-1

44- Fernandez-Cuesta L, Plenker D, Osada H, Sun R, Menon R, Leenders F, Ortiz-Cuaran S, Peifer M, Bos M, Daßler J, Malchers F, Schöttle J, Vogel W, Dahmen I, Koker M, Ullrich RT, Wright GM, Russell PA, Wainer Z, Solomon B, Brambilla E, Nagy-Mignotte H, Moro-Sibilot D, Brambilla CG, Lantuejoul S, Altmüller J, Becker C, Nürnberg P, Heuckmann JM, Stoelben E, Petersen I, Clement JH, Sänger J, Muscarella LA, la Torre A, Fazio VM, Lahortiga I, Perera T, Ogata S, Parade M, Brehmer D, Vingron M, Heukamp LC, Buettner R, Zander T, Wolf J, Perner S, Ansén S, Haas SA, Yatabe Y, Thomas RK. CD74-NRG1 fusions in lung adenocarcinoma. *Cancer Discov. 2014 Apr; 4(4):415-22.*

45- Le T, Gerber DE. Newer-Generation EGFR Inhibitors in Lung Cancer: How Are They Best Used?. *Cancers (Basel)*. 2019;11(3):366. Published 2019 Mar 15. doi:10.3390/cancers11030366

46- Fukuoka M, Wu YL, Thongprasert S, Sunpaweravong P, Leong S-S, Sriuranpong V, et al. Biomarker analyses and final overall survival results from a phase III, randomized, open-label, first-line study of gefitinib versus carboplatin/paclitaxel in clinically selected patients with advanced non-small-cell lung cancer in Asia (IPASS). J Clin Oncol. 2011;29(21):2866–74.

47- Ellis PM, Coakley N, Feld R, Kuruvilla S, Ung YC. Use of the epidermal growth factor receptor inhibitors gefitinib, erlotinib, afatinib, dacomitinib, and icotinib in the treatment of non-small-cell lung cancer: a systematic review. *Curr Oncol*. 2015;22(3):e183–e215. doi:10.3747/co.22.2566

48- T.S Mok, Y. Cheng, X. Zhou, et al. improvement in overall survival in a randomized study that compared dacomitinib with gefitinib in patients with advanced non-small cell lung cancer and EGFR-activating mutations. J Cli Oncol. 2018, pp. 2244-2250.

49- Morgillo F, Della Corte CM, Fasano M, et al. Mechanisms of resistance to EGFR-targeted drugs: lung cancer. ESMO Open. 2016;1:e000060.

50- Vidyullatha P. Lung cancer incidence in never smokers: genetic and gender basis. Gene Rep 2016;4:19-207

51- Rodriguez-Lara V, Hernandez-Martinez JM, Arrieta O. Influence of estrogen in non-small cell lung cancer and its clinical implications. *J Thorac Dis*. 2018;10(1):482–497. doi:10.21037/jtd.2017.12.61

52- Ganti A.K., et al: Hormone replacement therapy is associated with decreased survival in women with lung cancer. J. Clin. Oncol. 2006; 24: pp. 59-63
53- Chlebowski RT, Schwartz AG, Wakelee H, Anderson GL, Stefanick ML, Manson JE, Rodabough RJ, Chien JW, Wactawski-Wende J, Gass M, Kotchen JM, Johnson KC, O'Sullivan MJ, Ockene JK, Chen C, Hubbell FA, Women's Health Initiative Investigators. Oestrogen plus progestin and lung cancer in postmenopausal women (Women's Health Initiative trial): a post-hoc analysis of a randomized controlled trial. *Lancet. 2009 Oct 10; 374(9697):1243-51.*
54- Kumar R, Zakharov MN, Khan SH, Miki R, Jang H, Toraldo G, Singh R, Bhasin S, Jasuja R. The dynamic structure of the estrogen receptor. J Amino Acids. 2011;2011:812540.
55- Hsu L., Chu N., Kao S. Estrogen, Estrogen Receptor and Lung Cancer. Int. J. Mol. Sci. 2017;18:1713
56- Marino M, Galluzzo P, Ascenzi P. Estrogen signaling multiple pathways to impact gene transcription. Current Genomics. 2006;7(8):497–508
57- Patrone C., Cassel T.N., Pettersson K., Piao Y.S., Cheng G., Ciana P., Maggi A., Warner M., Gustafsson J.A., Nord M. Regulation of postnatal lung development and homeostasis by estrogen receptor beta. Mol. Cell. Biol. 2003;23:8542–8552.
58- Siegfried JM. Smoking out reproductive hormone actions in lung cancer. *Mol Cancer Res*. 2014;12(1):24–31. doi:10.1158/1541-7786.MCR-13-0580
59- Chakraborty S, Ganti AK, Marr A, Batra SK. Lung cancer in women: role of estrogens. *Expert Rev Respir Med*. 2010;4(4):509–518. doi:10.1586/ers.10.50
60- Rodriguez-Lara V, Ignacio GS, Cerbon Cervantes MA. Estrogen induces CXCR4 overexpression and CXCR4/CXL12 pathway activation in lung adenocarcinoma cells in vitro. Endoc Res. 2017 Aug;42(3):219-231
61- *Stabile LP, Lyker JS, Gubish CT, Zhang W, Grandis JR, Siegfried JM.* Combined targeting of the estrogen receptor and the epidermal growth factor receptor in non-small cell lung cancer shows enhanced antiproliferative effects. *Cancer Res. 2005 Feb 15; 65(4):1459-70.*
62- Ding, X., Li, L., Tang, C., Meng, C., Xu, W., Wei, X., et al. Cytoplasmic expression of estrogen receptor β may predict poor outcome of EGFR-TKI therapy in metastatic lung adenocarcinoma. Oncology Letters. (2018) 16, 2382-2390. https://doi.org/10.3892/ol.2018.8936
63- Thrane S, Lykkesfeldt AE, Larsen MS, Sorensen BS, Yde CW. Estrogen receptor alpha is the major driving factor for growth in tamoxifen-resistant breast cancer and supported by HER/ERK signaling. Breast Cancer Res Treat. 2013; 139: 71–80
64- E.B. Garon, J.M. Siegfried, L.P. Stabile, et al. Randomized phase II study of fulvestrant and erlotinib compared with erlotinib alone in patients with advanced or metastatic non-small cell lung cancer. Lung Cancer. 123(2018), pp. 91-98
65- Siegfried JM, Lin Y, Diergaarde B, et al. Expression of PAM50 Genes in Lung Cancer: Evidence that Interactions between Hormone Receptors and HER2/HER3

Contribute to Poor Outcome. *Neoplasia*. 2015;17(11):817–825. doi:10.1016/j.neo.2015.11.002

66- *Chen DSm Mellman I. Oncology meets immunology: the cancer-immunity cycle. Immunity. 2013 Jul 25;39(1):1-10*

67- Soo RA, Chen Z, Yan Teng RS, et al. Prognostic significance of immune cells in non-small cell lung cancer: meta-analysis. *Oncotarget*. 2018;9(37):24801–24820. Published 2018 May 15. doi:10.18632/oncotarget.24835

68- Yu H, Boyle TA, Zhou C, Rimm DL, Hirsch FR. PD-L1 Expression in Lung Cancer [published correction appears in J Thorac Oncol. 2017 Jan;12 (1):157-159]. *J Thorac Oncol*. 2016;11(7):964–975. doi:10.1016/j.jtho.2016.04.014

69- Tian, Y., Zhai, X., Han, A. *et al.* Potential immune escape mechanisms underlying the distinct clinical outcome of immune checkpoint blockades in small cell lung cancer. *J Hematol Oncol* **12,** 67 (2019). https://doi.org/10.1186/s13045-019-0753-2

70- Jain P, Jain C, Velcheti V. Role of immune-checkpoint inhibitors in lung cancer. *Ther Adv Respir Dis*. 2018;12:1753465817750075. doi:10.1177/1753465817750075

71- Brahmer JR, et al. Safety and activity of anti-PD-L1 antibody in patients with advanced cancer. *N Engl J Med*. 2012;366(26):2455–2465.

72- Gettinger SN, et al. Overall survival and long-term safety of nivolumab (anti-programmed death 1 antibody, BMS-936558, ONO-4538) in patients with previously treated advanced non-small-cell lung cancer. *J Clin Oncol*. 2015;33(18):2004–2012

73- Weinberg F, Gadgeel S. Combination pembrolizumab plus chemotherapy: a new standard of care for patients with advanced non-small-cell lung cancer. *Lung Cancer (Auckl)*. 2019;10:47–56. Published 2019 Jun 4. doi:10.2147/LCTT.S176391

74- Maimela NR, Liu S, Zhang Y. Fates of CD8+ T cells in Tumor Microenvironment. *Comput Struct Biotechnol J*. 2018;17:1–13. Published 2018 Nov 22. doi:10.1016/j.csbj.2018.11.004

75- Driessens G, Kline J, Gajewski TF. Costimulatory and coinhibitory receptors in anti-tumor immunity. *Immunol Rev*. 2009;229(1):126–144. doi:10.1111/j.1600-065X.2009.00771.x

76- Jiang, X., Wang, J., Deng, X. *et al.* Role of the tumor microenvironment in PD-L1/PD-1-mediated tumor immune escape. *Mol Cancer* **18,** 10 (2019). https://doi.org/10.1186/s12943-018-0928-4

77- Nielsen SR, Schmid MC. Macrophages as Key Drivers of Cancer Progression and Metastasis. *Mediators Inflamm*. 2017;2017:9624760. doi:10.1155/2017/9624760

78- Yousef Ahmed Fouad and Carmen Aanej. Revisiting the hallmarks of cancer. Am J Cancer Res. 2017;7(5):1016-1036

79- Gordon SR, Maute RL, Dulken BW, et al. PD-1 expression by tumour-associated macrophages inhibits phagocytosis and tumour immunity. *Nature*. 2017;545(7655):495–499. doi:10.1038/nature22396

80- Palacios, E., Weiss, A. Function of the Src-family kinases, Lck and Fyn, in T-cell development and activation. *Oncogene* **23,** 7990–8000 (2004). https://doi.org/10.1038/sj.onc.1208074

81- Bommhardt U, Schraven B, Simeoni L. Beyond TCR Signaling: Emerging Functions of Lck in Cancer and Immunotherapy. *Int J Mol Sci*. 2019;20(14):3500. Published 2019 Jul 16. doi:10.3390/ijms20143500

82- Arasanz H, Gato-Cañas M, Zuazo M, et al. PD1 signal transduction pathways in T cells. *Oncotarget*. 2017;8(31):51936–51945. Published 2017 Apr 19. doi:10.18632/oncotarget.17232

83- Arulraj T, Barik D. Mathematical modeling identifies Lck as a potential mediator for PD-1 induced inhibition of early TCR signaling. *PLoS One*. 2018;13(10):e0206232. Published 2018 Oct 24. doi:10.1371/journal.pone.0206232

84- Stephen Rapecki, Rodger Allen. Inhibition of human T cell activation by novel Src kinase inhibitors is dependent upon the complexity of the signal delivered to the cells. Journal of Pharmacology and Experimental Therapeutics December 2002, 303 (3) 1325-1333; DOI: https://doi.org/10.1124/jpet.102.038380

85- Katrin Mestermann, Theodoros Giavridis, Justus Weber, Julian Rydzk et al. The tyrosine kinase inhibitor dasatinib acts as a pharmacologic on/off switch for CAR T cells. Science Translational Medicine. 2019 Jul 3;11(499).

86- Hekim C, Ilander M, Yan J, Michaud E, Smykla R, et al. Dasatinib changes immune cell profiles concomitant with reduced tumor growth in several murine solid tumor models. Cancer Immunol Res. 2017 Feb;5(2):157-169

87- Ling Y, Xie Q, Zhang Z, Zhang H. Protein kinase inhibitors for acute leukemia. *Biomark Res*. 2018;6:8. Published 2018 Feb 13. doi:10.1186/s40364-018-0123-1

88- Kiefer F, Brumell J, Al-Alawi N, et al. The Syk protein tyrosine kinase is essential for Fcgamma receptor signaling in macrophages and neutrophils. *Mol Cell Biol*. 1998;18(7):4209–4220. doi:10.1128/mcb.18.7.4209

89- Yi YS, Son YJ, Ryou C, Sung GH, Kim JH, Cho JY. Functional roles of Syk in macrophage-mediated inflammatory responses. *Mediators Inflamm*. 2014;2014:270302. doi:10.1155/2014/270302

90- Crowley MT, Costello PS, Fitzer-Attas CJ, et al. A critical role for Syk in signal transduction and phagocytosis mediated by Fcgamma receptors on macrophages. *J Exp Med*. 1997;186(7):1027–1039. doi:10.1084/jem.186.7.1027

91- Wellenstein MD, de Visser KE. Cancer-cell-intrinsic mechanisms shaping the tumor immune landscape. Immunity. 2018 Mar 20;48(3):399-416.

92- E.A. Akbay, S. Koyama, J. Carretero, A. Altabef, J.H. Tchaicha, C.L. Christensen , O.R. Mikse, A.D. Cherniack, E.M. Beauchamp, T.J. Pugh, *et al.* Activation of

the PD-1 pathway contributes to immune escape in EGFR-driven lung tumors. Cancer Discov., 3 (2013), pp. 1355-1363
93- Patrick H. Lizotte, Ruey-Long Hong, Tony A. Luster, Megan E. Cavanaugh, et al. A high-throughput immune-oncology screen identifies EGFR inhibitors as potent enhancers of antigen-specific cytotoxic T-lymphocyte tumor cell killing. Cancer Immunol Res. 2018 Dec;6(12):1511-1523
94- Eri Suglyama, Yosuka Togashi, Yoshiko Takeuchi, Sayoko Shinya, et al. Blockade of EGFR improves responsiveness to PD-1 blockade in EGFR-mutated non-small cell lung cancer. Sci Immunol. 2020 Jan.
95- Pollack BP. EGFR inhibitors, MHC expression and immune responses: Can EGFR inhibitors be used as immune response modifiers?. *Oncoimmunology*. 2012;1(1):71–74. doi:10.4161/onci.1.1.18073
96- Dielschneider RF, Xiao W, Yoon JY, et al. Gefitinib targets ZAP-70-expressing chronic lymphocytic leukemia cells and inhibits B-cell receptor signaling. *Cell Death Dis*. 2014;5(10):e1439. Published 2014 Oct 2. doi:10.1038/cddis.2014.391
97- Zeboudj L, Maitre M, Guyonnet L, Laurans L, Joffre J, et al. Selective EGF-receptor inhibition in CD4+ T cells induces anergy and limits atherosclerosis. J Am Coll Cardiol. 2018 Jan 16;71(2):160-172.
98- Jeffrey A. Engelman, Kreshnik Zejnullahu, Christopher-Michael Gale, Eugene Lifshifts, et al. PF00299804, an irreversible pan-ERBB inhibitor, is effective in lung cancer models with EGFR and ERBB2 mutations that are resistant to gefitinib. Cancer Res. 2007 Dec 15;67(24): 11924-32.
99- Saito H, Fukuhara T, Furuya N, et al. Erlotinib plus bevacizumab versus erlotinib alone in patients with EGFR-positive advanced non-squamous non-small cell lung cancer (NEJ026): interim analysis of an open-label, randomized, multicenter, phase 3 trial. Lancet Oncol. 2019.
100-Zhang F, Huang D, Li T, et al. Anti-PD-1 Therapy plus Chemotherapy and/or Bevacizumab as Second Line or later Treatment for Patients with Advanced Non-Small Cell Lung Cancer. *J Cancer*. 2020;11(3):741–749. Published 2020 Jan 1. doi:10.7150/jca.37966
101-Markowitz GJ, Havel LS, Crowley MJ, et al. Immune reprogramming via PD-1 inhibition enhances early-stage lung cancer survival. *JCI Insight*. 2018;3(13):e96836. Published 2018 Jul 12. doi:10.1172/jci.insight.96836
102-Alexander M, Galeas J, Cheng H. Tumor mutation burden in lung cancer: a new predictive biomarker for immunotherapy or too soon to tell?. *J Thorac Dis*. 2018;10(Suppl 33):S3994–S3998. doi:10.21037/jtd.2018.09.35
103– Uprety D. Chemo-immunotherapy: the beginning of a new era in lung cancer. Clin Lung Cancer. 2019 Mar;20(2):63-65.
104- Svoronos N, Perales-Puchalt A, Allegrezza MJ, et al. Tumor Cell-Independent Estrogen Signaling Drives Disease Progression through Mobilization of Myeloid-Derived Suppressor Cells. *Cancer Discov*. 2017;7(1):72–85. doi:10.1158/2159-8290.CD-16-0502
105- Rothenberger NJ, Somasundaram A, Stabile LP. The Role of the Estrogen Pathway in the Tumor Microenvironment. *Int J Mol Sci*. 2018;19(2):611. Published 2018 Feb 19. doi:10.3390/ijms19020611

106- Hamilton D.H., Griner L.M., Keller J.M., Hu X., Southall N., Marugan J., David J.M., Ferrer M., Palena C. Targeting estrogen receptor signaling with fulvestrant enhances immune and chemotherapy-mediated cytotoxicity of human lung cancer. Clin. Cancer Res. 2016;22:6204–6216. doi: 10.1158/1078-0432.CCR-15-3059
107- Chou TC. Drug combination studies and their synergy quantification using the Chou-Talalay method. Cancer Res. 2010 Jan 15;70(2):440-6
108- F. Simpkins, K. Jang, H. Yoon, *et al.* Dual Src and MEK inhibition decreases ovarian cancer growth and targets tumor initiating stem-like cells. Clin Cancer Res, 24 (2018), pp. 4874-4886
109- Almotlak AA, Farooqui M, Siegfried JM. Inhibiting pathways predicted from a steroid hormone gene signature yields synergistic antitumor effects in NSCLC. J Thorac Oncol. 2020 Jan;15(1):62-79.
110- Barros, F.F., Abdel-Fatah, T.M., Moseley, P. et al. Characterization of HER heterodimers in breast cancer using in situ proximity ligation assay. *Breast Cancer Res Tret*. 2014; 144: 273–285
111- Green, A.R., Barros, F.F., Abdel-Fatah, T.M. et al. HER2/HER3 heterodimers and p21 expression are capable of predicting adjuvant trastuzumab response in HER2+ breast cancer. *Breast Cancer Res Treat*. 2014; 145: 33–44
112- Zhang, X., Diaz, M.R., and Yee, D. Fulvestrant regulates epidermal growth factor (EGF) family ligands to activate EGF receptor (EGFR) signaling in breast cancer cells. *Breast Cancer Res Treat*. 2013; 139: 351–360
113- Osborne, C.K., Shou, J., Massarweh, S., and Schiff, R. Crosstalk between estrogen receptor and growth factor receptor pathways as a cause for endocrine therapy resistance in breast cancer. *Clin Cancer Res*. 2005; 11: 865s–870s
114- Addison, C.L., Ding, K., Zhao, H. et al. Plasma transforming growth factor alpha and amphiregulin protein levels in NCIC Clinical Trials Group BR.21. *J Clin Oncol*. 2010; 36: 5247–5256
115- Massarelli, E., Varella-Garcia, M., Tang, X. et al. KRAS mutation is an important predictor of resistance to therapy with epidermal growth factor receptor tyrosine kinase inhibitors in non–small-cell lung cancer. *Clin Cancer Res*. 2007; 13: 2890–2896
116- Moll, H.P., Pranz, K., Musteanu, M. et al. Afatinib restrains K-RAS driven lung tumorigenesis. (pii:eaao2301)*Sci Transl Med*. 2018; 10
117- Kruspig, B., Monteverde, T., Neidler, S. et al. The ERBB network facilitates KRAS-driven lung tumorigenesis. (pii:eaao2565)*Sci Transl Med*. 2018; 10
118- Lee, Y.J., Han, J.Y., Lee, G.K. et al. C-Met overexpression as resistance biomarker for epidermal growth factor receptor tyrosine kinase inhibitors in EGFR-mutant non–small cell lung cancer. *J Clin Oncol*. 2017; 34: e20660
119- Stabile, L.P., Davis, A.L., Gubish, C.T. et al. Human non–small cell lung tumors and cells derived from normal lung express both estrogen receptor α and β and show biological responses to estrogen. *Cancer Res*. 2002; 62: 2141–2150
120- Rahdar, M., Inoue, T., Meyer, T., Zhang, J., Vazquez, F., and Devreotes, P.N. A phosphorylation-dependent intramolecular interaction regulates the membrane association and activity of the tumor suppressor PTEN. *Proc Natl Acad Sci U S A*. 2009; 106: 480–485

121- Malaney, P., Palumbo, E., Semidey-Hurtado, J. et al. PTEN physically interacts with and regulates E2F1-mediated transcription in lung cancer. *Cell Cycle*. 2018; 17: 947–962
122- Panni, R.Z.; Linehan, D.C.; DeNardo, D.G. Targeting tumor-infiltrating macrophages to combat cancer. Immunotherapy 2013, 5, 1075–1087
123- A Sica, P Larghi, A Mancino, L Rubino, C Porta, MG Totaro, et al. Macrophage polarization in tumour progression. Semin Cancer Biol, 18 (5) (2008), pp. 349-355.
124– Speiser DE, Ho PC, Verdeil G. Regulatory circuits of T cell function in cancer. Nat Rev Immunol. 2016 Oct;16(10):599-611
125-Anderson KG, Stromnes IM, Greenberg PD. Obstacles Posed by the Tumor Microenvironment to T cell Activity: A Case for Synergistic Therapies. *Cancer Cell*. 2017;31(3):311–325. doi:10.1016/j.ccell.2017.02.008
126– Natalie J. Rothenberger, Laura P. Stabile. Induction of lung tumors and mutational analysis in FVB/N mice treated with the tobacco carcinogen 4-(Methylnitrosamino)-1-(3-pyridyl)-1-butanon. Molecular Toxicology Protocols. 2020 Jan. pp 149-160
127- Ayeni, D., Miller, B., Kuhlmann, A. *et al*. Tumor regression mediated by oncogene withdrawal or erlotinib stimulates infiltration of inflammatory immune cells in EGFR mutant lung tumors. *J Immunotherapy Cancer* 7, 172 (2019). https://doi.org/10.1186/s40425-019-0643-8
128- Kohsuke Isomoto, Koji Haratani, Hidetoshi Hayashi, Shigeki Shimizu, et al. Impact of EGFR-TKI treatment on the tumor immune microenvironment in EGFR mutation-positive non-small cell lung cancer. Clin Cancer Res. 2020 Jan. [published onlinefirst] doi: 10.1158/1078-0432.CCR-19-2027
129- Kumai T, Ohkuri T, Nagato T, et al. Targeting HER-3 to elicit antitumor helper T cells against head and neck squamous cell carcinoma. *Sci Rep*. 2015;5:16280. Published 2015 Nov 5. doi:10.1038/srep16280
130- Liu D, Mamorska-Dyga A. Syk inhibitors in clinical development for hematological malignancies. *J Hematol Oncol*. 2017;10(1):145. Published 2017 Jul 28. doi:10.1186/s13045-017-0512-1
131- Geahlen RL. Getting Syk: spleen tyrosine kinase as a therapeutic target. *Trends Pharmacol Sci*. 2014;35(8):414–422. doi:10.1016/j.tips.2014.05.007
132– Hassane M. Zarour. Reversing T-cell dysfunction and exhaustion in cancer. Clin Cancer Res. 2016 Apr 15:22(8):1856-1864
133– Anliang Xia, Yan Zhang, Jiang Xu, Tailang Yin and Xiao-Jie Lu. T cell dysfunction in cancer immunity and immunotherapy. Frontiers in Immunology. 2019 July. | https://doi.org/10.3389/fimmu.2019.01719
134- Havel JJ, Chowell D, Chan TA. The evolving landscape of biomarkers for checkpoint inhibitor immunotherapy. *Nat Rev Cancer*. 2019;19(3):133–150. doi:10.1038/s41568-019-0116-x
135- Qianqin Ni, Fuwu Zhang, Yijing Liu, Zhantong Wang, Guocan Yu, et al. A bi-adjuvant nanovaccine that potentiates immunogenicity of neoantigen for combination immunotherapy of colorectal cancer. Sci Advances. 2020 Mar. 6(12). DOI: 10.1126/sciadv.aaw6071

136- Li B, VanRoey M, Wang C, Chen TH, Korman A, Jooss K. Anti-programmed death-1 synergizes with granulocyte macrophage colony-stimulating factor – secreting tumor cell immunotherapy providing therapeutic benefit to mice with established tumors. *Clin Cancer Res* (2009) 15:1623–34. doi:10.1158/1078-0432.CCR-08-1825
137- Duraiswamy J, Kaluza KM, Freeman GJ, Coukos G. Dual blockade of PD-1 and CTLA-4 combined with tumor vaccine effectively restores T-cell rejection function in tumors. *Cancer Res* (2013) 73:3591–603. doi:10.1158/0008-5472.CAN-12-4100
138– Schaer DA, Beckmann RP, Dempsey JA, Huber L, Forest A, et al. The CDK4/6 inhibitor abemaciclib induces a T cell inflamed tumor microenvironment and enhances the efficacy of PD-L1 checkpoint blockade. Cell Rep. 2018 Mar 13:22(11):2978-2994
139- Moya-Horno I, Viteri S, Karachaliou N, Rosell R. Combination of immunotherapy with targeted therapies in advanced non-small cell lung cancer (NSCLC). *Ther Adv Med Oncol*. 2018;10:1758834017745012. Published 2018 Jan 9. doi:10.1177/1758834017745012
140- Spigel DR, Schrock AB, Fabrizio D, et al. Total mutation burden (TMB) in lung cancer (LC) and relationship with response to PD-1/PD-L1 targeted therapies. J Clin Oncol 2016; 34(Suppl.): abstract 9017
141– Derek De-Rui Huang, James Chih-Hsin Yang. Chekpoint inhibitor combined with tyrosine kinase inhibitor-the end or the beginning?J Thorac Oncol. 2020 Mar;15(3):305-307.
142–Impact of EGFR-TKIs combined with PD-L1 antibody on the lung tissue of EGFR-driven tumor-bearing mice. Lung Cancer. 2019 Nov;137:85-93
143-Vartanian, R., Masri, J., Martin, J. et al. AP-1 regulates cyclin D1 and c-MYC transcription in an AKT-dependent manner in response to mTOR inhibition: role of AIP4/Itch-mediated JUNB degradation. *Mol Cancer Res*. 2011; 9: 115–130
144-Castaño, Z., Marsh, T., Tadipatri, R. et al. Stromal EGF and igf-I together modulate plasticity of disseminated triple-negative breast tumors. *Cancer Discov*. 2013; 3: 922–935
145-Petz, L.N., Ziegler, Y.S., Schultz, J.R., and Nardulli, A.M. Fos and Jun inhibit estrogen-induced transcription of the human progesterone receptor gene through an activator protein-1 site. *Endocrinology*. 2004; 18: 521–532
146-Blonska, M., Zhu, Y., Chuang, H.H. et al. Jun-regulated genes promote interaction of diffuse large B-cell lymphoma with the microenvironment. *Blood*. 2015; 125: 981–991
147-Willis C, Fiander M, Tran D, et al. Tumor mutational burden in lung cancer: a systematic literature review. *Oncotarget*. 2019;10(61):6604–6622. Published 2019 Nov 12. doi:10.18632/oncotarget.27287
148-Gardner A, Ruffell B. Dendritic Cells and Cancer Immunity. *Trends Immunol*. 2016;37(12):855–865. doi:10.1016/j.it.2016.09.006
149-Fu B, Wang F, Sun R, Ling B, Tian Z, Wei H. CD11b and CD27 reflect distinct population and functional specialization in human natural killer cells. *Immunology*. 2011;133(3):350–359. doi:10.1111/j.1365-2567.2011.03446.x